ADVANCED LECTURES 1987

CLOUD PHYSICS

VOLUME 1

1. THE STRUCTURE OF SMALL MARITIME CUMULUS CLOUDS

1.1 HISTORICAL INTRODUCTION

Early studies of the structure of small warm cumulus were concerned with the water content and updraught within the clouds and with the evolution of the droplet spectrum. Despite the limited instrumentation available for the early aircraft based observational studies three basic features were demonstrated:

i. The liquid water content averaged across the cloud at any level is significantly less than the adiabatic water content (the water content of a parcel raised to that level from cloud base at which it is just saturated) and that the deficit increases with height above cloud base (Table 1.1).

ii. The liquid water content averaged over about 100 m is almost constant across the cloud with a sharp decrease at the edges of the cloud (Figure 1.1).

iii. The maximum drop size increases with height above cloud base but the breadth of the spectrum also increases with small drops being observed in significant concentrations at all levels (Figure 1.2). The dispersion of the droplet spectrum (ratio of standard deviation of radii to the mean radius) increases with height above cloud base

TABLE 1.1 Ratio of observed liquid water content in cumulus clouds (q) to the adiabatic water content (q_a)

Height above cloud base (km)	Number of Observations	Median Value q/q_a
0-0.33	24	0.33
0.33-0.67	119	0.26
0.67-1.0	66	0.18
1.0 -1.33	62	0.17
1.33-1.67	23	0.12
1.67-2.0	0	-
2.0 -2.33	27	0.08

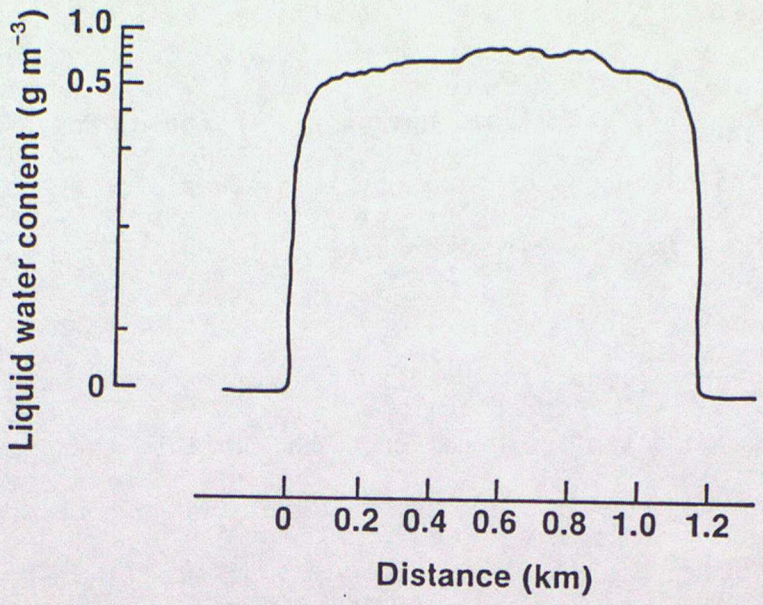

Figure 1.1. Observations of the variation of liquid water content across a small cumulus cloud.

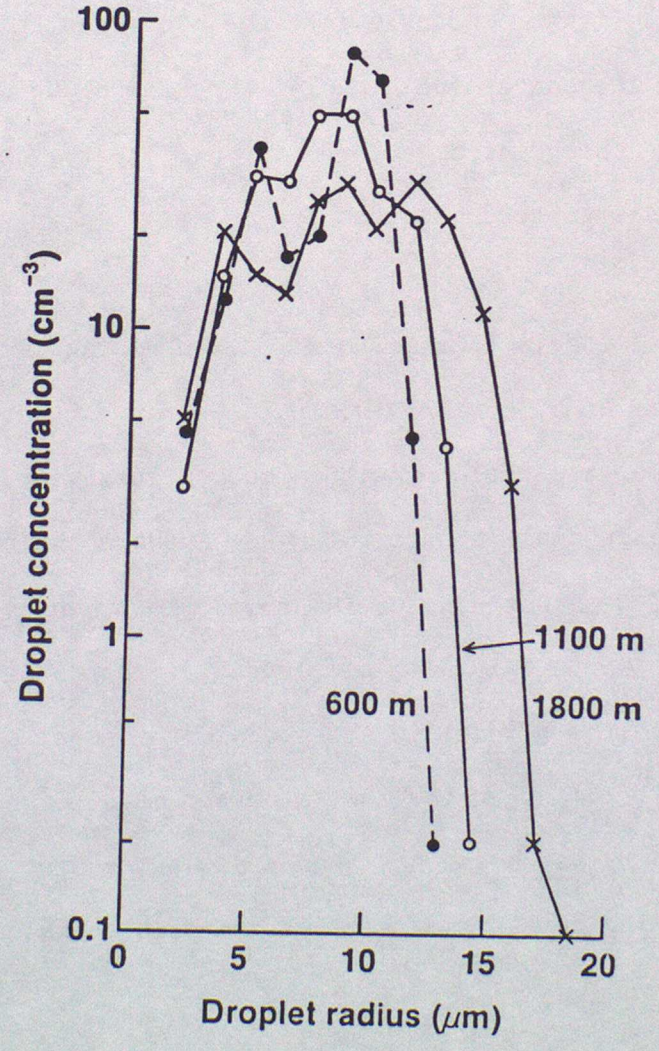

Figure 1.2. Observations of droplet spectra in maritime cumulus at the indicated height above cloud base averaged across the cloud.

(Figure 1.3) and it has recently been shown (Knight, 1987) that the dispersion increases slightly as the ratio of the cloud water content to the adiabatic value decreases (Figure 1.4).

The observations of sub-adiabatic water content can only be explained by the entrainment of dry environmental air into the clouds during their development including, since sub-adiabatic water contents were observed in growing clouds, the growth phase of the cloud. Since the water content profile is relatively uniform across the cloud it was believed that entrainment took place at the cloud top. Squires (1958b) suggested that such cloud top entrainment could give rise by evaporative cooling to downdraughts which might penetrate into the cloud hastening its decay. Entrainment also introduces fresh nuclei into the cloud which could become activated during subsequent ascent to give rise to the observed populations of small droplets even towards cloud top.

Simple parcel models of a uniformly mixed rising thermal demonstrated that without entrainment not only would the water content be adiabatic but the latent heat release would result in much higher vertical velocities than are observed in small clouds. Table 1.2 shows the results obtained from such a model when entrainment is assumed to be inversely proportional to the radius of the parcel which consequently expands as it rises. In an attempt to explain the bimodality observed in some mean droplet spectra Mason and Jonas (1974) suggested that a better model of cloud development might be obtained by assuming that second and subsequent thermals rise through the decaying remnants of earlier thermals entraining saturated air.

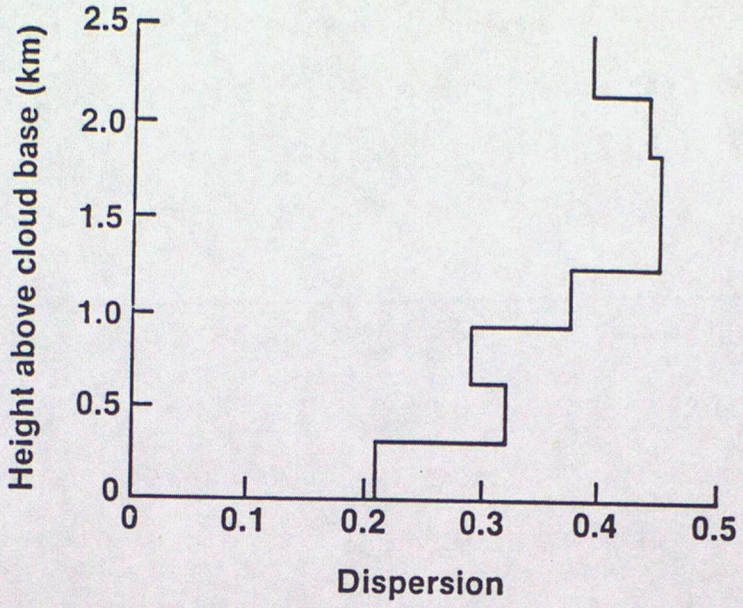

Figure 1.3. Variation of the average dispersion of the droplet spectrum in small maritime cumulus with height above cloud base.

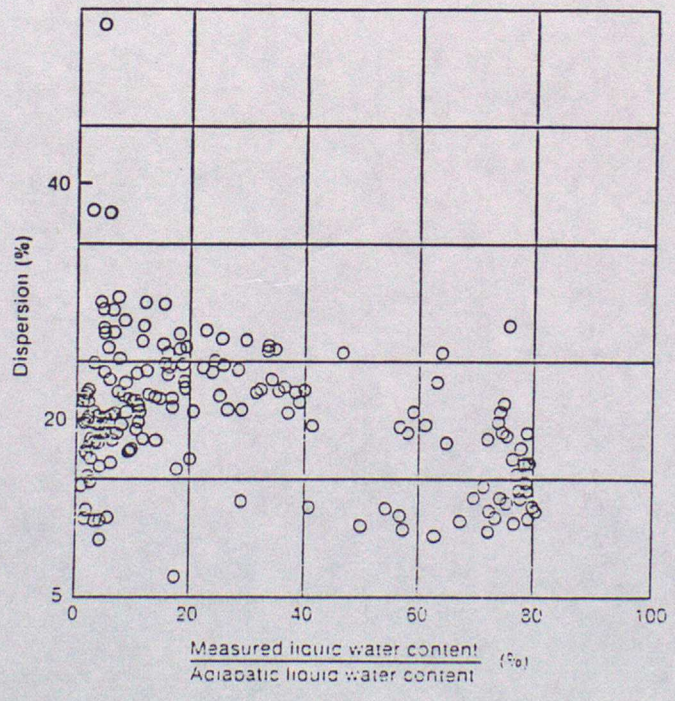

Figure 1.4. Observations of the dispersion of the droplet spectrum at various levels in small maritime cumulus clouds plotted against the ratio of the liquid water content to the adiabatic value.

TABLE 1.2 Calculated propeties of an entraining cloud parcel. Initial updraught 1.0 m s^{-1} and radius of parcel 350 m (250 m for last 3 rows of table).

Environment			Maximum Values		
Lapse rate (K km^{-1})	Relative humidity (%)	Initial Temperature (K)	Height (K m)	Updraught (m s^{-1})	Water Content (10^{-3})
7	85	0.1	1.61	1.0	0.3
7	85	0.2	2.16	1.2	0.4
8	85	0.1	6.57	5.7	1.2
7	80	0.1	0.85	1.0	0.1
7	90	0.1	4.06	2.1	1.4
7	85	0.1	0.72	1.0	0.1
7	85	0.2	0.95	1.1	0.2
7	87	0.2	1.32	1.1	0.2

Although this model reproduced some features of the droplet spectrum the predicted cloud structure differed little from that resulting from a single parcel model as can be seen from Figure 1.5.

One of the problems encountered in attempting to explain the details of the observations is the poor spatial resolution of the early observations which result from averaging of parameters over distances which have been shown subsequently to contain much detailed structure. It has also become apparent that detailed explanations of drop growth depend on the dynamical structure of the cloud on a scale which was hardly resolvable in the early studies.

1.2 OBSERVATIONS OF HORIZONTAL STRUCTURE OF SMALL CLOUDS

The development of instrumentation capable, even at aircraft speeds of resolving structure on a scale of a few meters has demonstrated the complexity of the dynamical structure of cumulus clouds. A series of observations by Knight (1987) in non-precipitating maritime clouds in the vicinity of the British Isles includes clouds at all stages of development. Although finite aircraft speeds make it impossible to obtain an instantaneous picture of cloud structure at any point in the life of the cloud, the synthesis of data from a large number of clouds enables the typical structure to be defined. The depth of the clouds was about 1 km with the cloud base 1 km above the sea surface; adiabatic water contents would be expected to be about 2 g kg^{-1} at cloud top.

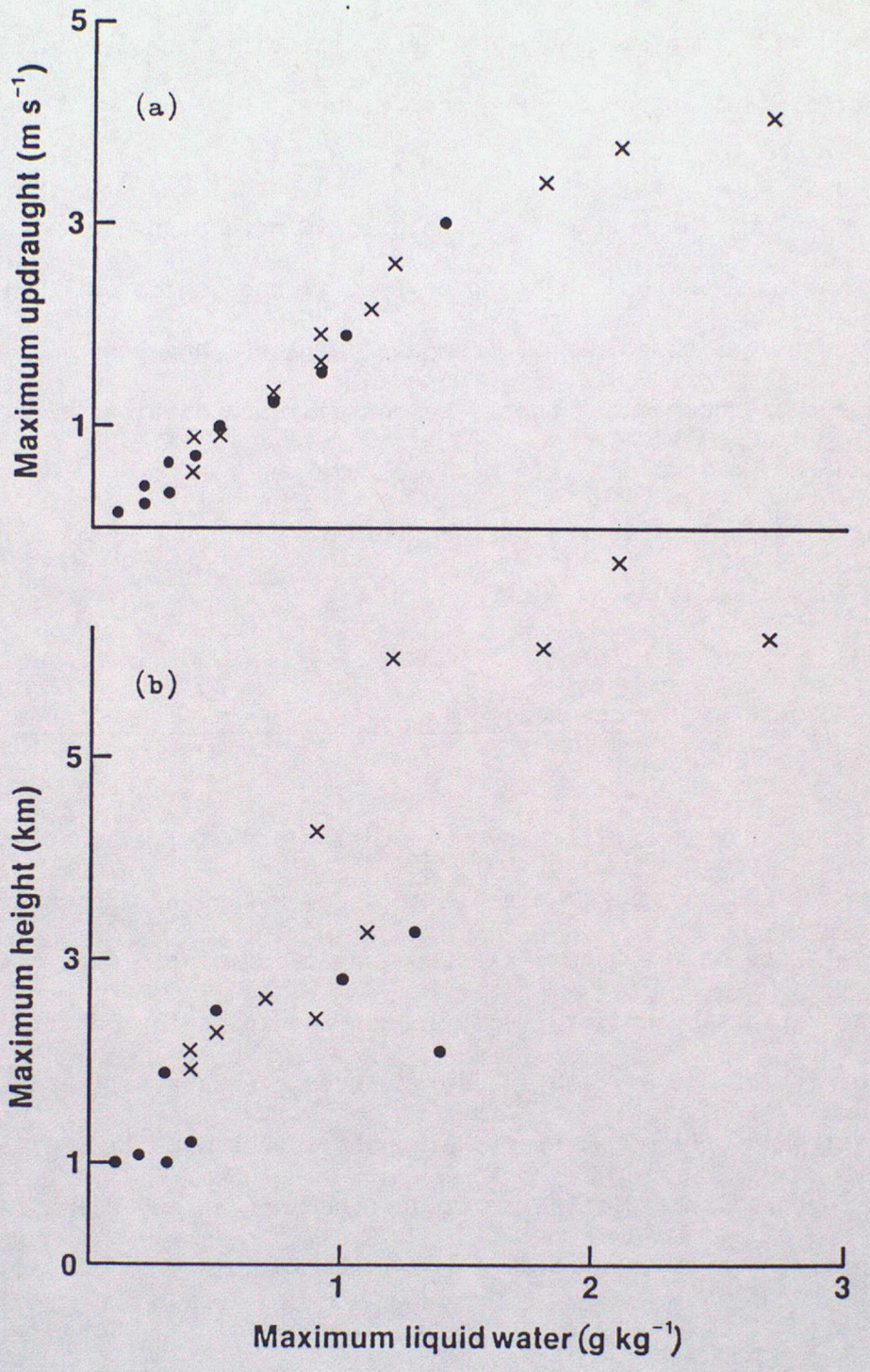

Figure 1.5. Calculated maximum ascent and height reached by entraining, uniformly mixed parcels. Circles represent single thermals, crosses represent parcels rising through the remnants of earlier thermals. A range of environmental lapse rates and initial temperatures were used in the calculations.

Typical results are seen in Figure 1.6 which shows at 5 Hz (about 20 m) profiles across a cloud of the vertical velocity, liquid water content, temperature and total water content. The measurements were made about 100 m above cloud base (Figure 1.6a), at about the middle level of the cloud (Figure 1.6b) and near the top of the cloud which in this case was about 950 m deep (Figure 1.6c). The measurements were made along straight lines approximately parallel to the mean wind in the cloud layer. Since the measurements extend over a period of about 6 min some cloud development must have occurred between the time of the highest (earliest) and lowest (latest) measurements. The observations demonstrate the cloud has much structure on a scale of less than 100 m and yet coherent motion is seen on a scale of about 500 m.

Near cloud base the updraught is weak and fluctuations are comparable with those beyond the edges of the cloud defined as the region with significant liquid water content. The liquid water content shows some peaks which approach the adiabatic value in regions about 500 m across. The temperature within the cloud differs little from that outside but the total water content is rather higher within the cloud than in its surroundings suggesting that the air had ascended from levels below cloud base. At the mid-level in the cloud (Figure 1.6b) the vertical velocity variance is significantly higher than outside the cloud and there is evidence of vertical motion on all scales. In general, regions of ascent are associated with high liquid water content. A further feature of these observations is the presence of a region of warm subsiding air close to the edge of the cloud. At cloud top (Figure 1.6c) several regions of descent (or less rapid ascent) can be identified within the cloud with a scale of

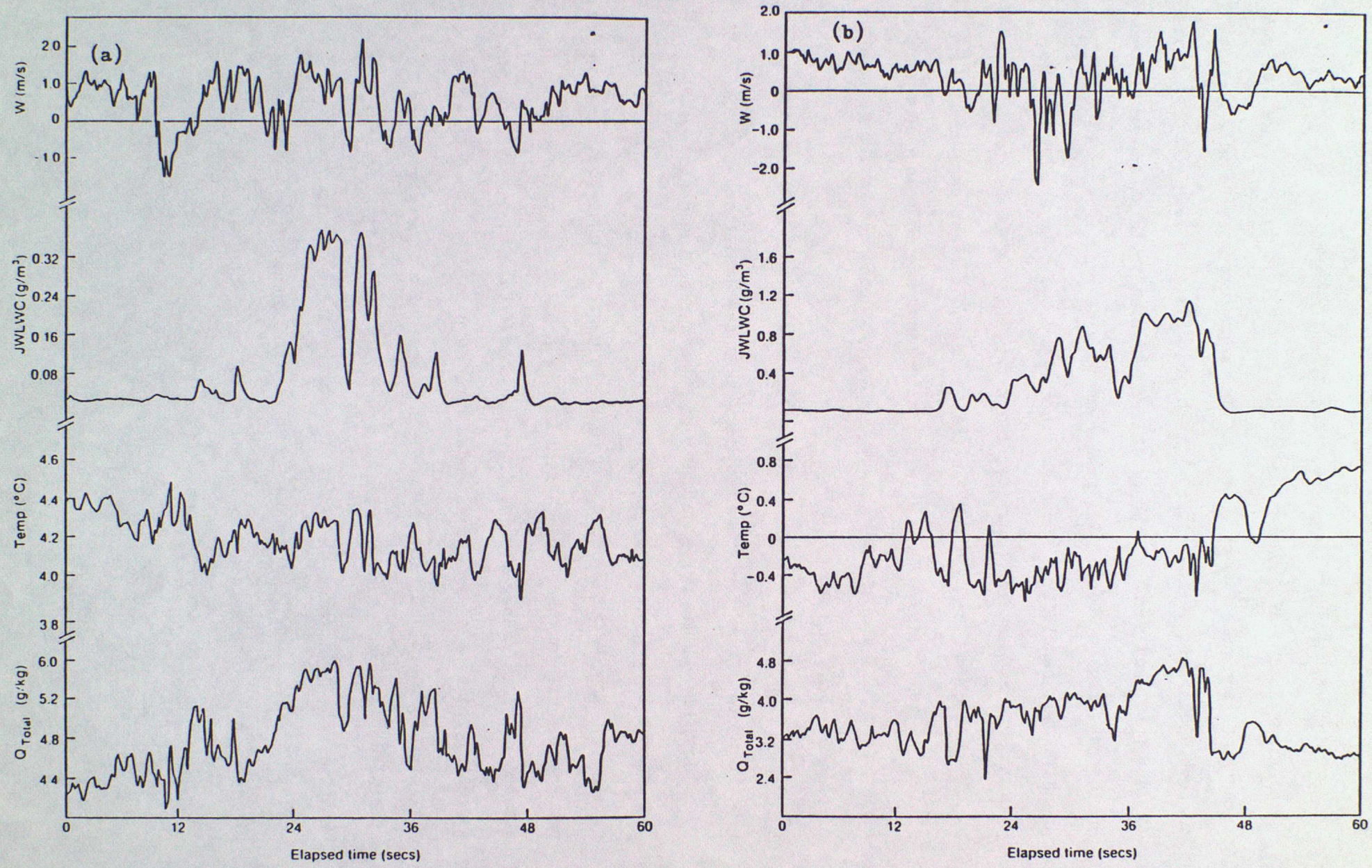
(a)
W (m/s)
2.0
1.0
0
-1.0
JWLWC (g/m³)
0.32
0.24
0.16
0.08
Temp (°C)
4.6
4.4
4.2
4.0
3.8
Q Total (g/kg)
6.0
5.2
4.8
4.4
0
12
24
36
48
60
Elapsed time (secs)
(b)
W (m/s)
2.0
1.0
0
-1.0
-2.0
JWLWC (g/m³)
1.6
1.2
0.8
0.4
Temp (°C)
0.8
0.4
0
-0.4
Q Total (g/kg)
4.8
4.0
3.2
2.4
0
12
24
36
48
60
Elapsed time (secs)

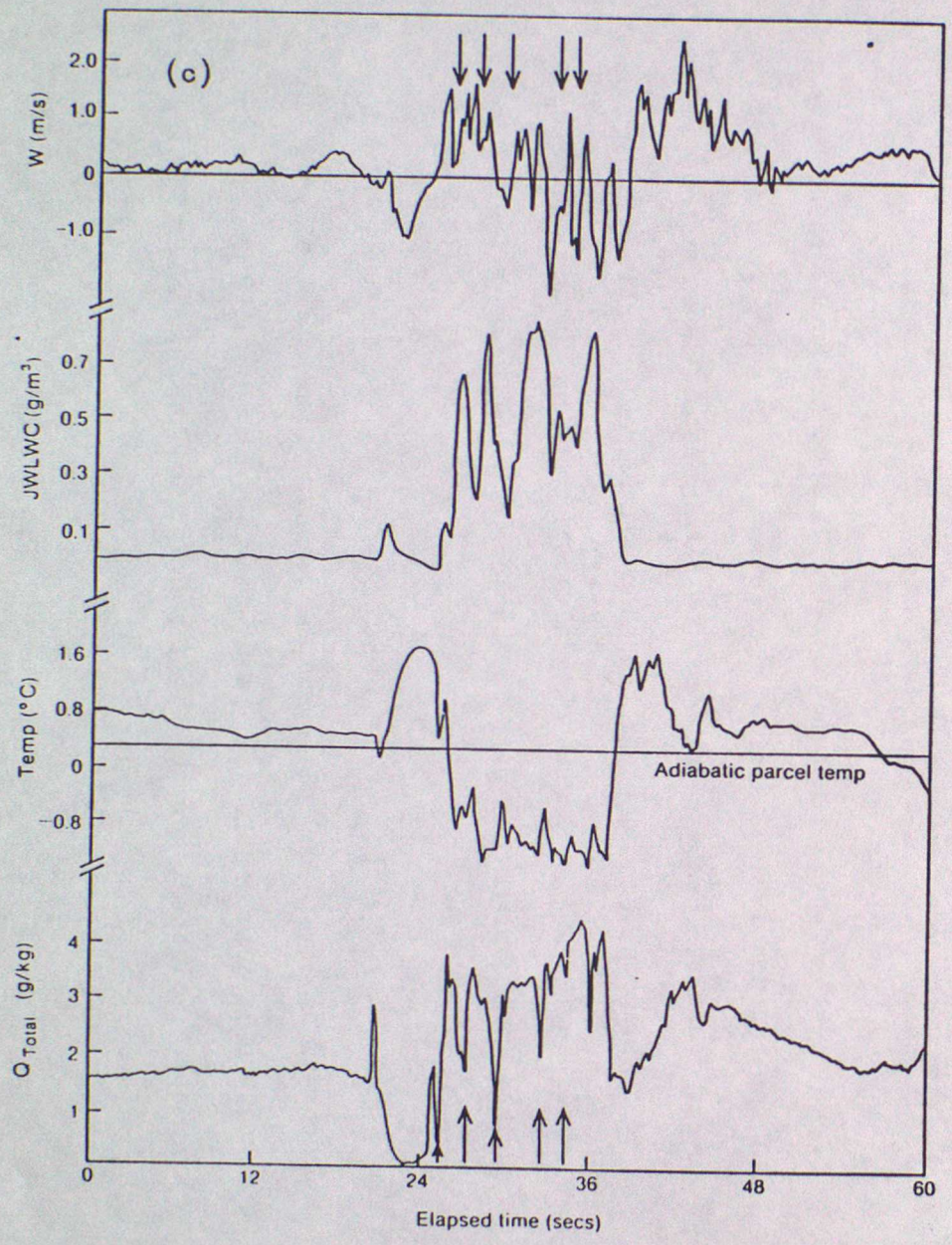

Figure 1.6. Typical observations of updraught, liquid water content, temperature and total water content across maritime cumulus clouds approximately 1 km deep. (a) 100 m above cloud base, (b) Near the mid-level of cloud. (c) About 100 m below cloud top.

about 100 m. These regions have lower than average cloud liquid water content and are warmer than the surrounding cloud. Examination of the total water content record shows that these downdraughts are also drier than the surrounding cloud suggesting that they are the result of entrainment of drier air at cloud top across the top of the cloud. The water content in these regions was recorded by the hot wire instrument but this has a slow response time. The fast response sampling instruments suggested that drops were not present in some of these regions and the specific humidity measurements (not shown) suggested a relative humidity as low as 50%. The air near the inversion on this occasion was very dry. The existence of a dry, warm subsiding region at the upwind cloud edge apparent at mid-level is even more apparent at cloud top at about 24 s. (The flight track is in the opposite direction to that in Figure 1.6b).

1.3 THE VERTICAL STRUCTURE OF SMALL CLOUDS

Aircraft mounted instruments make possible measurements of many clouds but the horizontal and vertical resolution is limited by the speed of movement and the response time of the instruments. Observations at several levels using balloon borne probes show considerable vertical coherence in the clouds (Figure 1.7) with slightly tilted updraught and downdraught regions. This structure will be considered later in more detail.

Knight (1987) attempted to use observations from several cloud penetrations on one day to develop a general picture of the vertical structure of cumulus clouds. Results shown in Figure 1.8 include data for many clouds plotted against height above cloud base normalised using the

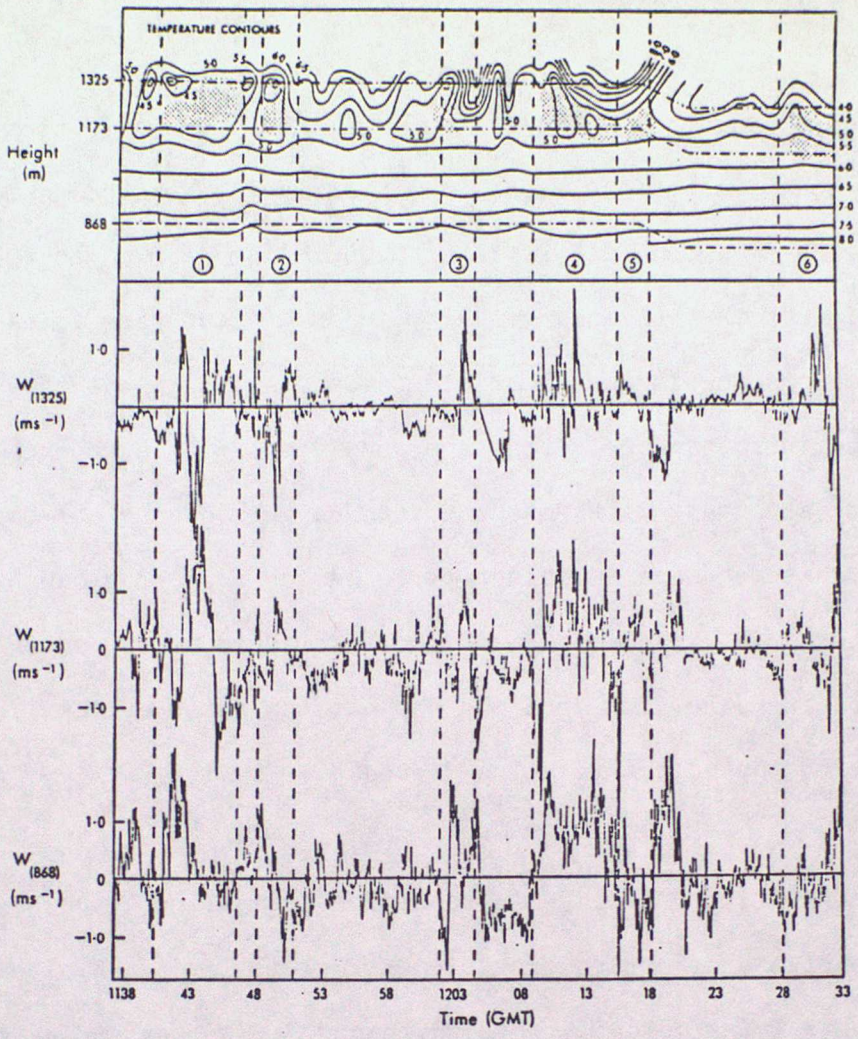

Figure 1.7. Temperature contours (0.5 K spacing) from balloon borne sensors at 3 marked levels through a field of small cumulus (clouds stippled). Vertical and horizontal coordinates are approximately equal. Below are vertical velocity traces. Dashed lines indicate location of cloud boundaries.

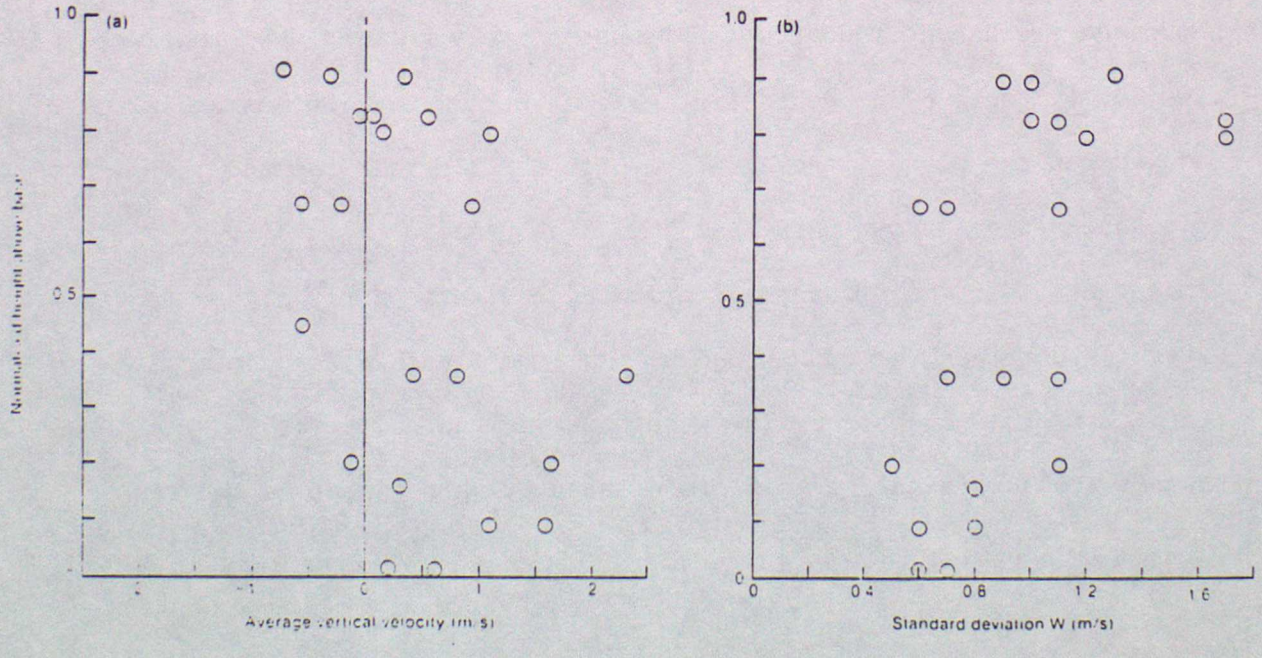

Figure 1.8. (a) Average vertical velocity in cloud from each penetration on one day plotted against normalised height. (b) Standard deviation of vertical velocity fluctuations about averages shown in (a).

observed cloud depth. The figure shows the average vertical velocity across the width of the clouds. Generally the vertical velocity is highest just below or around mid-level with a minimum near cloud top. The standard deviation of the vertical velocity in each cloud pass is also shown; fluctuations are largest near cloud top. Although the data were not obtained instantaneously they are consistent with a coherent vertical velocity structure with frequent downdraughts near cloud top. The downdaughts decrease in intensity or number towards cloud base. Consistent with the early experimental results the liquid water content and its variance increase towards cloud top but the ratio of the liquid water content to the adiabatic value decreases.

Knight (1987) employed a conditional sampling technique to obtain a picture of the structure of typical cumulus clouds. Regions of coherent updraughts (mean velocity greater than 0.1 m s^{-1} extending over 100 m) and downdraughts were identified. The data were classified according to the non-dimensional height above cloud base and according to whether within updraughts or downdraughts. The variations arising from the different stages of development of the clouds were therefore smoothed out although clouds were apparently near maturity or actively growing when they were sampled. Effects of condensation nucleus spectrum variations are also removed but the clouds were all formed in maritime air masses. Results of this analysis are shown in Figure 1.9. The results (Figure 1.9a) demonstrate that the updraught regions have significantly higher liquid water content than the downdraughts. Maximum liquid water contents approaching the adiabatic value were observed near cloud base. The results suggest that updraught regions are diluted by entrainment as the air

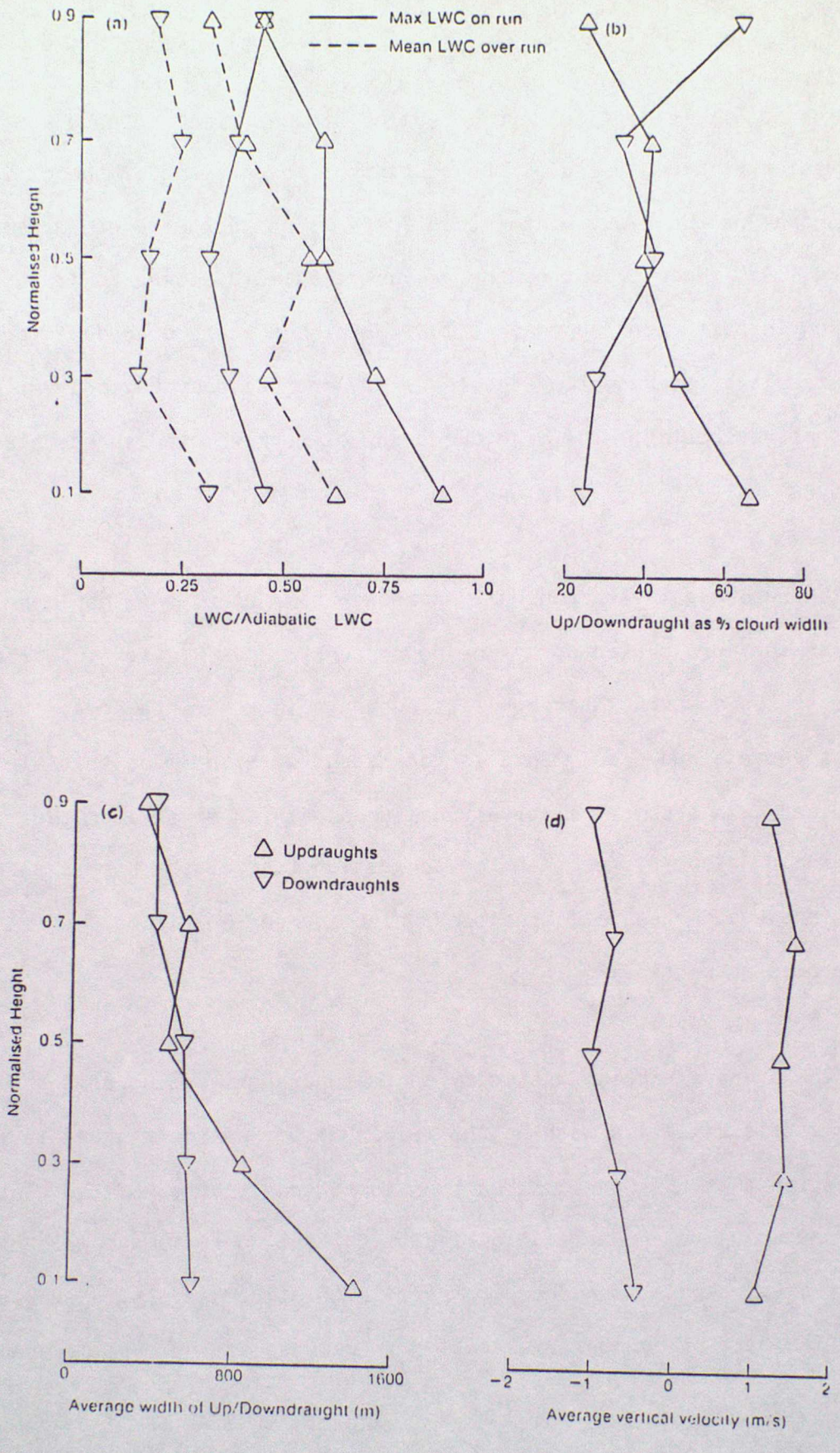

Figure 1.9. Variation with non dimensional height of (a) Ratio of liquid water content to adiabatic value; (b) Updraught or downdraught width as % of cloud width; (c) Updraught or downdraught width; (d) Vertical velocity. Data are averages from a large number of penetrations and are shown for updraught and downdraught regions only.

ascends but it is difficult to determine at what time and at what level the air was entrained because of the continuous development of the cloud. The percentage of the cloud width occupied by up and downdraughts is shown in Figure 1.9b. Near cloud top the region occupied by downdraughts is about 70% and in some cases approached 100% as clouds started to decay probably as a result of overshooting the level of zero buoyancy together with evaporative cooling. The high frequency of narrow downdraughts near cloud top suggests that they originate in this region.

The updraughts are generally narrower near cloud top than near cloud base as they are broken up by the downdraughts (see Figure 1.9). In contrast the downdraughts show little change in horizontal scale with height above cloud base. This is consistent with the idea that air entrained as a blob of relatively quiescent air is mixed into the surrounding cloud rather than the suggestion that cloudy air is entrained into (and evaporates into) the blob which increases in size (at least until it becomes saturated).

The average vertical velocity in the updraught and downdraught regions shows little variation with height (Figure 1.9d) although there is some suggestion that the updraught maximum is towards the top of the cloud. The peak downdraughts are at a slightly lower level where momentum exchange with the updraughts is reduced compared with higher levels. Towards cloud base, the rate of evaporative cooling is reduced as the rate of evaporation is reduced.

1.4 PENETRATIVE DOWNDRAUGHTS

Squires (1958b) suggested that under certain conditions downdraughts initiated by evaporative cooling due to air entrained at cloud top could penetrate deeply into a cloud. Jonas and Mason (1982) attempted to model this process and their results (shown in Figure 1.10) suggest that downdraught penetration almost to cloud base is possible. The downdraughts in these calculations were maintained close to saturation by cloud drop evaporation. The results show some resemblence to the observations of Knight (1987) (although he studied much shallower clouds) in that the peak downdraught is found to be below the level of the maximum updraught. The general structure of the liquid water content variation with height predicted by the model is also in reasonable agreement with the observations.

Deardorff (1980) and Randall (1980) showed that for entrainment to be capable of initiating downdraughts the difference in equivalent potential temperature across the cloud boundary must exceed a critical value typically about 1 or 2 K. The analysis is similar to that for conventional conditional instability of the atmosphere to heating but, of course, the sign is reversed. An analysis of the small cumulus observations by Knight (1987) showed that in the more vigorous clouds examined, entrainment was capable of generating downdraughts if the air remained saturated. The results shown in Table 1.3 have been calculated assuming either that air is only entrained from within 100 m of the cloud edge or over a much larger distance; the air close to the cloud often has a lower equivalent temperature than air further away due to subsidence. The data for a weaker

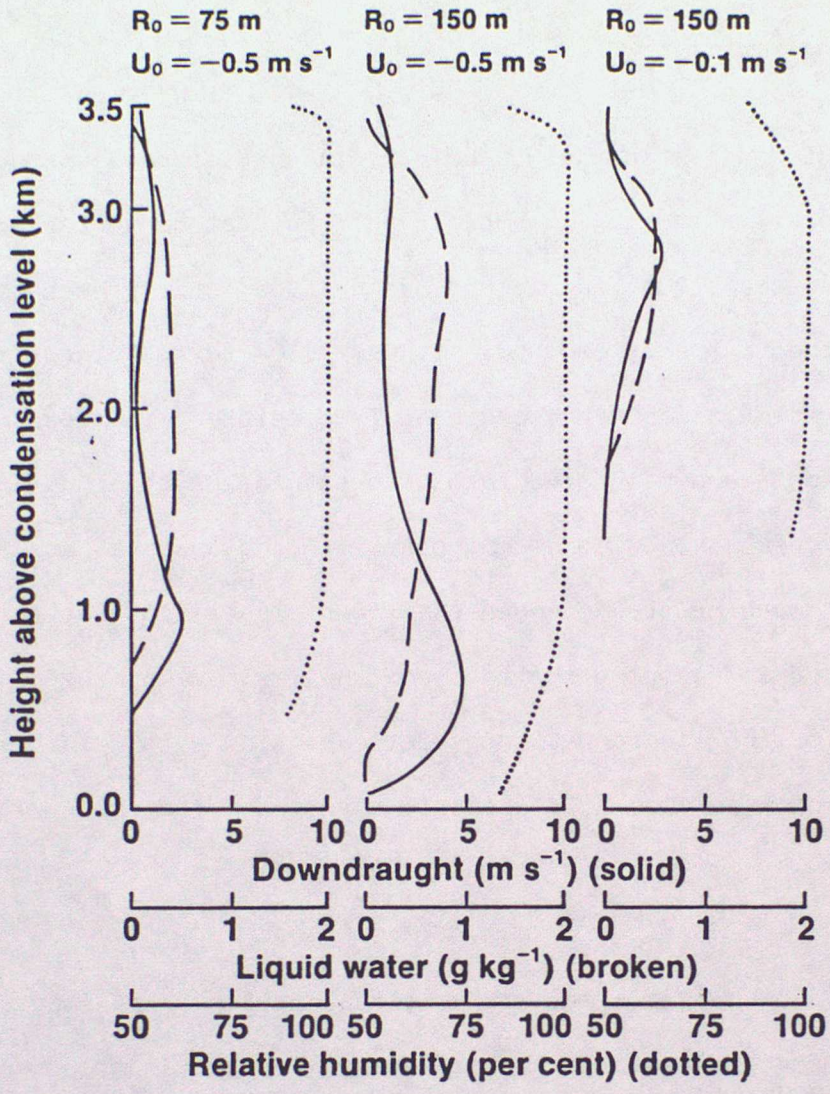

Figure 1.10. Calculated penetration of downdraught of initial radius R, upward velocity U into a 3.5 km deep cloud with maximum updraught 6.1 m s^{-1} at 1.4 km above cloud base and liquid water content 1.8 g kg^{-1} at 1.5 km above cloud base.

TABLE 1.3 The difference (K) between observed values of equivalent potential temperature across the boundaries of cumulus clouds ($\Delta\theta$) and the calculated critical values for instability. Values of $\Delta\theta$ are calculated from (a) data within 100 m of the cloud edge; (b) data within 1000 m of the cloud edge.

		Top	Middle Levels		Near Base
Vigorous Cloud					
	(a)	5.0	2.6	2.9	2.0
	(b)	3.7	1.8	2.3	2.2
Weak Cloud					
	(a)	-0.4	0.7		0.3
	(b)	-0.1	1.6		1.2

cloud suggest that penetrative downdraughts were much less likely to form, a result confirmed by the vertical velocity measurements through the cloud.

A further feature of the downdraughts in cumulus is their relationship to the droplet spectrum. In general regions of high liquid water content compared with the adiabatic value are associated with updraughts however high resolution data such as are shown in Figure 1.11, show that some downdraught or weak updraught regions have relatively high liquid water content. A feature of these results is that the largest drops may be found in regions of decreased water content and reduced updraughts but not in regions of strong downdraught. We are not concerned here with the mechanisms for the growth of large drops but these observations suggest that their growth cannot be treated in isolation from the structure of the clouds. It is possible for example that some drops could have been brought down in almost saturated downdraughts from higher levels in the cloud.

1.4 SOURCES OF ENTRAINED AIR

Some constraints on the origins of the air within the clouds can be obtained from the observed thermodynamic properties. Paluch (1979) showed that mixing diagrams based on total water content q_{Total} and wet equivalent potential temperature θ_q, which are conserved during ascent and descent in saturated and unsaturated air, could be used to deduce the level at which entrained into a cloud originated. She noted that if these parameters were plotted against each other for data within clouds they often fell on well defined straight lines implying that air from only 2 levels was mixed in varying quantities. Data from the environmental profile can similarly be

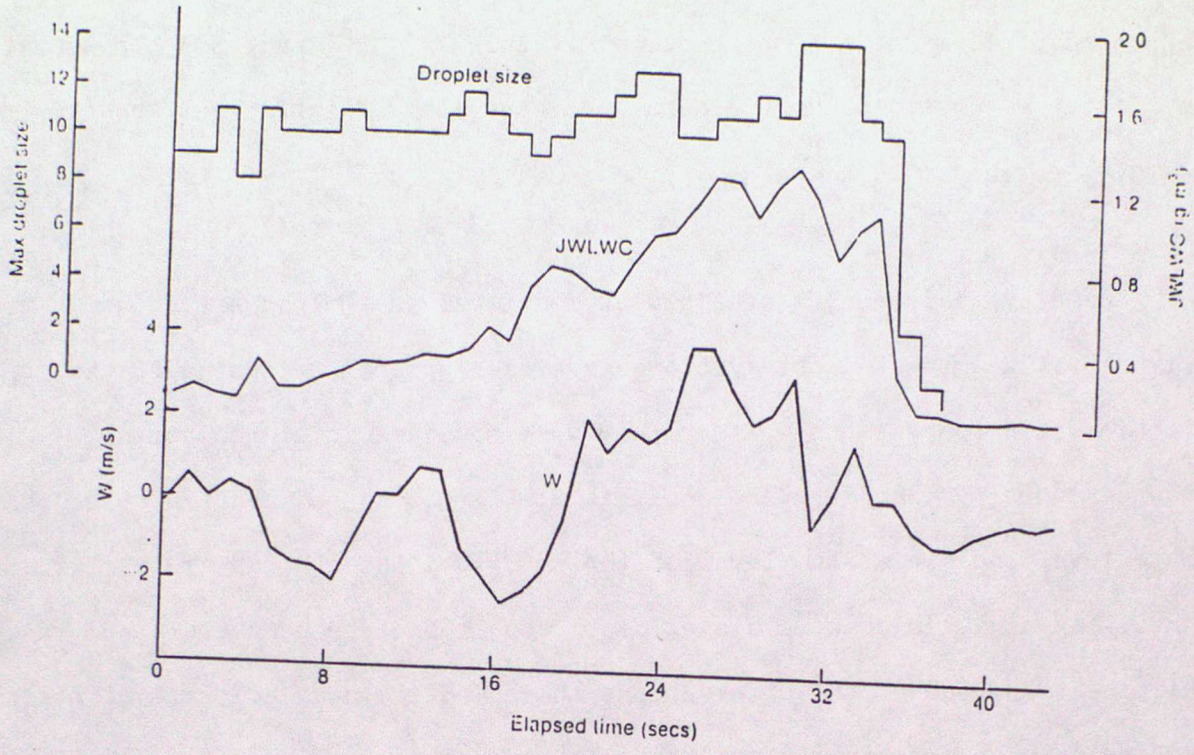

Figure 1.11. Maximum droplet size, liquid water content and updraught along a penetration at mid-level in a small cumulus cloud.

plotted and the intersections of the mixing line with the the environmental curve identifies the two source levels. Knight (1987) analysed his data in a similar way noting that the data were generally of sufficient accuracy to give θ_q to about 0.5 K and q_{Total} to about 0.1 g kg^{-1}.

Some typical results obtained at mid-level in a cloud are shown in Figure 1.12a where the observations have been grouped according to the liquid water content and whether they were obtained in updraughts or downdraughts. The results are consistent with mixing between air at cloud base level and air at the level of the observations although mixing involving air at higher levels eg cloud top, cannot be completely eliminated. None of the observations showed unambiguous evidence of mixing extending downwards from cloud top. In general the updraught regions show signs of little mixing while the downdraught regions have undergone more mixing.

The results obtained close to the cloud top, Figure 1.12b show rather more scatter. Relatively unmixed samples with high liquid water content are observed at this level but other points show evidence of substantial mixing with air from the inversion.

These results suggested that there was little vertical mixing within the clouds and that dilution occurred either by lateral entrainment or by entrainment at cloud top at the earlier time when the cloud top was close to the observation level. This picture is however at variance with observations by Paluch (1979) and also the observations of Kitchen and Caughey (1981) shown in Figure 1.7 which suggested that coherent

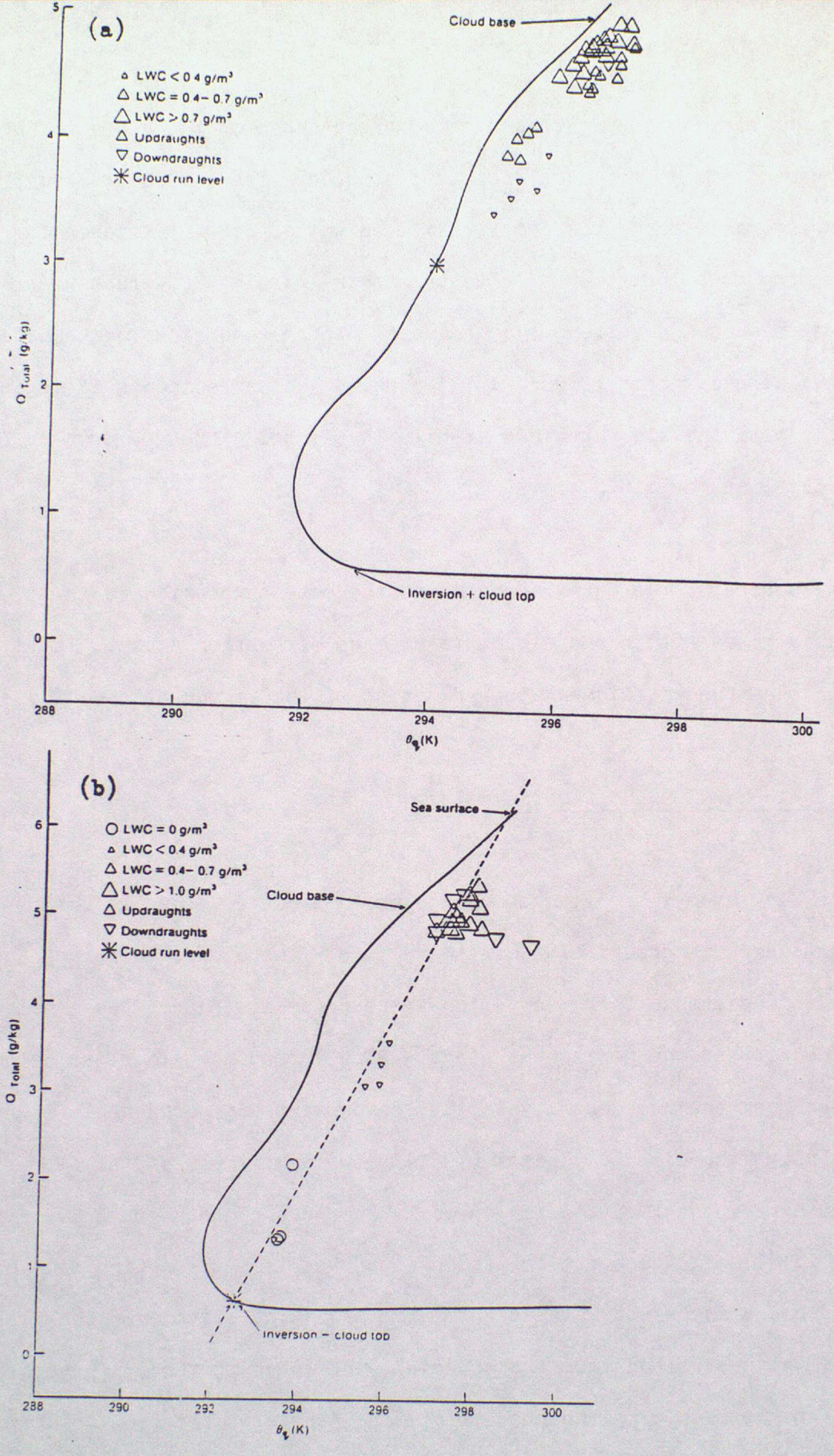

Figure 1.12. Diagrams showing total water content plotted against wet equivalent potential temperature from penetrations of small cumulus at (a) mid-level and (b) near cloud top. Solid lines represent environmental soundings while in-cloud data along horizontal penetrations are grouped according to updraught and water content. An asterisk on the sounding indicates the level of the penetration.

downdraught structures were found through the depth of the cloud. There were however some differences the cases studied. The clouds studied by Knight were maritime clouds about 1 km deep while those of Kitchen and Caughey were much shallower. In contrast, the results of Paluch were obtained in much more vigorous continental clouds several kilometers deep but her mixing diagrams (Figure 1.13) show very clear evidence of mixing at cloud top with the air entrained at high levels being brought down at least to mid level in the cloud.

The source of the entrained air and the extent to which it is vertically mixed within the clouds is an area of further study. It is possible that the entrainment is a function of the vigour of the clouds.

1.5. FLOW AROUND CUMULUS CLOUDS

The flow associated with cumulus clouds is not confined to the updraughts and downdraughts within the clouds. The clouds influence the flow at some distance from the region where drops are found. We consider first the flow in the horizontal plane. Flow around the cloud can be estimated from the horizontal velocity measurements on horizontal flight paths through the clouds. Knight (1987) shows an example of the fluctuating component of the air velocity around a cloud about 2 km deep (Figure 1.14). The penetration of the cloud was from the upwind side and the wind speed increased with height. The mean wind speed over the traverse was subtracted from the observed wind speed so that, if the cloud moves with the mean wind the gust velocities represent the flow relative to the cloud. The reversal of the fluctuations on each side of the cloud seen

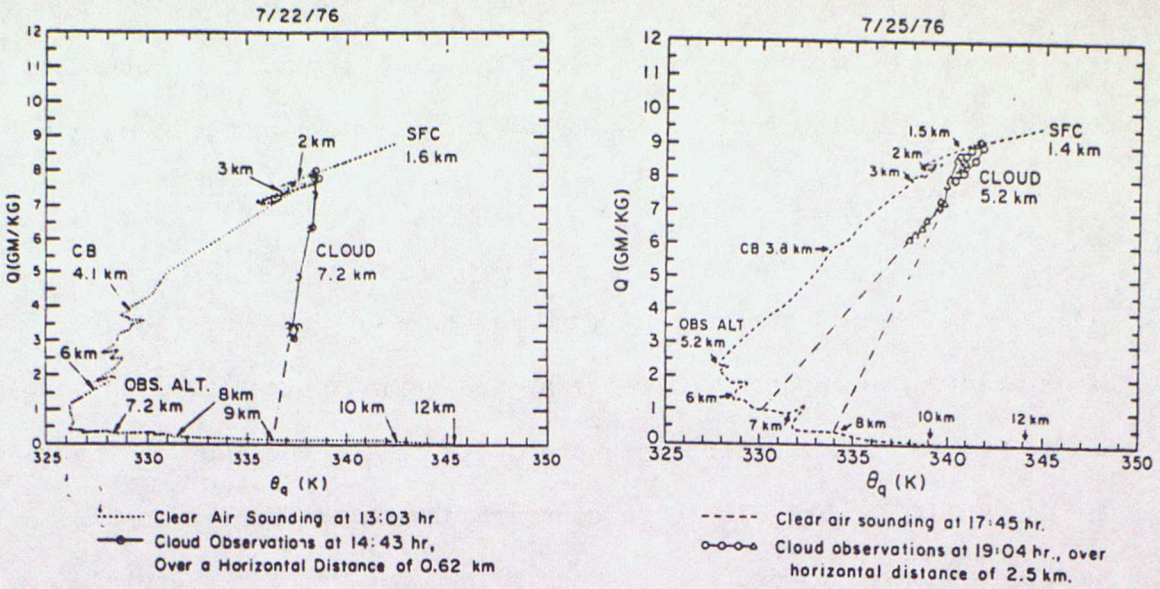

Figure 1.13. As figure 1.12 except that the data are from two moderate continental clouds.

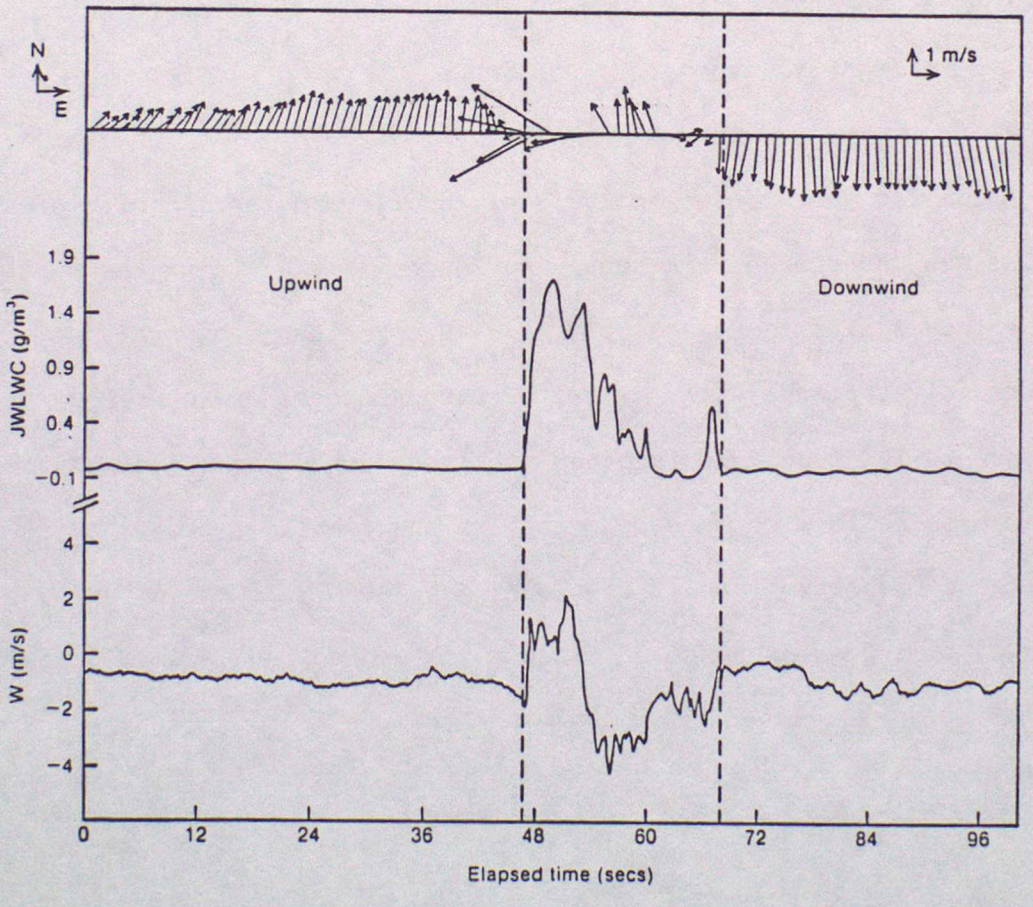

Figure 1.14. Observations of the fluctuations about the mean horizontal wind component, the liquid water content and the vertical velocity from a penetration near the top of a small cumulus cloud delineated by the dashed lines.

in Figure 1.14 is consistent with the hypothesis that the cloud acts as an obstacle to the flow and air is forced around the cloud producing a downwind wake.

It has been suggested that turbulence levels are increased in the wakes leading to enhanced entrainment and in many examples such as this at mid level the liquid water content profile is saw toothed with the peak on the upwind side. This is to be contrasted with the more symmetrical profiles observed by Squires (1958a). The wake extends downwind several times the cloud diameter and in most cases is still apparent 3 km behind the cloud where the measurements were terminated. The results shown in Figure 1.14 also demonstrate that the vertical velocity is negative on the downwind cloud edge while there is ascent in the upwind high water content region. This also suggests that mechanically driven lateral entrainment may occur at the downstream edge of the cloud in addition to entrainment at cloud top driven by evaporative cooling.

A similar gust vector analysis of the flow in the vicinity of small cumulus was undertaken by Kitchen and Caughey (1981) using their balloon data. The results in Figure 1.15 show an organised updraught and downdraught structure with regions of strong ascent surrounded by regions of descent. The updraught is often inclined due to the effect of shear. Although there is much more coherence in these balloon observations than in the aircraft observations it is clear that these measurements need to be extended to a greater range of cloud sizes and to levels well below cloud

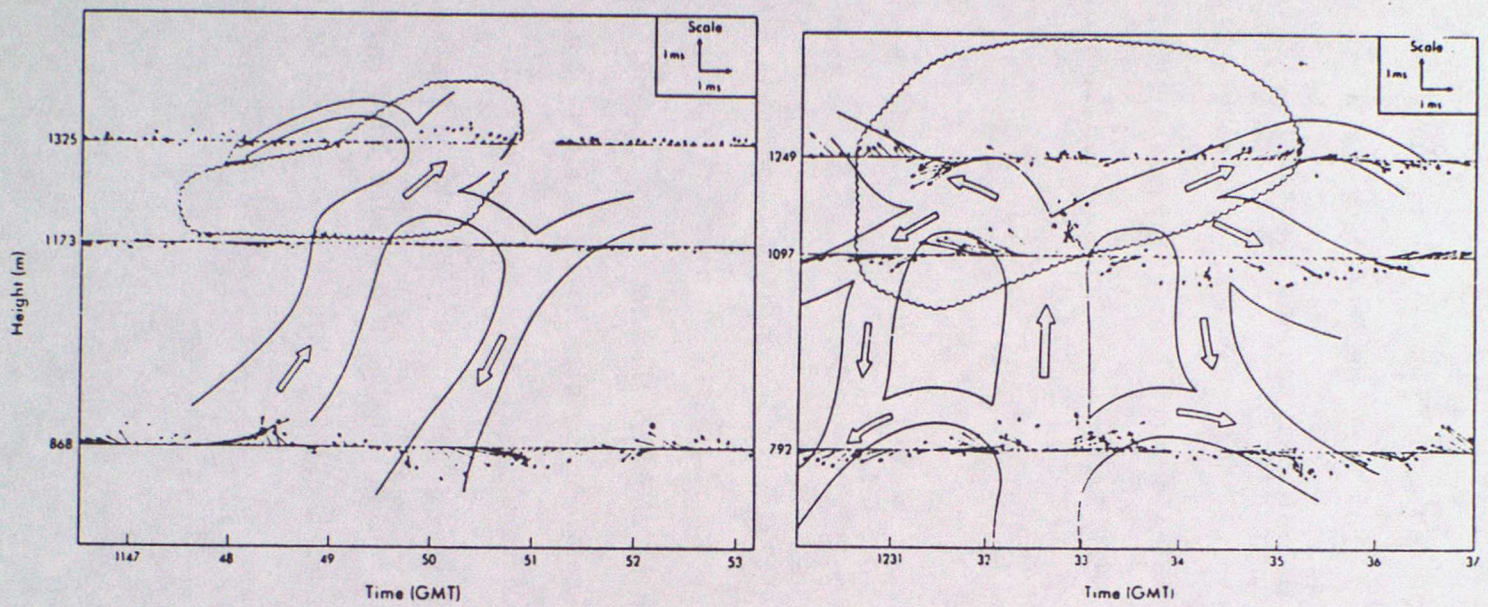

Figure 1.15. Gust vectors (5 s) and suggested flow patterns in a vertical plane obtained from balloon borne sensors in the vicinity of two small cumulus clouds. The cloud boundaries are shown schematically.

base to determine whether air may be recirculated through the cloud. Such recycling may be important for the growth of large drops if any remain in the subsaturated downdraughts.

The aircraft traverses reported by Knight (1987) and described earlier suggested that in many cases a narrow layer of subsiding air surrounded the growing cumulus clouds. This air was warm and had low total water content suggesting origins at higher level. The observation is consistent with the motion of liquid plumes although the observations of plumes with rising cores and subsiding edges were made in liquids with no internal buoyancy source.

Although some of Knight's results suggest that the subsiding air is confined to the clear air surrounding the clouds other observations suggest that the downward moving air extends into the cloud. Indeed Knight's observations in more vigorous clouds also suggest that the strongest subsidence is within the region of non-zero liquid water content. Data presented in Figure 1.16 which shows three dimensional gust vectors at mid-level in a 1.5 km deep cloud clearly show descent regions which are within the cloud. The conditions under which the descending region contains no liquid water are not known but it is possible that this depends on the humidity at cloud top level and the size of the droplets which determine the rapidity with which the drops will evaporate if they should be entrained into this subsiding region.

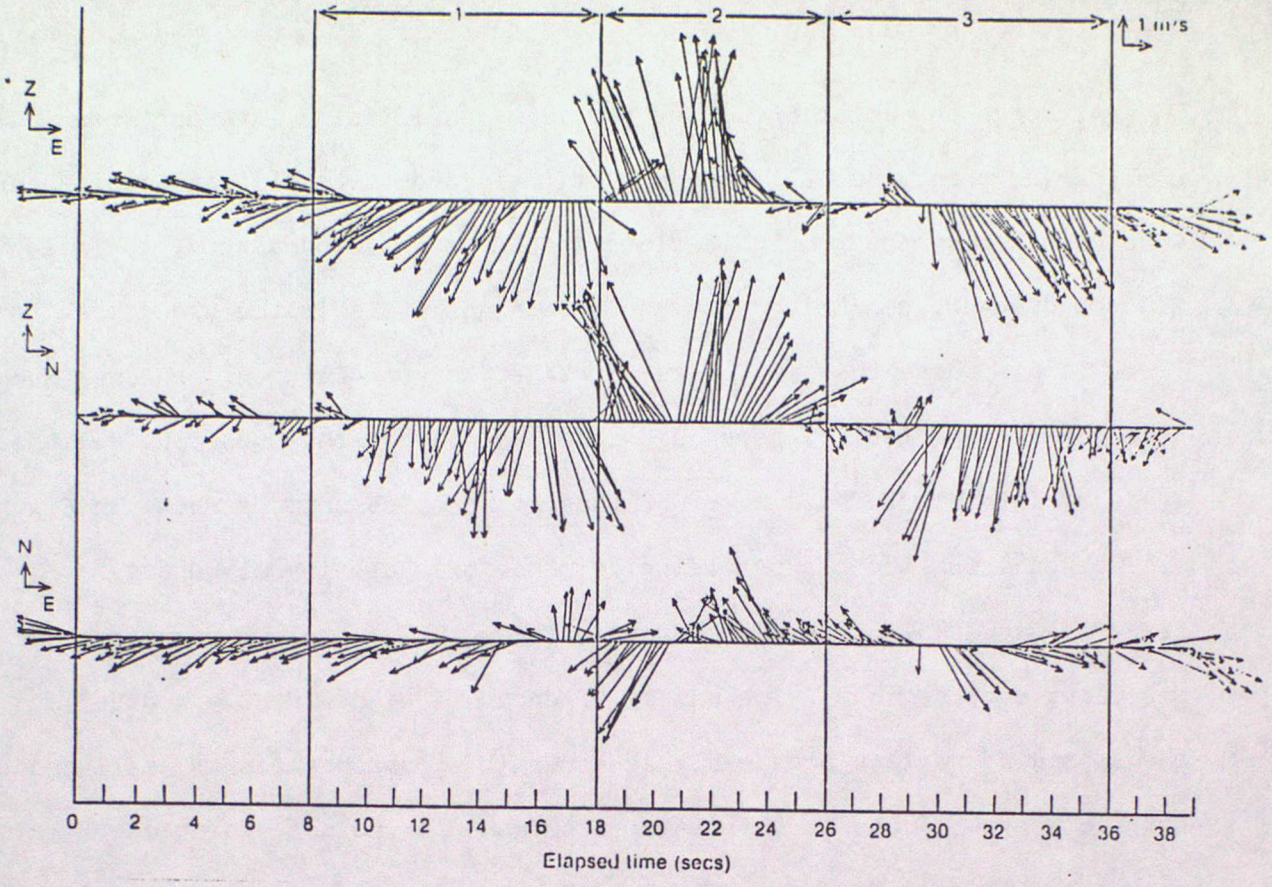

Figure 1.16. Fluctuations of velocity components about the mean wind at mid-level in a vigorous cumulus cloud. Regions 1, 2 and 3 are in cloud.

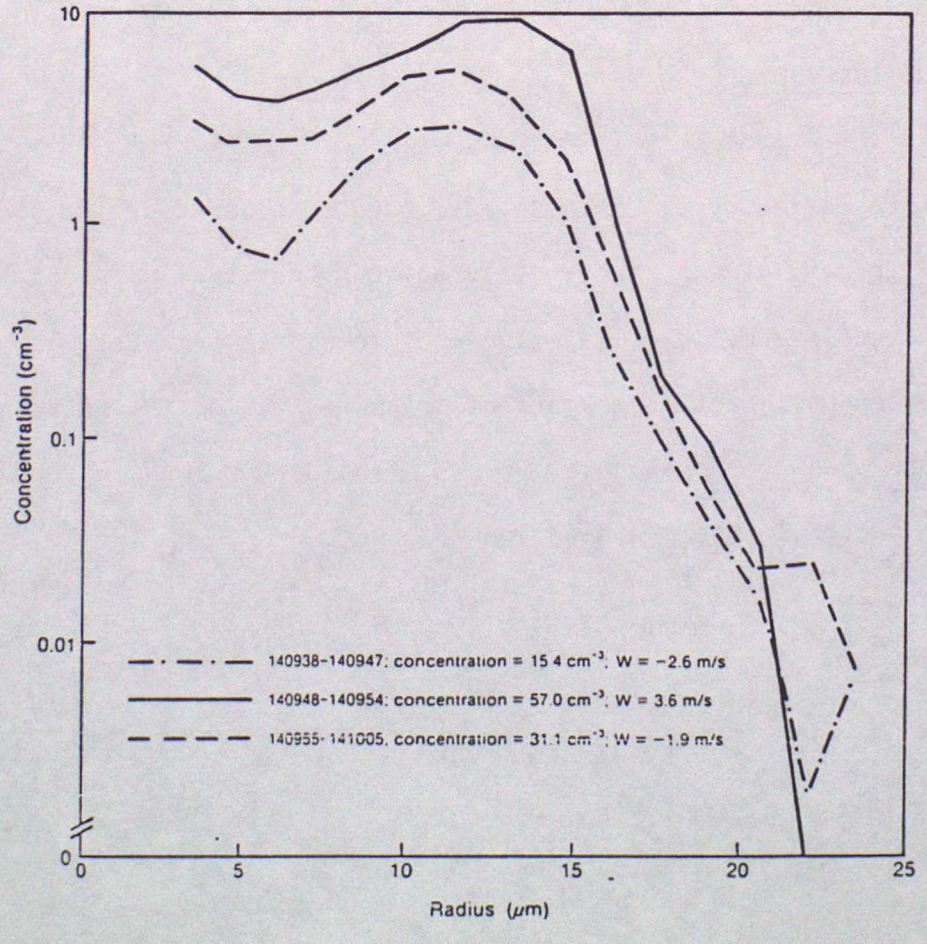

Figure 1.17. Average droplet spectra for each of the region 1, 2 and 3 shown in Figure 1.16.

Although the location of the subsiding shell is of interest when considering the dynamical structure of the cloud it is also of importance when considering the growth of cloud drops. Such downdraughts, as indeed any downdraught, can bring droplets from high levels in the cloud back to lower levels where they may be re-entrained to grow further. Whether such a mechanism is effective depends on the humidity in the subsiding regions. It is of interest to note however, that the droplet spectra shown in Figure 1.17 taken along the run providing evidence of subsiding cloud edges (Figure 1.16) show clear differences between the central core and the subsiding edge regions. The number of drops is significantly reduced in the subsiding regions presumably as a result of evaporation of small drops, but the largest drops at this level are found in the descending air. This suggests that they may have been brought down from higher levels in the clouds but whether they survive to be re-entrained into the updraught core is not known.

1.6 CLOUD INTERACTIONS

In this review cumulus clouds have been considered as isolated systems. In many circumstances it is obvious that the individual clouds are organised in some way. Examples include clouds organised as lines, where they probably act as tracers of organised motion in the sub-cloud layer or as open or closed cells where latent heat release may be an important factor in the organisation.

Although clouds may be initiated by essentially random processes, either humidity or temperature fluctuations, or by some organised convergence and ascent, when they become sufficiently large some degree of interaction is possible. The mechanism for such an interaction is not well established but attempts are being made to clarify the problem using numerical models of the development of cloud fields. Unfortunately the present computing resources are adequate only to consider evolution in one horizontal dimension unless models with a coarse resolution are used. It is generally found that when an unstable but uniformly stratified atmosphere is subject to random perturbations a number of small clouds develop. As the clouds grow, some are suppressed and those remaining increase in depth and horizontal extent.

Hill (1974) showed (using a relatively simple numerical model) that the predicted evolution of individual clouds reproduced reasonably well the observed rate of cloud development on a particular occasion when an observed sounding was used. The evolution of the modelled cloud field (Figure 1.18) shows the suppression of some of the smaller clouds as the larger ones develop. It appears from these results that the interactions between the circulations in the sub-cloud layer leads to the initial suppression of some clouds rather than to an interaction at cloud level which occurs later.

More detailed studies of the mechanism of cloud interaction have been reported by Clark et al (1986) again using a two dimensional numerical model. As was observed by Kitchen and Caughey (1981) the clouds appear to have little effect on the eddy structure in the boundary layer. However

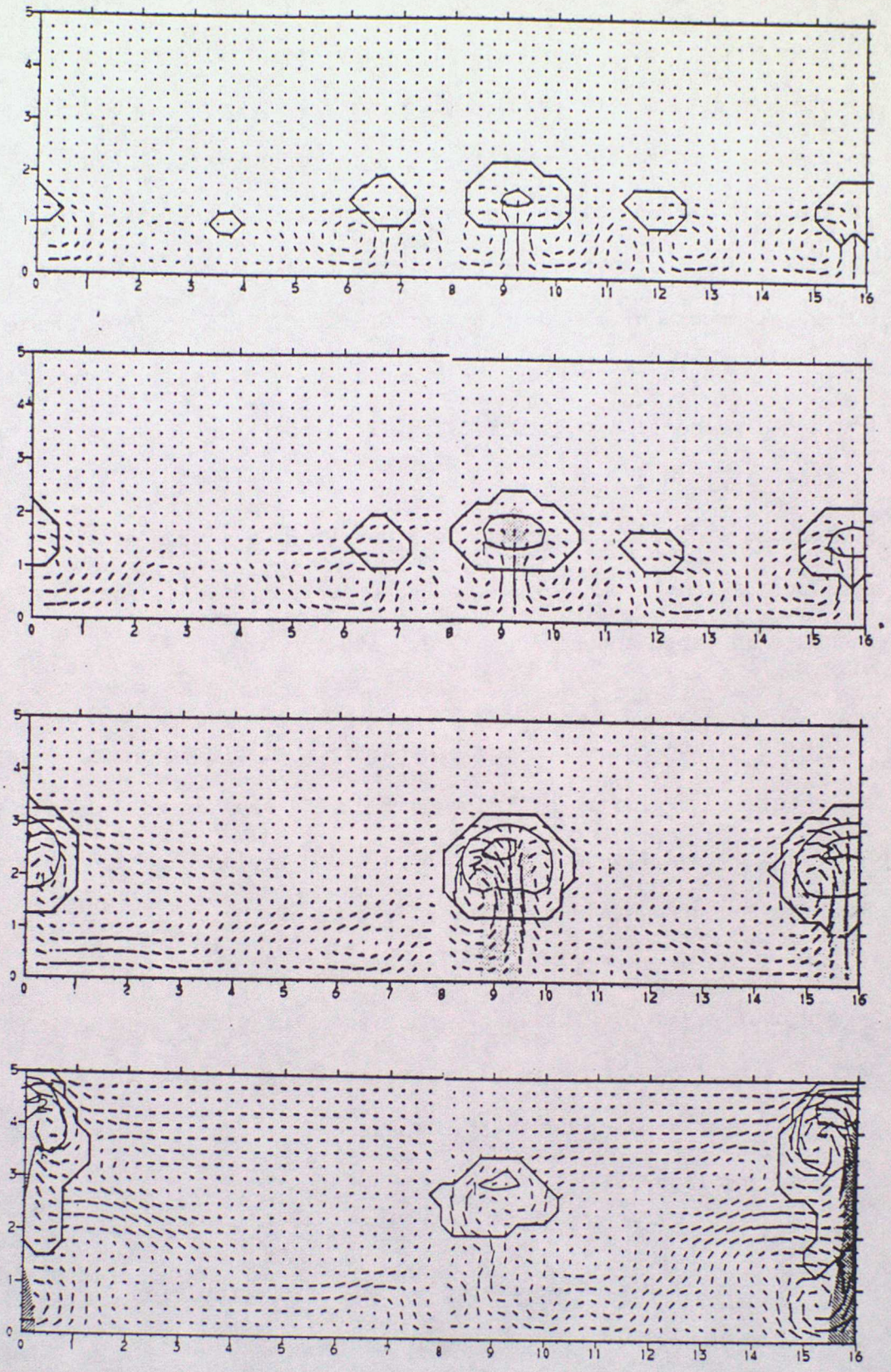

Figure 1.16. Simulations using a 2-d model, of development of a field of cumulus clouds at 180, 186, 201 and 213 min from model initiation. Axes are km vertically and horizontally. Contours of liquid water content are at 1 g kg^{-1} intervals and precipitation is stippled.

the clouds were themselves strongly influenced by interactions between gravity waves excited by thermal forcing and by the clouds acting as obstacles to the flow Cumulus clouds tended to develop on the upshear side of developed clouds. This is believed to be due to an interaction between the excited gravity waves and the convection such that the relative phase velocity between the gravity waves and the clouds plays a crucial role in determing the cloud growth. The results suggest that the dynamical structure of the atmosphere well beyond the cloud boundary is important in determining how cumulus clouds grow and interact. In particular even the structure above cloud top is important since this influences gravity wave propagation.

1.7 CONCLUSIONS

The observations described above enable a general picture of the structure of cumulus clouds to be drawn. A typical cumulus cloud consists of a generally rising region of air which is saturated and warmed by latent heat of condensation. As the parcel rises it may entrain air at its upper surface but in more vigorous clouds such entrainment is rather restricted to the regions close to the edge of the cloud where the updraught is weaker. However in a more mature cloud instability at the top surface can lead to the formation of penetrative downdraughts which extend downwards through the cloud almost to cloud base and play a role in causing the cloud to dissipate. Some entrainment may take place through the edges of the cloud particularly on the downwind edge but this is generally small compared with cloud top entrainment.

The flow of air in the vicinity of the clouds is influenced by their presence, and in turn influences cloud structure. The updraughts and downdraughts are tilted in the presence of a shear. Flow around the cloud gives rise to a wake which enhances lateral entrainment on the downwind side of the cloud. Factors influencing the development of the clouds have received rather little attention but it is apparent that fields of clouds develop rather differently from isolated clouds.

The effects of cloud structure on the droplet spectra has not been considered in detail in this review but several areas of interaction are apparent. The reduction of the cloud water content by mixing will reduce the average growth of droplets unless the numbers are significantly reduced from those expected in an adiabatic parcel. Locally however the downdraughts may reduce droplet concentrations and subsequent ascent of the entrained air could lead to enhanced droplet growth. Paluch and Knight (1986) have however cast some doubt on the generality of such a mechanism. Another possible cause of enhanced droplet growth is the recycling of drops in saturated or almost saturated downdraughts which leads to an extended growth time for the drops.

Some outstanding problems remain however and it is clear that all clouds cannot be described using the above simply model. Areas which merit further study include:

i. The preferred scale for the initial cloud development and its relation to boundary layer structure.

ii. The scale of instability leading to cloud top entrainment.

iii. The degree to which cumulus clouds are vertically mixed and the factors affecting this.

iv. The importance of lateral entrainment especially in the early stages of cloud development.

v. The extent of the wake behind clouds and its vertical structure.

vi. The manner in which the spacing, height and width of clouds is determined.

These problems can only be tackled by a considerable programme of observations. For these, aircraft in situ measurements will be helpful but some of the problems can only be solved using multi-level balloon borne instruments or remote sensing techniques such as millimetric radar. Modelling studies are also necessary but in view of the importance of the turbulent motions on scales of about 10 m such work requires high resolution models. Since the flow around the cloud appears to be important in determining the regions of entrainment and since the atmospheric wind direction is seldom constant with height such models should eventually provide a three dimensional description of cloud development. It seems likely however, that detailed microphysical representation is not required in such dynamical models.

It is only when the structure of the clouds is better understood that it will be possible to evaluate the various theories concerning the growth of droplets in cumulus clouds. Models of the growth of droplets require specification of quantities such as the local supersaturation which, although small in comparison with the water content is crucial to the problem of the activation of condensation nuclei and hence to the growth of a population of droplets. Again the scales of turbulence within the cloud are such that evaporation time scales for droplets and mixing time scales become comparable. Clearly the models of uniformly mixed entraining thermals contained many simplications but in view of the complexity of the structure of cumulus it is not yet possible to develop a model which is both dynamically consistent and which can be used to analyse cloud droplet growth.

1.8 REFERENCES

Clark, T.L.; Hauf, T. and Kuettner, J.P. 1986 Convectively forced internal gravity waves: Results from two-dimensional numerical experiments. Q.J. Meteorol. Soc., 112, 899-925.

Deardorff, J.W. 1980 Cloud top entrainment instability. J. Atmos. Sci., 37, 131-147.

Hill, G.E. 1974 Factors controlling the size and spacing of cumulus clouds as revealed by numerical experiments. J. Atmos. Sci., 31, 646-673.

Jonas, P.R. and Mason, B.J. 1982 Entrainment and the droplet spectrum in cumulus clouds. Q. J. Meteorol. Soc., 108, 857-869.

Kitchen, M. and Caughey, S.G. 1981 Tethered balloon observations of the structure of small cumulus clouds. Q.J. Meteorol. Soc., 107, 853-874.

Knight, K.A. 1987 The structure and development of small cumulus. Submitted to Q.J. Meteorol. Soc.

Mason, B.J. and Jonas, P.R. 1974 The evolution of droplet spectra and large droplets by condensation in cumulus clouds. Q.J. Meteorol. Soc., 100, 23-38.

Paluch, I.R. 1979 The entrainment mechanism in Colorado cumuli. J. Atmos. Sci., 36, 2467-2478.

Paluch, I.R. and Knight, C.A. 1986 Does mixing promote cloud droplet growth? J. Atmos. Sci., 43, 1994-1998.

Randall, D.A. 1980 Entrainment into a stratocumulus layer with distributed radiative cooling. J. Atmos. Sci., 37, 198-159.

Squires, P. 1958a The spatial variation of liquid water and droplet concentration in cumuli. Tellus, 10, 372-380.

Squires, P. 1958b Penetrative downdraughts in cumuli. Tellus, 10, 381-389.

2. ELECTRIFICATION AND LIGHTNING

2.1 INTRODUCTION

Thunderstorms are electrostatic generators that produce positive and negative electrical charges; the positive charge becoming concentrated in one region of a cloud and the negative charge becoming concentrated in another. As physical separation of the charges of different polarity proceeds, the electric field and potential difference between the charge regions (or between one of them and the earth or ionosphere) increases until a lightning flash is initiated. At least part of the separated charge is neutralised by the discharge but the field builds up again and the sequence of events is repeated.

A satisfactory theory of charge separation must explain quantitatively how charge is generated, and separated at a sufficient rate to account for its dissipation in lightning flashes. It must account for the observed distribution of positive and negative charges and the observed changes of electric field produced by the discharges. The theory must also be consistent with the size and life cycle of the storm and its microphysical properties, represented typically by the scale, intensity and duration of the precipitation that accompany it.

2.2 OBSERVATIONS OF THUNDERSTORMS

2.2.1 General properties

Exploration by aircraft and radar reveals that thunderstorms generally consist of one or more 'cells' with strong vertical motions. Each cell grows, reaches maturity and decays. The growth stage lasts for about 10-25 minutes, is characterised by updraughts of about 10 m s^{-1}, and the initiation of precipitation in the form of rain or hail in the middle troposphere. The onset of the mature stage coincides with the spread of precipitation towards the ground and the appearance of updraughts and downdraughts in the lower part of the cell. The mature stage lasts about 30 minutes.

The cell may be about 1 km across when first detected by radar, but it usually develops rapidly up towards the -20°C isotherm and beyond, and extends to several kilometres in all directions. A feature some 10 km high and 8 km across results. The base of the thunderstorm is almost invariably warmer than 0°C, and the cloud top is often cooler than -40°C. It is to be expected therefore that the cloud and precipitation contains both ice and liquid water forms. Lightning activity occurs predominantly during the mature phase. Thus any theory must be capable of explaining the generation and separation of the charge sufficient to supply the first lightning stroke within about 10 to 20 minutes of

the appearance of precipitation particles of radar detectable size. This activity should be capable of being sustained for up to 30 minutes.

2.2.2 Charge distribution

The distribution of charge inside a thundercloud can be deduced from the variation of electric field at the ground caused by lightning flashes, as a function of distance from the storm. Early observations showed that there was a positively charged upper region and negative charge lower down. The existence of a pocket of positive charge in the base of some thunderclouds has been inferred from balloon borne measurements of electric field. More recent measurements confirm this general picture shown in Figure 2.1 as well as providing additional insight.

Typical multistation measurements of the electric field change induced by lightning in New Mexico storms are shown in Figure 2.2. The equivalent charge centres neutralised by the ground flash have been located from such data (Figure 2.3). The field changes are found to be reasonably consistent with the lowering to ground of a localised, spherically symmetrical negative charge. The centres of charge lowered to ground originate over large horizontal distances within the cloud (up to 8 km) at more or less constant height between the -9°C and the -17°C clear- air-temperature isotherms. Comparison

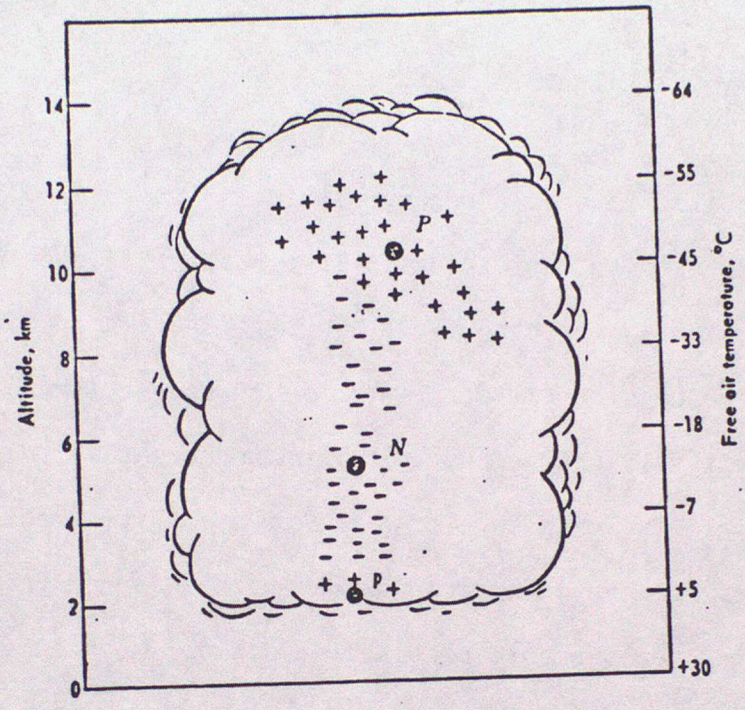

Figure 2.1. Schematic diagram of the charge distribution in sub-tropical storms.

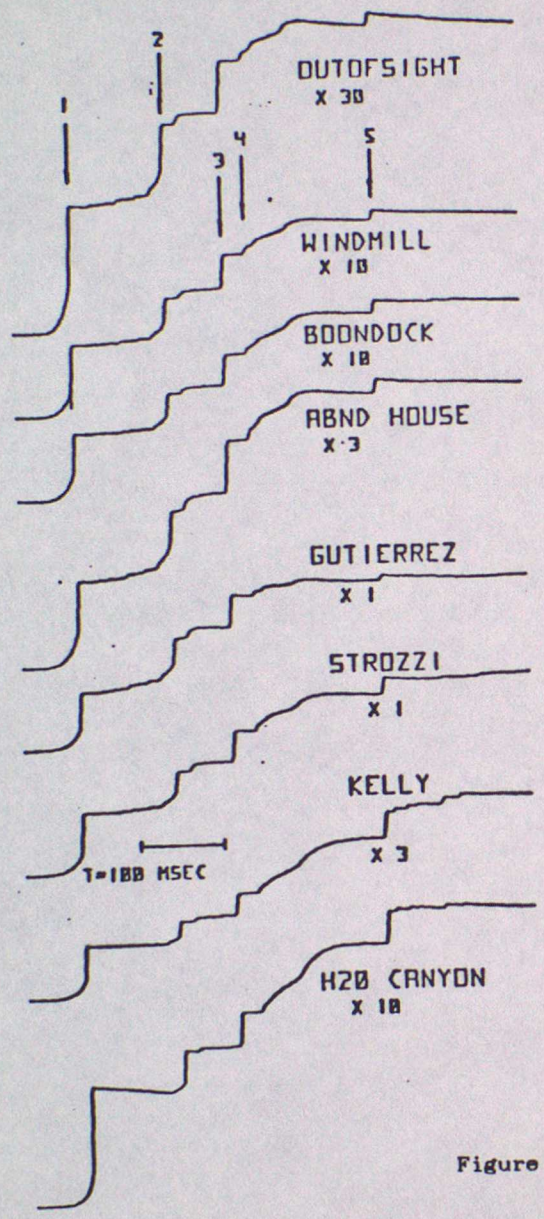

Figure 2.2. The electric field changes at several sites during a single lightning flash.

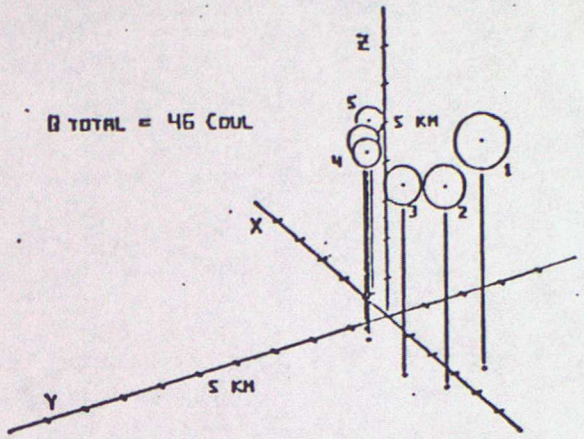

Figure 2.3. The infered charge distributions giving rise to individual strokes in the lightning flash of Figure 2.2. Circles denote the size of spherical charged regions neutralised during the strokes assuming a charge density of 20 C km^{-3}.

with 3 cm radar measurements of precipitation structure, shows that the discharge develops through a full horizontal extent of the region within the storm and appear to be bounded within its extent. In one instance where cellular structure of the storm was apparent, the lightning strokes selectively discharged regions where the precipitation echo was strongest. The vertical extent of the charge locations is, in contrast, small in comparison with the vertical extent of the storm.

The observations suggest that the negative charge centres are located within a supercooled region of relatively small vertical dimension. They show also that the negative charge lies within a relatively limited height range between the -10 and -25°C isotherms, and coincides predominantly with precipitation at these levels. Figure 2.4 shows a striking results from studies in Florida, New Mexico and Japan - where convective winter storms were investigated - that the temperatures at which the negative charge centres are located are similar in all three, even though the cloud bases are at very different pressure levels.

2.2.3 Charge separation

Bennetts et al (1980) reported measurements of electric field in aircraft traverses of convective cloud. The clouds, although electrically active, did not produce lightning. The data suggest that significant charge generation does not occur

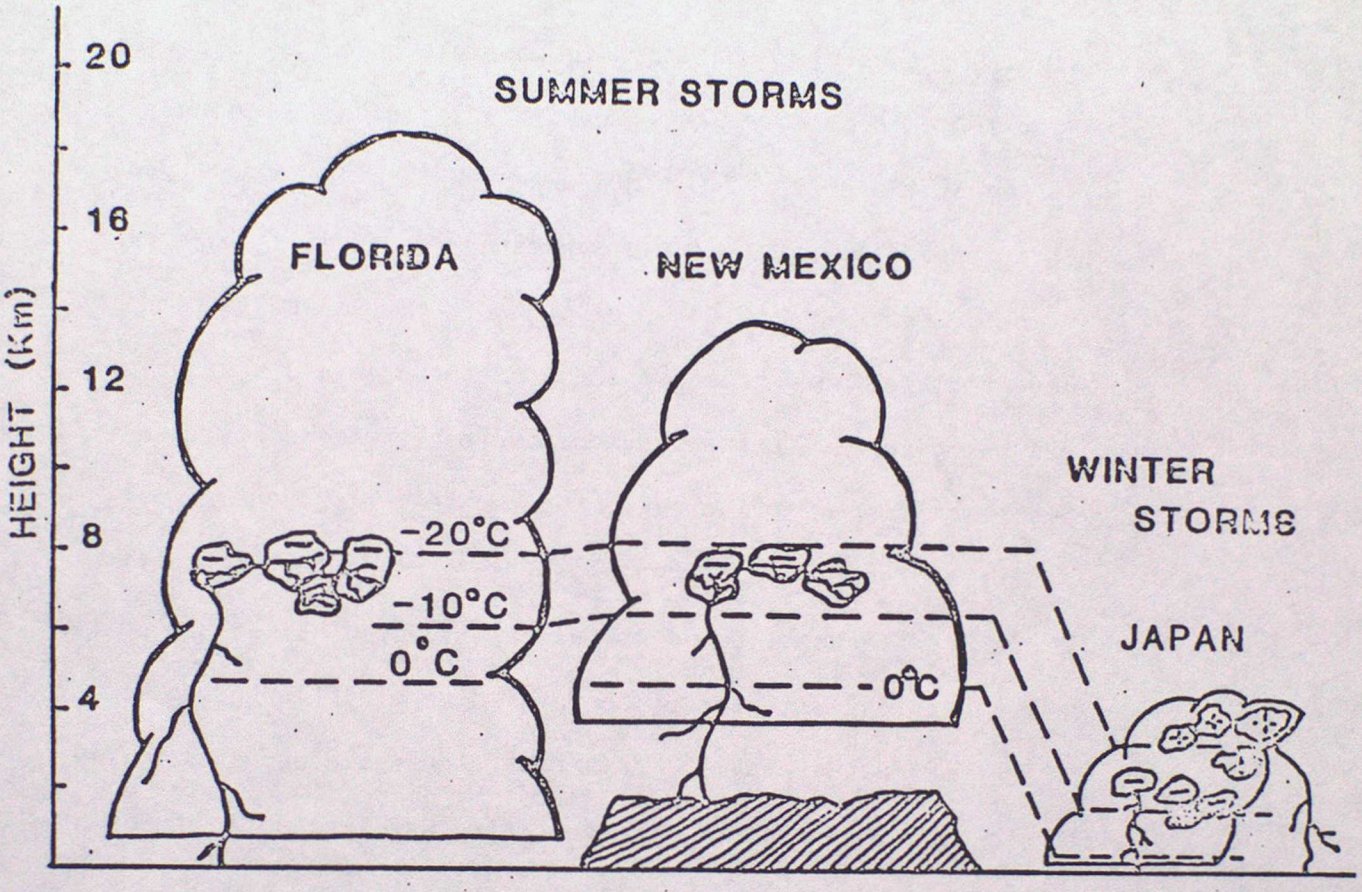

Figure 2.4. Schematic diagram of the level and distribution of charge centres for flashes to ground in storms at different locations and seasons.

before the ice phase is present within the cloud. However between two successive traverses through cloud, made in snow at about -8°C some 4 minutes apart, fields of both signs increased by a factor of 4 to about 3 kV m^{-1} suggesting that significant charge separation is possible once ice is present. Figure 2.5 is a composite of electric field data obtained during 14 traverses of a cloud which reached the -26°C level. It is probable that features separated 'vertically' by more than 100 mb or so reflect evolution of the charge distribution nevertheless, some gross features of the charge distribution can be inferred. Between successive penetrations just above and below the -12°C isotherm, the vertical field changes sign on the southern side of the cloud, suggesting that a positive charge centre was located at this altitude. The measurements are consistent with the presence of a more diffuse negative charge below this region, but no substantial accumulations are indicated. The positive charge centre was located in a region bounded above by almost total glaciation in the form of ice crystals and below by a mixture of snow and hail. It is suggested that the circulation of the cloud, which probably generated at least two interacting cells during its lifetime of more than one hour, was insufficient to separate charge and maintain regions of net charge within the cloud volume. If negative charge resides on precipitation much of it probably fell out of the cloud in the cloud lifetime. Nevertheless charge was being generated in the region of interaction

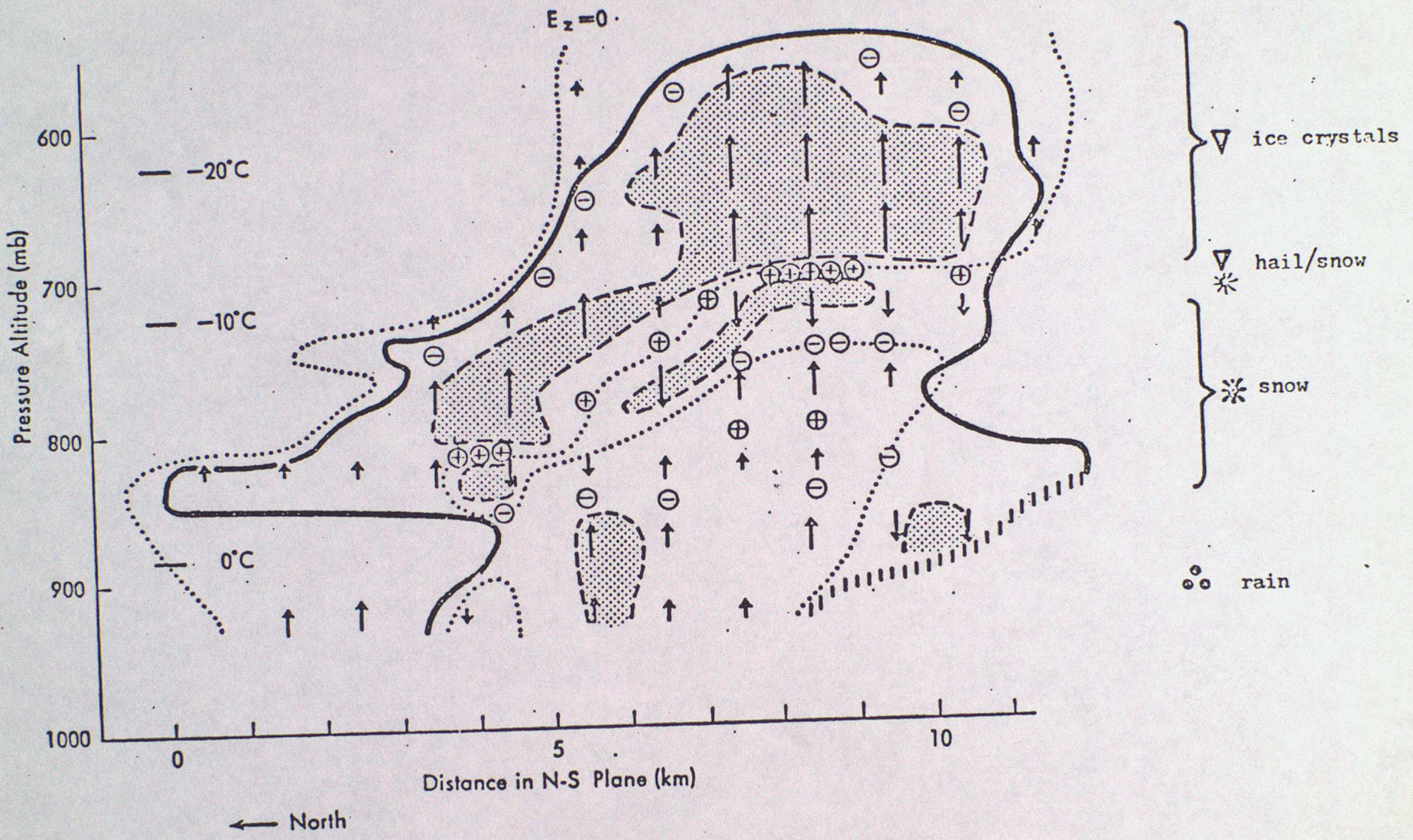

Figure 2.5. Distribution of the vertical component of electric field in a cumulonimbus derived from aircraft measurements. No lightning was observed. Arrows show the sense and magnitude of the field, areas with

between precipitation size particles and ice crystals; the very strong fields in the upper region of the cloud are consistent with positive charges on the latter.

Krehbiel et al (1980) found that in one storm system for which Doppler derived wind field and radar reflectivity data had been obtained, the onset of lightning activity in one of the storm cells followed the development of intense precipitation above the 0°C level and coincided with a rapid increase in the speed of the updraught (25 m s^{-1}) carrying this precipitation. Discharges tended to originate above the region of strongest radar reflectivity and in the region of maximum updraught (Figure 2.6).

From aircraft and ground based studies of thunderstorms it has been concluded that substantial charge densities (5 nC m^{-3}) are carried on precipitation elements. Charged hydrometeors are present over horizontal distances of several kilometres in the vicinity of the freezing level. The charges on individual elements are mainly, but not exclusively, negative. No relationship is discernible between the size of particles and the charges carried. Lightning activity within a cell is associated with upward motion of precipitation, and is sometimes evident where the precipitation rates do not exceed a few millimetres per hour.

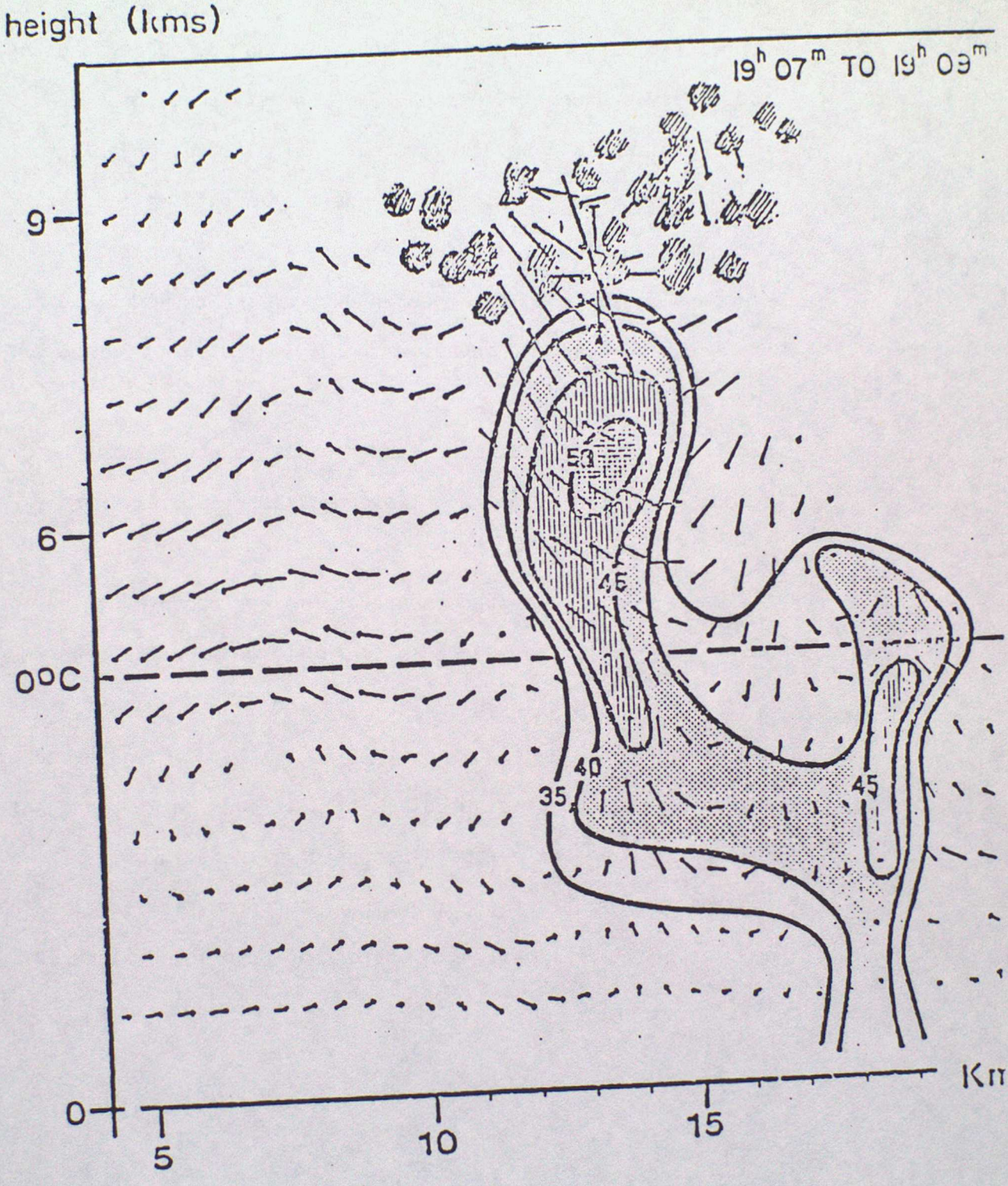

Figure 2.6. Contours of radar reflectivity (dBZ) and the doppler wind field in an electrically active cloud. Radiation sources for observed discharges near this time are hatched.

The facts that the lightning discharges are strongly correlated with precipitation and that the source regions are found between about -5°C and -25°C suggests that ice precipitation is a pre-requisite for significant charging rates. Observations made in thunderstorms capping the Zugspitze in Germany, indicate that solid precipitation elements dominate in the greater part of the thundercloud and are present on 93% of occasions. Snow pellets and pellets of soft hail are the most frequent form of hydrometeor, being present on 75% of occasions, and are always accompanied by strong electric fields, but large hail is relatively rare.

The maximum fields around thunderstorms are observed to be about 4 kV cm^{-1}, the charge is typically 40 C or more and some 5 to 10 C is discharged in lightning strokes. The charge density must therefore be about 10 to 20 nC m^{-3}. The evidence suggests the importance of small hail in carrying the charges that constitute the negative centre of a thunderstorm. It appears likely that the primary charging processes involve the collision of small hail with either supercooled droplets or ice crystals.

2.3 CHARGE SEPARATION MECHANISMS

2.3.1 Ion capture

Wilson (1956) pointed out that an electrically polarised hydrometeor falling through a cloud of ions or small cloud droplets could, by a process of selective ion capture, acquire a net charge. In a field acting to move positive ions downwards, a hail pellet becomes polarised with a net negative charge on the lower surface; negative ions are attracted to it, while positive ions are repelled. The rear surface has an equal positive polarisation charge of course, but if the terminal velocity of the pellet exceeds the drift velocity of the positive ions, then the latter are not captured. Thus the precipitation particle acquires a net negative charge (see Figure 2.7). The fundamental requirement is that $V>K+E$ where V is the terminal velocity, K_+ is the positive ion mobility and E the electric field. V rarely exceeds 8 m s^{-1} for hydrometeors other than large hail, and for unattached ions K ~ 1.5 cm^2 s^{-1} V^{-1}. Thus the maximum field which can result from this process is ~ 0.5 kV cm^{-1}. Larger fields are possible in principle, through the capture of slow ions or charged cloud drops but this is seldom a significant effect. Secondary sources of ions can be invoked but in general these tend to be productive only in the late stages of electric field growth.

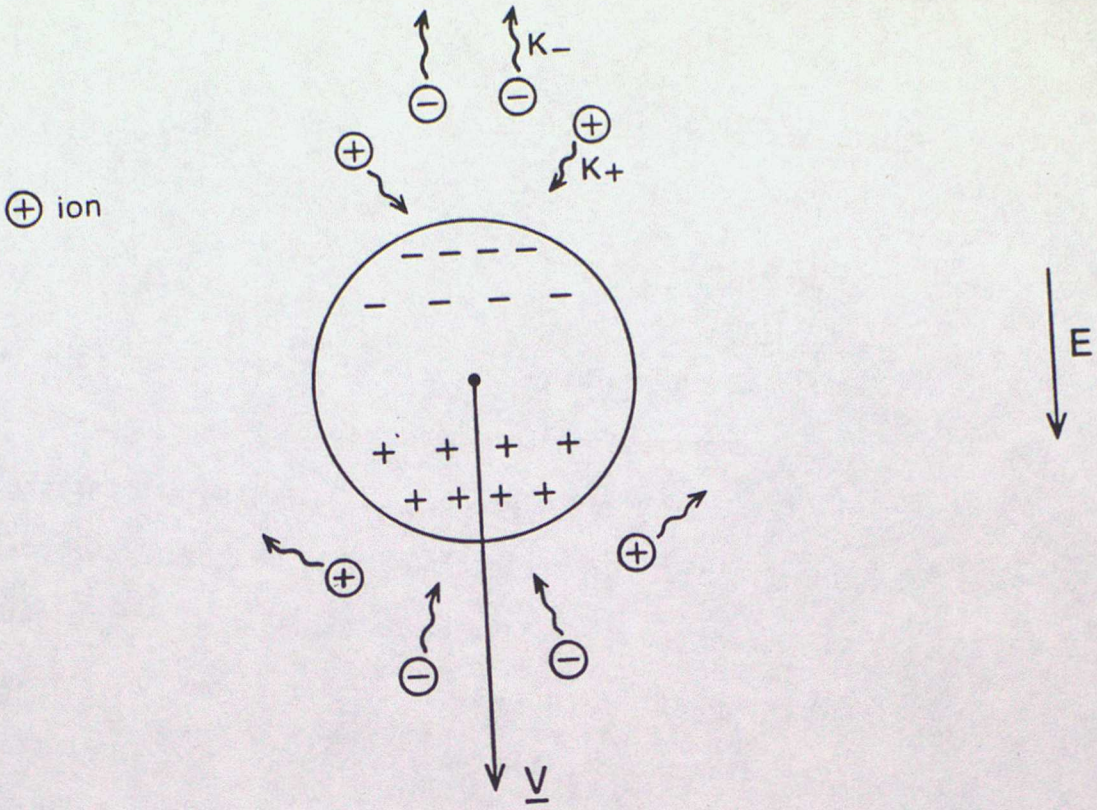

Figure 2.7. Diagram showing the Wilson ion capture theory of charge separation. Negative ion mobility is greater than that of the positive ions.

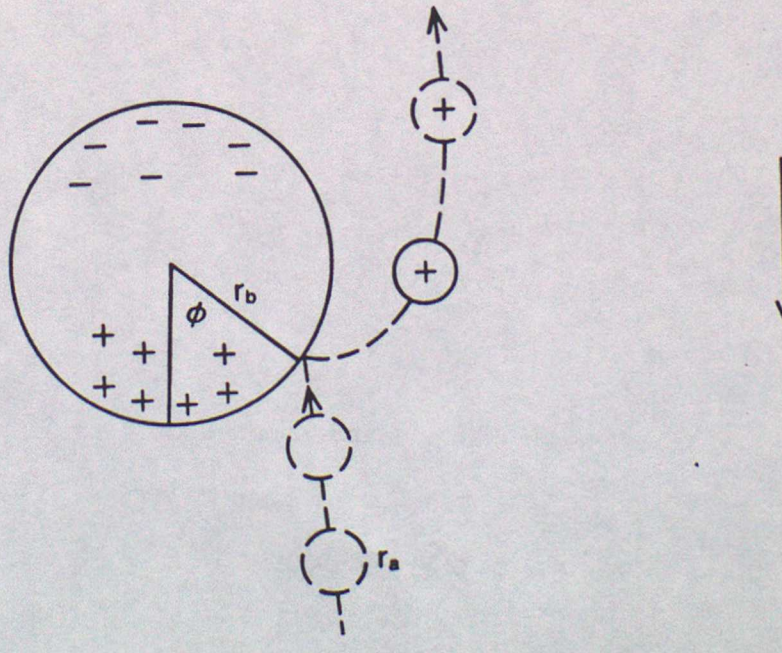

Figure 2.8. Diagram showing the inductive mechanism of charge separation. Particles of radius r_a bounce off the larger particle of radius r_b.

2.3.2 Inductive mechanisms

The inductive theory of precipitation charging in which a cloud particle (radius, r_a) collides with the underside of a larger precipitation particle (radius, r_b) polarised in an electric field, and separates charge of magnitude proportional to the field strength (E), is an attractive one because of the inherent positive feedback between charge separation and field strength. This contrasts with ion capture which is self limiting. The mechanism shown in Figure 2.8 has received considerable attention from modellers who have concluded that, in principle, water-water, water-ice as well as ice-ice collisions may separate charge at a sufficient rate to explain the observed field growth.

The charge transfer (q) per bouncing interaction, if the large particle has charge Q_B is:

$$q = \frac{\pi^2}{6} \left(\frac{r_a}{r_b}\right)^2 [12 \pi \varepsilon_o r_b^2 E \cos \phi + Q_B] [1 - \exp (t/\tau)] \quad (2.1)$$

where τ is the contact time and ϕ is the angle between the direction of the field and the radius to the point of contact. The maximum achievable charge on the precipitation element is:

$$Q_{MAX} = - 12 \pi \varepsilon_o E r_b^2 \cos \phi \quad (2.2)$$

Water droplet-raindrop collision experiments show that separation only occurs when the trajectory of the centre of the droplet passes the drop, otherwise they coalesce. The effective value of cos ϕ allowing bouncing is very small. Furthermore, experiments suggest that all collisions result in permanent coalescence for $E > 0.25$ kV cm^{-1}.

Aufdermauer and Johnson (1972) showed that a small fraction (~ 0.1%) of supercooled droplets, colliding with a hailstone in the presence of an electric field, separate after a collision and transfer charge in accordance with the expression above. They suggested that these are likely to be glancing collisions, so again cos ϕ is likely to be small. In view of the high concentration of droplets and the fact that for spherical hail pellets the aerodynamic and electrical 'equators' may be significantly different, it is not possible to discard the mechanism for ice-water inductive mechanism out of hand.

Although separation nearly always occurs following ice-ice collisions, leading to an average cos $\phi = {}^{2}/_{3}$, it is not obvious that the charges can flow through the ice during the available time of contact. Hertizan theory for a collision between a 100 μm ice crystal and a hailstone results in a contact time of ~0.3 μs. The bulk resistivity of ice predicts

a relaxation time of 10 ms and possibly a tenth of this if surface conductivity dominates. Practical evidence supports these ideas.

Rawlins (1982) carried out numerical modelling experiments testing the sensitivity of the inductive process to a number of microphysical assumptions, in a three dimensional model of cumulonimbus. He found that the electric field can reach breakdown threshold within half an hour of the appearance of precipitation, providing that multiple collisions between ice crystals and hail pellets are neglected; these latter act to discharge earlier charge separation events. As it was found necessary to maximise the charging rate by invoking large numbers of small hail particles and ice crystals, this assumption may be questionable. The importance of the various inductive processes has therefore not been demonstrated unambiguously.

2.3.3 Charging during wet hail growth

As water freezes on the surface of a hail stone, large potential differences may develop across the ice-water interface, as a result of the selective incorporation of ions of one sign into the ice lattice. The sign and magnitude of the effect depends on the concentration of the ionic species. In most cases this generates negatively charged ice, so that rapidly growing hailstones, being able to freeze only a

fraction of the impinging cloud water, acquire a liquid coat which is shed in the form of small positively charged drops as shown in Figure 2.9. A similar result is expected to follow from splashing collisions, between hail and large drops.

The requirement of large hail, the low probability of splashing events and sensitivity to trace solutes make this an unlikely candidate for a universal charging mechanism. The effect may be swamped by inductive charging when the ambient field exceeds about 1 V cm^{-1} since, because since in most splashing events water is shed from the rear surface, the inductive process is dissipative.

2.3.4 Temperature/gradient effect

Latham and Mason (1961) reported a process of charge separation associated with ice-splinter production during the growth of rime. The process depends on the fact that the concentrations of positive and negative ions in water increase quite rapidly with increasing temperature, and that the hydrogen ions diffuse more rapidly under a concentration gradient than the hydroxyl ions. Thus the cold end of a piece of ice acquires a greater fraction of positive ions (Figure 2.10a). It was suggested that a shell of ice would form around the outside of the supercooled drop soon after nucleation. It was conceived that the inside of the shell being at 0°C and the outside of some lower temperature, would

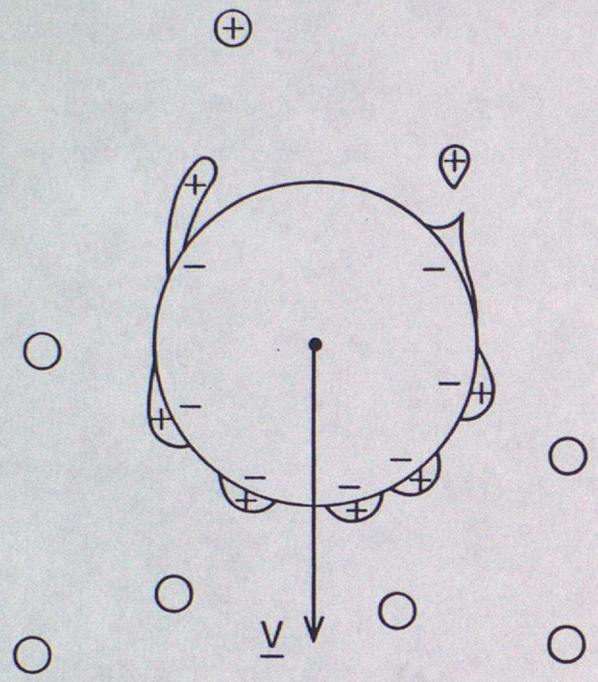

Figure 2.9. Diagram showing charge separation during the growth of wet hail and the shedding of drops from the wet surface layer.

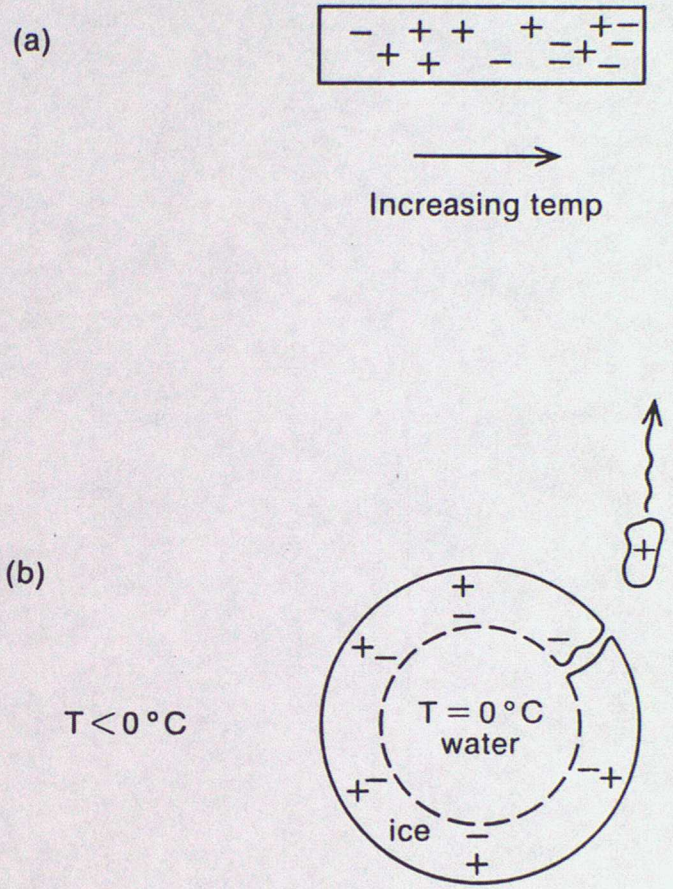

Figure 2.10. Diagram showing the temperature gradient mechanism for charge separation. (a) The charge distribution in an ice specimen subject to a temperature gradient. (b) Ejection of splinters during the symmetrical freezing of a drop in air below 0°C.

produce positively charged ice splinters as the shell thickened and fractured as freezing proceeded (Figure 2.10b). Unfortunately the mechanism requires unrealistically high rates of splintering to separate sufficient charge.

2.3.5 Charging due to rime growth

Results from laboratory experiments have been variable since the classical studies of Reynolds et al (1957) revealed large charging (hail pellet negative) when ice crystals and supercooled droplets coexisted in the cloud through which a hail pellet moved. It has been shown that, over a crystal diameter range of 10 to 300 μm, the charge transfer is roughly proportional to the square of the ice crystal diameter.

Laboratory studies suggest that charge carriers are actually present at the contact interface and do not flow along the surface thereby avoiding the time constant problems of the inductive theory. Such charge transfer is possible in collisions between particles having different surface work functions. Charge transfer takes place to establish the required contact potential. At present there is no time-dependent theory for this, but experiments confirm that charge transfer can take place. Calculations suggest that a charge transfer of about 10^{-14} - 10^{-13} C is required per collision to provide the necessary charging rate. As the capacitance of a 100 μm sphere close to plane surface is about

10^{-14} - 10^{-13} farad, the required difference in surface potential is between 0.1 and 1 volt. Such potential differences are believed to exist between evaporating and condensing drops or between rimed and non-rimed ice (see Figure 2.11). The potential differences are of the correct sign to produce negatively charge hail pellets when these are riming in a region colder than about -10°C and colliding with unrimed vapour grown crystals. Such a mechanism fits the observations described earlier very well qualitatively, but more work is necessary to confirm this quantitatively, and to elucidate the physics of charge transfer.

2.4 LIGHTNING

2.4.1 The lightning flash

The most common producer of lightning is cumulonimbus cloud. However lightning also occurs in snow storms, sand storms and in the clouds over erupting volcanos. Very little is known about the latter and almost all of the following discussion will be based upon discharges from cumulonimbus. Such lightning can take place entirely within a cloud, between two clouds, between a cloud and the earth or between the top of the cloud and the ionosphere.

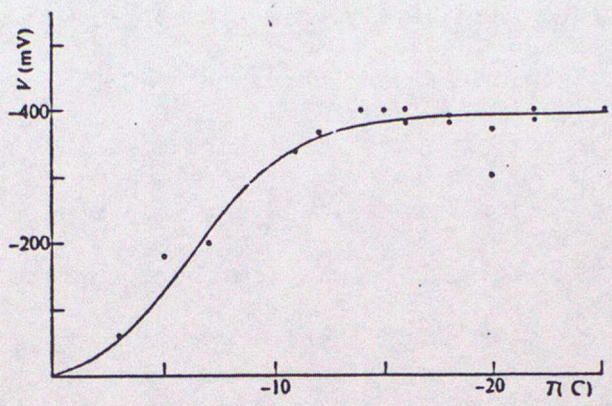

Figure 2.11. The surface potential of ice after riming as a function of temperature; potential is relative to an unrimed ice surface.

A cloud-to-ground lightning flash, which typically lasts about 0.5, is composed of several intermittent discharges called strokes, each of which has a duration of milliseconds. A stroke, in turn, is made up of a leader phase and return stroke phase. The leader initiates the return stroke by lowering the cloud charge (usually of negative sign) and cloud potential towards the earth. First or stepped leaders are heavily branched and carry charges of a few coulombs; dart leaders which precede subsequent strokes carry less charge and follow the main channels of previous strokes.

The negatively charged region of the thundercloud provides the negative charge which flows to ground in the cloud-to-ground flash. If it is assumed to be isolated and spherical with radius a then a lower limit can be estimated for a, by requiring that the maximum field (to be found at its boundary) is less than the breakdown field of the atmosphere. This varies inversely with pressure and is about 21 kV cm^{-1} at 3 km or 30 kV cm^{-1} at sea level. In practice, cloud lightning is initiated at a much lower threshold ~ 4 kV cm^{-1}. A typical value for the negative charge is -40 C so that since

$$a^2 \geq Q/4\,\pi\varepsilon_o\, E_{MAX} \qquad (2.3)$$

a must be greater than 1 km. It is evident that the lightning process must be able to drain charge in less than 1 s from a volume of about 4 km^3.

A similar analysis can be carried out, in a cylinderical volume, for the minimum leader radius a_l. If the leader is typically 5 km or so in length, its charge per unit length must be $\sim 10^{-3}$ C m^{-1} to contain the typical charge of 5C dissipated in each stroke. Assuming a maximum field of 30 kV cm^{-1},

$$a_l \geq \rho/2\pi\varepsilon_o E_{MAX}$$

then $a_l \geq 6$ m. The luminous radius is likely to be less than this as the existence of charge does not guarantee the emission of radiative energy.

The potential of an isolated sphere of radius 1 km and carrying a charge of 40 C is

$$V = \frac{Q}{4\pi\varepsilon_o a} \approx 3 \times 10^8 \text{ volts} \qquad (2.4)$$

The presence of the earth's surface reduces this but the order of magnitude of the potential difference between ground and charge is $\sim 10^8$ V. Thus the energy available for dissipation is $\sim 4 \times 10^9$ J. A single lightning stroke brings ~ 5 C to ground so if the channel is 5 km long the energy dissipated per metre is $\sim 10^5$ J m^{-1}. This is capable of vapourising some 40 g of water per metre in buildings, trees or people while in the atmosphere the energy is converted to dissociation,

ionisation, excition and kinetic energy of the channel particles, to the energy of expansion of the channel and to radiation.

2.4.2 Initiation of lightning

Since the breakdown field in dry air, at normal atmospheric pressure, in the absence of particles, is about 30 kV cm^{-1}, while the largest fields that have been recorded within thunderstorms are about 4 kV cm^{-1}, some initiating process must be invoked. In recent years it has become clear that the emission of corona from the extremities of hydrometres is a very likely candidate for this.

For a pointed electrode, the discharge process begins in a small volume near the tip, where the local electric field is high enough to permit ionisation of the gas molecules by any stray electrons. These latter must have been accelerated sufficiently by the electric field operating over their mean free path so that their kinetic energy exceeds the ionisation potential of the gas. Such activity releases further electrons at each subsequent collision. This process of cumulative ionisation is known as an electron avalanche, and is at the root of all forms of corona discharge. The threshold for corona reduces with reducing pressure as the mean free path increases.

The possibility that a positive corona is emitted from the surface of a raindrop, highly deformed by a strong electric fields, has been studied in considerable detail in the laboratory. It was shown that corona occurred from pointed regions of drops resulting from hydrodynamic instability under the influence of strong electric forces. The lower surface of the drops tended to be flattened by aerodynamic pressure and corona were initiated from the rear surface as shown in Figure 2.12. For uncharged drops of radii greater than 2 mm the critical onset was about 9.5 kV cm^{-1}. If the drops carried a high charge of the appropriate polarity the threshold corona field was reduced to about 5.5 kV cm^{-1} and somewhat lower if the field was inclined to the vertical. However, even under the most advantageous conditions, the corona fields were higher than the maximum fields observed in thunderstorms.

Griffiths and Latham (1974) have examined the possibility that ice hydrometeors may emit coronas. They demonstrated that corona currents of both signs can be initiated at low threshold fields from ice specimens in the form of needles and plates, prisms and artificial hailstones provided the temperature is warmer than a critical value, which is fixed by the electrical conductivity of the ice surface. This critical temperature is ~ -18°C for natural ice hydrometers (see Figure 2.13).

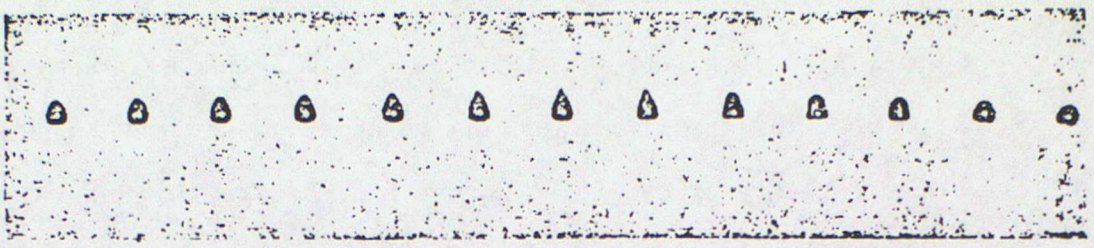

Figure 2.12. Instability of a 2 mm radius freely falling drop in a steadily increasing vertical electric field. Frames are 2.5 ms apart. The distortion and sudden collapse of the upper surface can be seen.

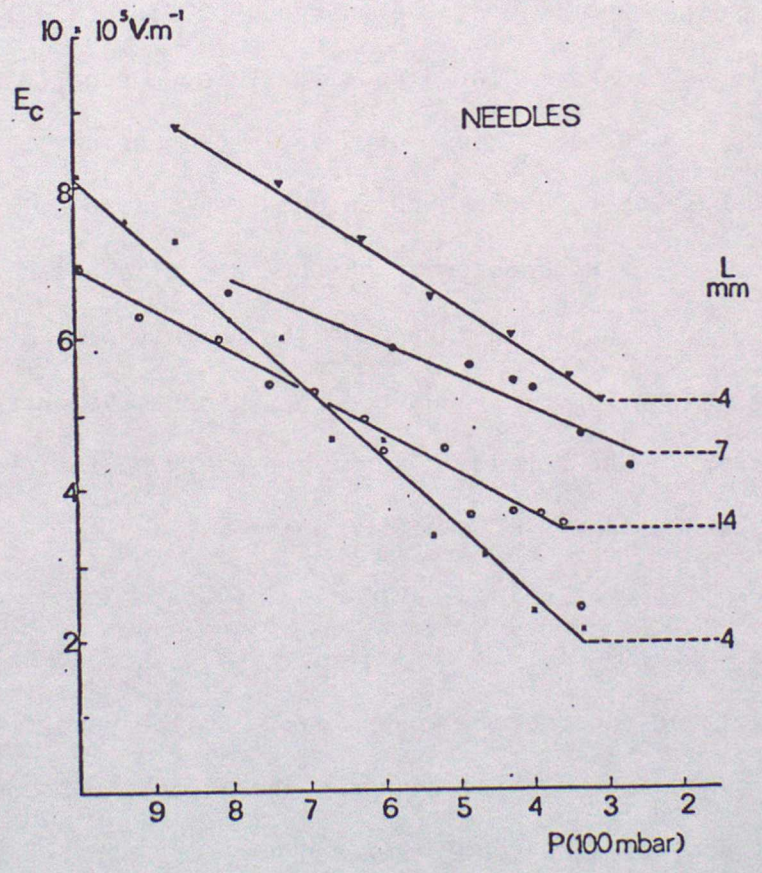

Figure 2.13. Measurements of the critical field for corona discharge from ice needles of length L at a temperature of 12°C.

Crabb and Latham (1974) studied the possibility that the collision of a pair of raindrops within a thundercloud may produce momentarily, a grossly deformed object whose shape is particularly conducive to corona onset. They found corona at fields as low as 2.5 kV cm^{-1} for glancing collisions. Such events are probably rather rare and transitory but the authors suggest that one such event per cubic metre per minute is likely in precipitation of about 20 mm hr^{-1}.

Given that a positive corona is likely to be produced on hydrometeors in the regions of strong field close to the dge of the negatively charged region (perhaps enhanced by the lower pocket of positive charge) how does this initiate the stepped leader? The direction of the corona is directed along the local field lines; upwards in the region between the charge centre and ground as shown in Figure 2.14. By comparison with observations of such discharges from power lines, it has been suggested that highly branched streamers expanding laterally and toward the negative charge centre result. The streamers adopt a broadly conical form. The net upward movement of positive charge effectively increases the negative charge in the vicinity of the original corona site effectively lowering negative charge. New corona streamers are then promoted at lower levels by the resulting field enhancement. In the process, charge from the upper broad end of a conical region is lowered and concentrated towards the earthward apex with consequent field enhancement there. This

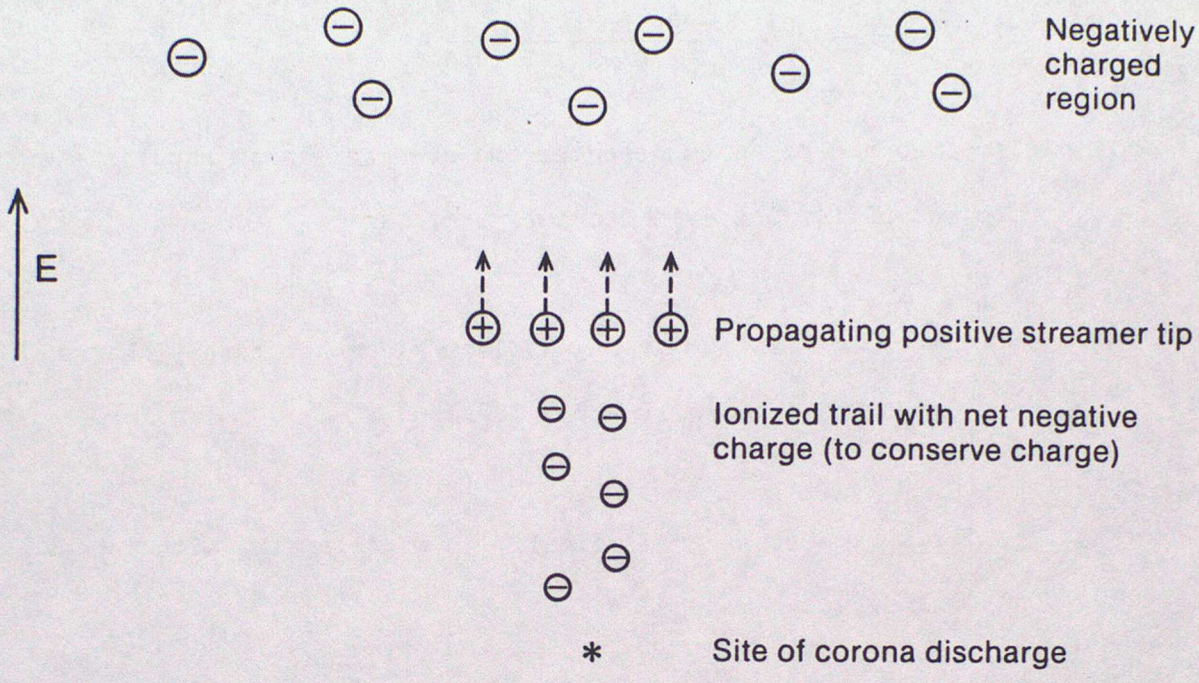

Figure 2.14. Diagram showing the initiation of the lightning stroke following a corona discharge at a point below the main region of negative charge.

may reach the breakdown field of 30 kV cm^{-1} and promote the propagation of a negative streamer; the first step of the stepped leader.

2.4.3 The discharge processes

Any theory devised to describe the stepped leader should take account of its observed characteristics:

i. the minimum average velocity for negatively charged downward leaders is about 10^5 m s^{-1},

ii. the steps are typically 50 m in length, with a pause time between steps of ~ 50 μs,

iii. some 5 C of negative charge are deposited over the length of the leader, requiring a current of about 100 A flowing for a few tens of milliseconds.

It has been suggested that the leader is formed by negative corona streamers as shown in Figure 2.15(a). These die out rapidly except in the strongest fields so that radial and peripheral branches do not develop. The stepped nature of the leader is a further manifestation of this tendancy to dissipate. Qualitatively it is possible to view the process as one which lowers negative charge and the potential of the

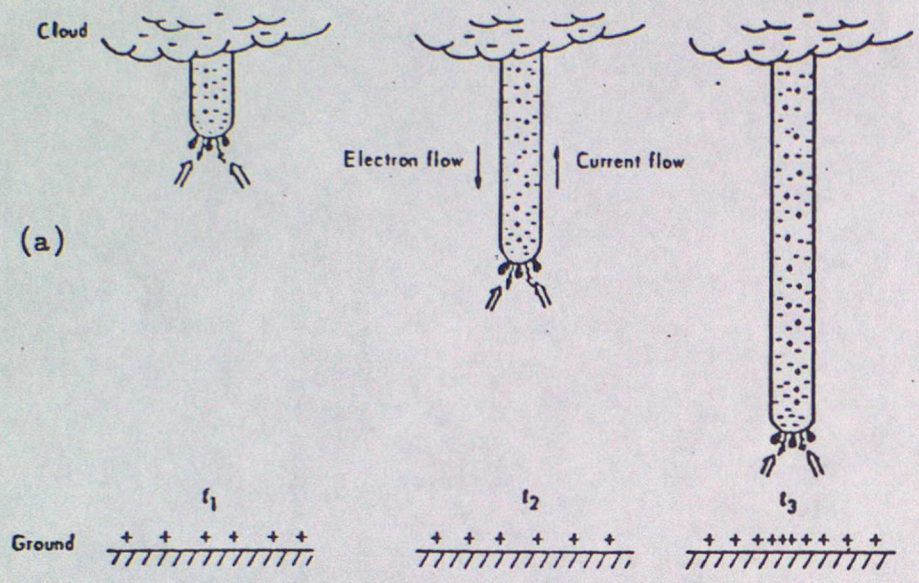

Diagram showing general features of streamer mechanism as applied to lightning leader into virgin air in absence of step mechanism. The times $t_3 > t_2 > t_1$.

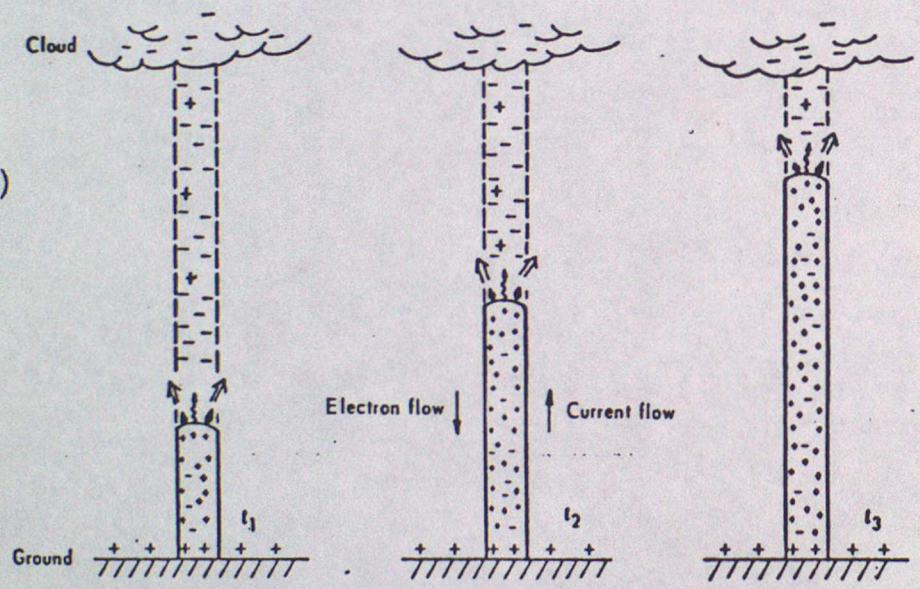

Diagram showing general features of streamer mechanism as applied to return stroke. Times $t_3 > t_2 > t_1$. Note that all current is carried by electrons since the mobility of positive ions is low.

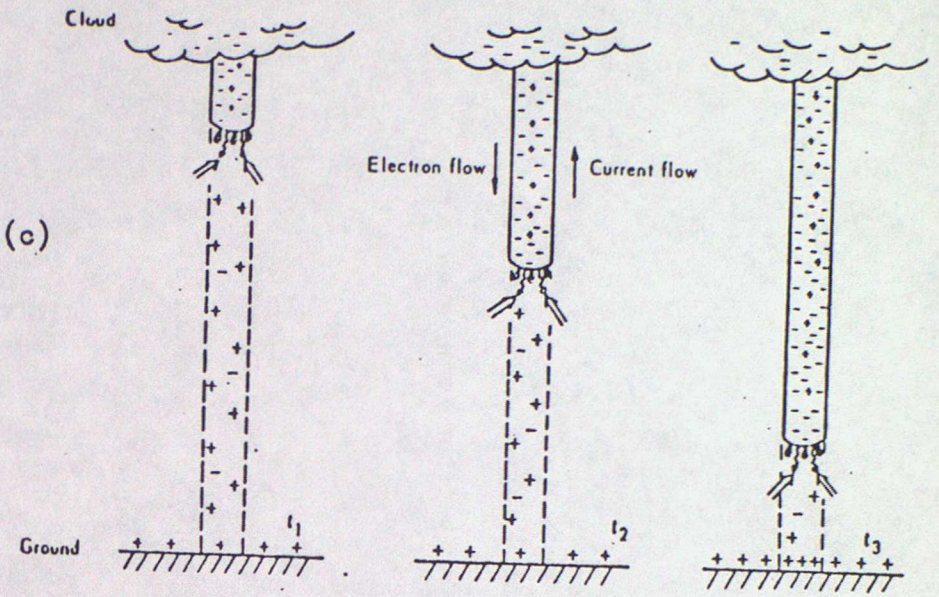

Diagram showing general features of streamer mechanism as applied to dart leader. The times $t_3 > t_2 > t_1$.

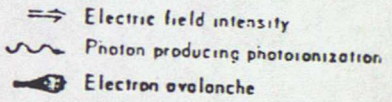

Figure 2.15. Schematic diagrams showing the mechanisms active at different times during the lightning flash. (a) The stepped leader. (b) The return stroke. (c) The dart leader. The dart leader - return stroke cycle may be repeated several times during the flash.

negatively charged region but since the channel is conducting, charge is distributed along it and the quantitative nature of the process has not evaluated.

When a stepped leader is within a few tens of metres of the ground, an upward propogating positive streamer may result. When the junction is complete the first return stroke is initiated.

The negatively charged leader, which may have a tip potential of 10^7 to 10^8 V with respect to the earth, is effectively short circuited to ground. Ground potential is then propogated up the channel. The intense electric field present between the ground potential and the negative charge potential forms a front which propogates at a third to a tenth of the velocity of light, making the trip between ground and cloud in about 70 μs. The excess negative charge deposited in the leader channel is lowered to ground in the form of mobile electrons (Figure 2.15(b)). The current measured at the ground rises typically to 10 to 20,000 A in a few microseconds, and falls to one half of the peak value, typically in 20 to 60 μs. Currents of the order of hundreds of amps may continue to flow for several milliseconds.

When the very sharp voltage gradient reaches the source regions of negative charge, most of the charge from the channel must have passed to ground. The stroke current

therefore reduces. However the proximity of earth potential to the negative region can initiate a new era of charge drainage by upwards positive streamer action as before. This drainage then funnels a new wave of negative charge from the area of propagating streamers to the relatively confined but somewhat decayed conducting channel of the previous stroke. This sweeps down the channel, presumably as a streamer but in a continuous fashion in a time less than about 100 ms. The degree of ionisation increases and charge is again deposited in the channel; albeit to a lesser extent than by the stepped leader. Cloud potential is carried earthward once more to initiate a new return stroke as shown in Figure 2.15(c).

2.4.4 Special forms of lightning

Bead or chain lightning is a visually well documented phenomenon in which the lightning channel breaks up or appears to do so, into luminous fragments generally reported to be metres to tens of metres long. The beads appear to persist for a longer time than does the usual cloud to ground discharge channel. The most plausible theory of bead lightning is that the phenomenon is due to a pinch effect instability by which the current carrying channel is distorted into a 'string of sausages' with the strong light emission coming from the necked off regions of high current density.

Ball lightning is the name given to the mobile luminous spheres which have been observed, usually during thunderstorms. A typical ball lightning is said to have the dimensions of an orange or grapefruit and a lifetime of a few seconds. The phenomenon has not been reproduced in the laboratory and observations are very limited and subjective. Some attempts have been made to place bounds of energetics of ball lightning by inspection of damage caused. The fact that such damage does occur suggests that the phenomenon is not an optical illusion; as has been claimed. Nevertheless there is no known theory to explain how a luminous sphere capable of a lifetime of several seconds can move rather slowly horizontally and vertically, apparently of its own volition, and disappear either silently or explosively.

2.4.5 Effects of lightning

It is to be expected that aircraft often intercept cloud to cloud flashes as well as those from cloud to ground. Very little is known about the former, but it is usually assumed that the currents are not greater than those of typical ground strokes. As a lightning leader approaches an aircraft, high electric fields are to be expected at sharp points and edges. The high fields give rise to streamer discharges which propogate away from the aircraft until one of them contacts the approaching leader. Further development of the stepped leader away from other extremities is then envisaged until a

branch reaches ground or another charge centre. There have been documented cases of aircraft triggering lightning discharges to themselves under conditions where the clouds would, although electrically active, not be expected to produce lightning. These are probably due to the local enhancement of the field at sharp points on the aircraft possibly helped by static charge field up on the aircraft

Two sorts of damage to aircraft are to be expected; one results from the energy dissipated in the structure due to the high current. For a given current this energy is a function of resistance, so efforts are expended to ensure the lowest possible impedance between aircraft structures by efficient bonding. The other sort of damage is a consequence of the high peak current and its high rate of change - which can approach 80 kA s^{-1}. This produces strong, varying electromagnetic fields which can damage electrical apparatus. Again, 'low impedance-at-high-frequency' bonding and the enclosures of sensitive components in shielded structures are sought for protection.

Annual deaths in England and Wales from lightning have been between 1 and 6 per 10 million of the population since the 1920s. Death from lightning results when current through the heart or respiratory centre causes them to malfunction. The body acts as a structureless gel for the sort of currents which result in death or injury so that the position of the

points of exit and entry play a crucial role in defining the current path and hence whether or not the heart or brain are at risk. It is not certain whether cardiac or respiratory arrest are functions of charge or energy dissipation but almost certainly the threshold is often not reached until the low current stage.

When a tree is struck, people or animals beneath it may be at risk from induced effects. The electrical impedance of a tree trunk to the lightning current is a complex function of many variables but between the ground and the height of a person, it is thought to be typically a few kilohms compared with a tyipcal body resistance of one kilohm. A person standing alongside the trunk is at earth potential. As current through the trunk increases, a point may be reached when the potential drop across the lower part of the trunk exceeds the breakdown potential between the trunk and person. A side flash results as in Figure 2.16(a). Obviously this phenomenon can occur in a number of situations and provides a mechanism for injury of people within buildings and possibly for multiple deaths when a strike occurs to several individuals in a crowd. Figure 2.16(b) shows how an ohmic and inductive current may result in a person standing beneath a tree.

A direct strike to open ground results in current flow into the surrounding earth. This creates potential gradients in the soil/rock around the strike point which are proportional

(a)

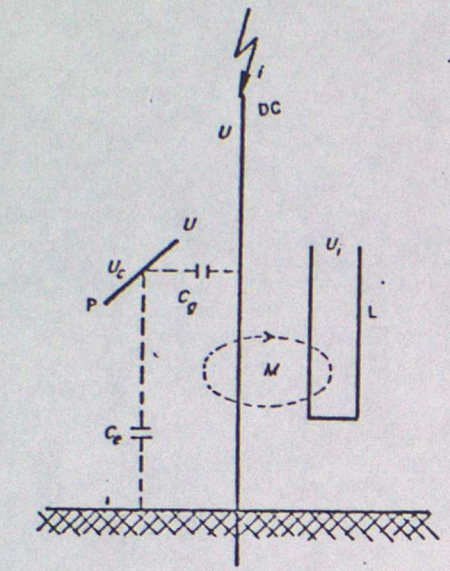

Inductive effects of the lightning current; i = lightning current, U = voltage of down conductor, DC = down conductor, P = isolated metal component with capacitance C_e to down conductor and capacitance C_e to earth, $U_c = UC_e/(C_e + C_e)$ capacitatively induced voltage on P, L = metallic loop with mutual inductance M to down conductor, $U_i = M(\mathrm{d}i/\mathrm{d}t,)$ the inductively induced voltage.

(b)

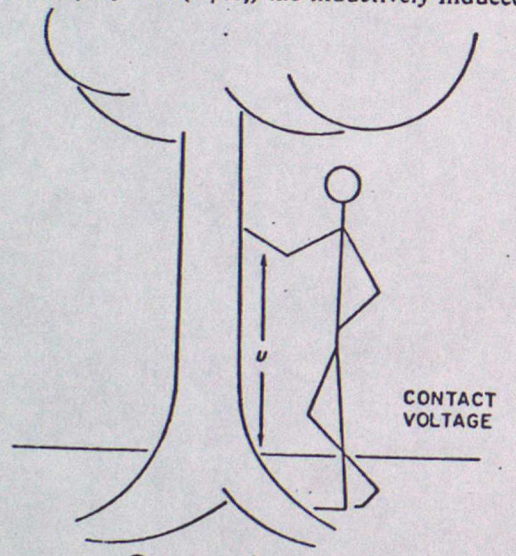

Contact voltage: $u = i(R + R_e) + L\,\mathrm{d}i/\mathrm{d}t + u_s$, where, i is current flowing through the tree, R is the resistance of the tree between the highest point of the body touching the tree and earth, R_e is the "effective" earthing resistance of the tree, L is the inductance between the highest point where the body touches the tree and earth, and u_s is the potential drop between the bottom of the tree and the feet.

(c)

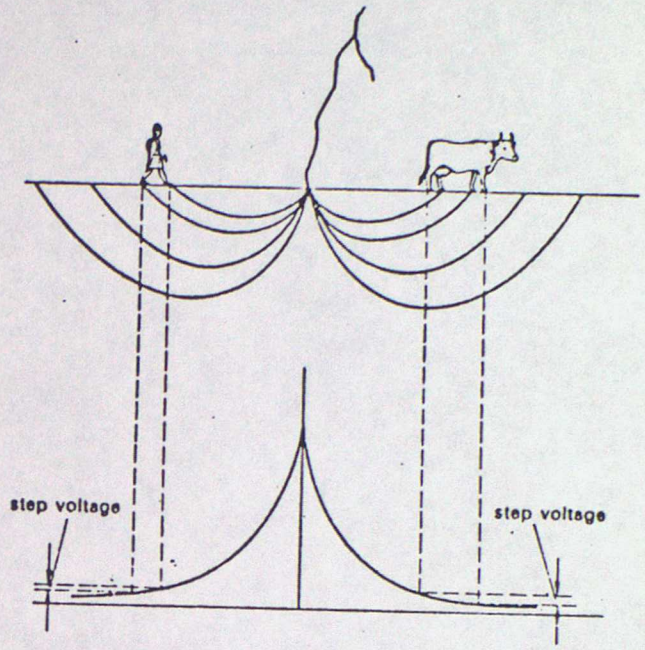

Figure 2.16. Schematic diagrams showing the effects of a lightning discharge to ground. (a) Induction may cause high fields in adjacent objects. (b) High fields may result from contact with a resistive path to ground. (c) Horizontal field variations at the surface may drive currents through four legged animals.

to the current density and earth impedance. Feet in contact with the ground can be at a different potential resulting in current through the body. Such currents are unlikely to be fatal to bipeds but may pass through the hearts of animals causing death (Figure 2.16(c)).

2.5 THUNDER

It is generally accepted that thunder is the result of intense, rapid heating of the lightning channel to form a high pressure shock wave which degenerates into a loud audible sound at large distances. In work carried out at the New Mexico Institute of Mining and Technology data recorded by a network of microphones have been analysed to display the joint temporal and frequency distributions of sound energy shown in Figure 2.17. The general characteristics of such plots are the wide-band tongues of intense sound indictative of so called thunder 'claps', superimposed upon low frequency 'rumbles'. The presence of significant energy at a few Hertz is also apparent.

The thunder signature depends on the tortursity of the lightning channel. The sound from an element of the channel observed from the side gives a sharp crack (since the sound arrives simultaneously) while heard from one end the sound is a rumble due to the time difference between arrival of sound from each end; the thunder from a typical tortuous channel is a mixture of cracks and rumbles.

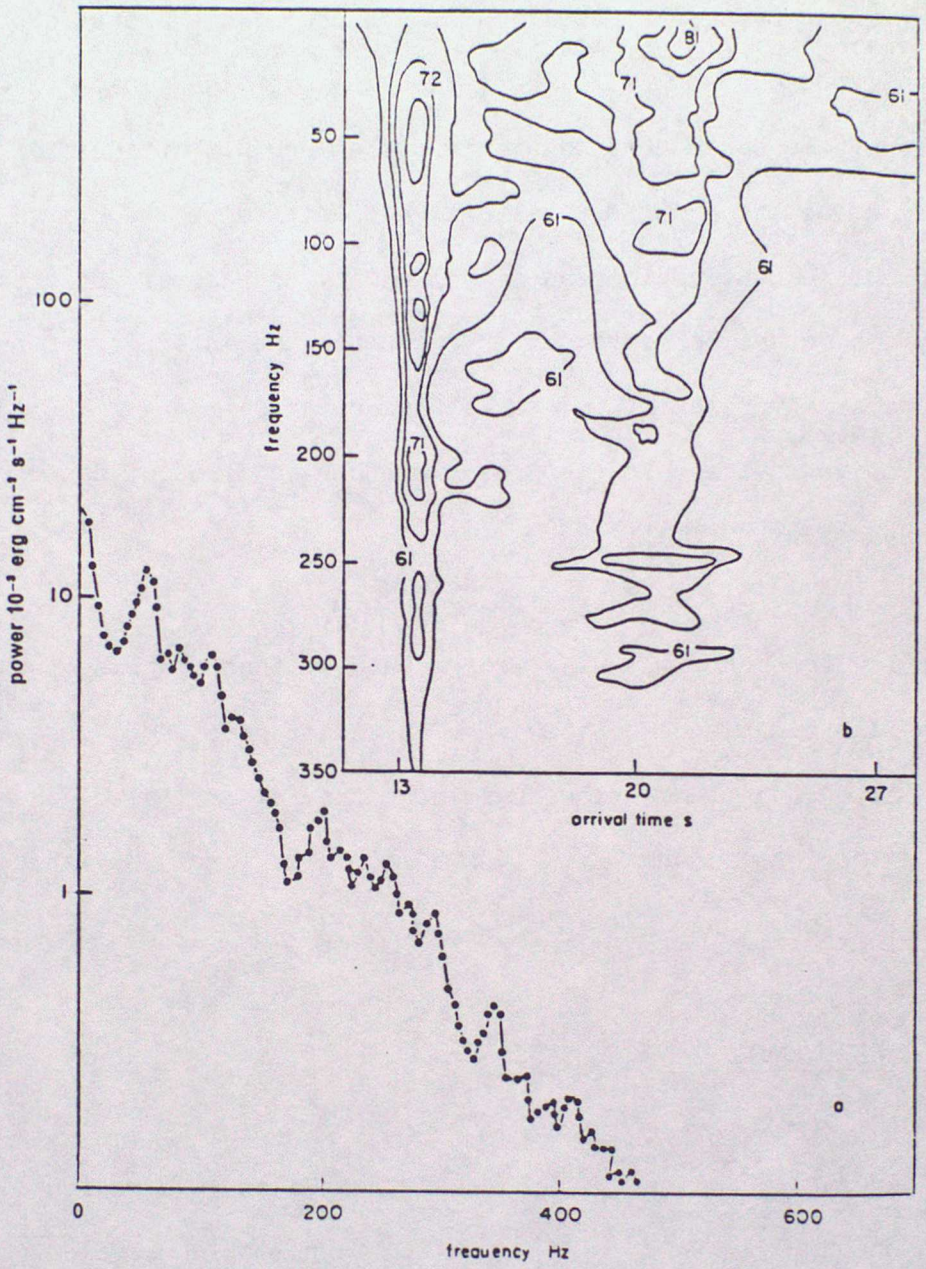

Figure 2.17. Distributions of energy in a roll of thunder showing the intense, broad frequency range thunder clap followed by lower intensity rumbles and the presence of energy at very low frequencies. (a) Power spectrum against frequency. (b) Power contours (arbitrary units) against frequency and arrival time.

Non-linear processes result in stretching of the acoustic pulse with, according to Few (1982), doubling over the first kilometre with little subsequent change in pusle length. Attenuation results from molecular processes, is insignificant below 100 Hz and at higher frequencies increases as humidity decreases. Scattering, refraction and reflection also influence the intensity of thunder heard at any point. Since attenuation and scattering are less effective at lower frequencies the observed pitch of thunder often decreases with time.

The low frequency ($\leq$ 20 Hz) components of thunder arise partly from the lightning induced shock wave but also from sudden changes in the size of a thundercloud resulting from electrical discharge from large regions. Sound from such a mechanism is of low frequency and highly directional.

2.6 REFERENCES

Aufdermaur, A.N. and Johnson, D.A. 1972 Charge separation due to riming in an electric field. Q.J.R. Meteorol. Soc., 98, 369-382.

Bennetts, D.A.; Ryder, P.; Latham, J. and Stromberg, I.M. 1980 The electric field structure of convective cloud. Abstr. VI Int. Conf. Atmos. Elec., UMIST 28 July-1 August.

Crabb, J.A. and Latham, J. 1974 Corona from colliding drops as a possible mechanism for the triggering of lightning. Q.J.R. Meteorol. Soc., 100, 191-202.

Few, A.A. 1982 Acoustic radiation from lightning. CRC Handbook of atmospherics, 2, Boca Raton, 258-290.

Griffiths, R.F. and Latham, J. 1974 Electrical corona from ice hydrometeors. Q.J.R. Meteorol. Soc., 100, 163-180.

Krehbiel, P.R. and others 1980 Lightning charge structure in thunderstorms. Abst. VI Int. Conf. Atmos. Elec., UMIST 28 July-1 August.

Latham, J. and Mason, B.J. 1961 Electric charge transfer associated with temperature gradients in ice Proc. R. Soc., 260A, 523-536.

Rawlins, F. 1982 A numerical study of thunderstorm electrification using a three dimensional model incorporating the ice phase. Q. J. R. Meteorol. Soc., 108, 779-800.

Reynolds, S.E.; Brook, M. and Gourley, M.F. 1957 Thunderstorm charge separation. J. Meteorol., 14, 426-436.

Wilson, C.T.R. 1956 A theory of thundercloud electricity. Proc. R. Soc., 236A, 297-317.

2.7 BIBLIOGRAPHY

Barry, J.D. 1980 Ball lightning and heat lightning-extreme forms of atmospheric electricity. Plenum Press. New York. 298 pp.

Brook, M. and others 1980 Positive ground stroke observations in Japanese and Florida storms. Abst. VI Int. Conf. Atmos. Elec., UMIST 28 July-1 August.

Caranti, J.M.; Illingworth, A.J. and Marsh, S.J. 1985 The charging of ice by differences in contact potential. J. Geophys. Res., 90, 6041-6046.

Golde, R.H. 1977 Lightning, vols 1 and 2. Academic Press, London. 849 pp.

Illingworth, A.J. and Latham, J. 1977 Calculations of electric field growth, field structure and charge distributions in thunderstorms. Q.J.R. Meteorol. Soc., 103, 281-295.

Latham, J. and Warwicker, R. 1980 Charge transfer accompanying the splashing of supercooled raindrops on hailstones. Q.J.R. Meteorol. Soc., 106, 559-568.

Macgorman, D.R. and Few, A.A. 1978 Correlations between radar reflectivity contours and lightning channels for a Colorado storm on 25 July 1972. Proc. AMS Conf. on Cloud Phys. and Atmos. Elec., Issaquah. 31 July-4 August.

Mason, B.J. 1972 The physics of the thunderstorm. Proc. R. Soc., 327A, 433-466.

Scott, W.D. and Levin, Z. 1970 The effect of potential gradient on the charge separation during interactions of snow crystals with an ice sphere. J. Atmos. Sci., 27, 463-473.

Uman, M.A. 1984 Lightning. Dover Publications, New York, 298 pp.

Warwick, J.W.; Hayenga, C.O. and Brosnahan, J.W. 1979 Interferometric directions of lightning sources at 34 MHz. J. Geophys. Res., 84, 2457-2468.

Winn, W.P. and Moore, C.B. 1971 Electric field measurements in thunder clouds using instrumented rockets. J. Geophys. Res., 76, 5003-5017.

JM

3. WEATHER MODIFICATION

3.1 INTRODUCTION

Discussions of ways of deliberately changing the weather to benefit mankind has been going on for many years but it is only in the last few tens of years that practical means have become available which may make this possible. We shall consider techniques which affect the microphysical processes in clouds and which have been tried in the field, sometimes with success, to modify weather over areas from tens to thousands of square kilometers.

Clouds form when air is cooled below its dew-point so that condensation takes place upon sub-microscopic particles; the cooling may be the result of radiation to space, of convective ascent of buoyant air masses or mesoscale or synoptic-scale motions which produce lifting, or of the mixing of two air masses at different initial temperatures and humidities.

As a cloud grows, the droplets increase in size with height above cloud base. If there are very large concentrations of condensation nuclei however, precipitation may grow only slowly even if the cloud grows quite large and clouds often form, grow and evaporate over inland areas without producing significant rain (see figure 3.1). However, if the concentrations of nuclei and droplets are relatively low and there are a few giant nuclei resulting in a few much larger than average droplets, both

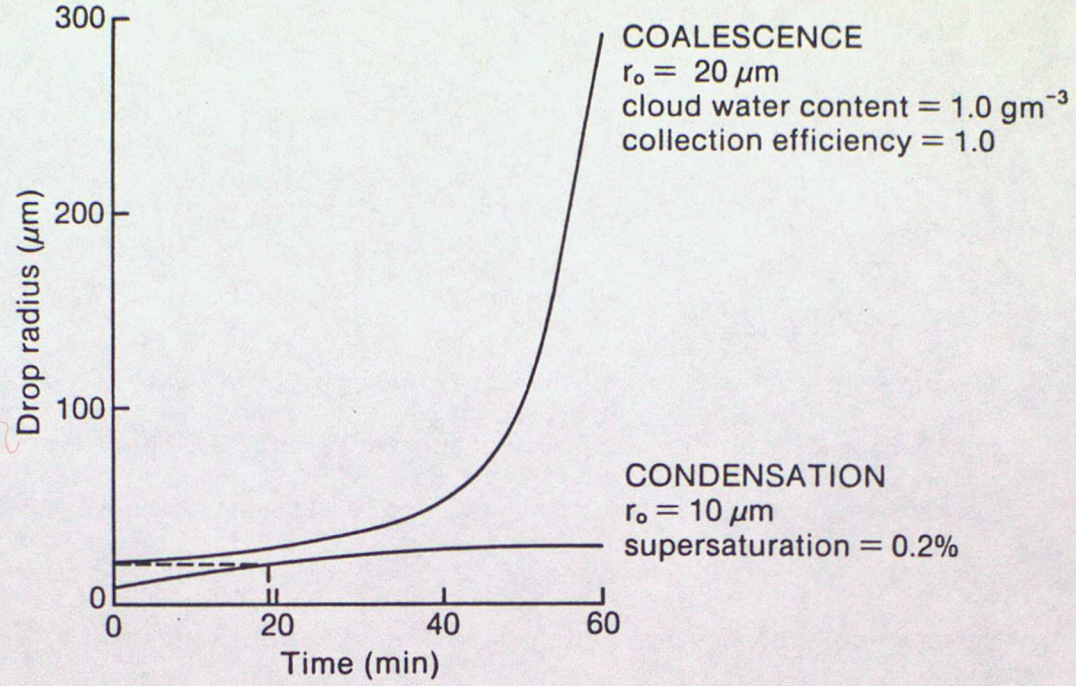

Figure 3.1. Comparison of the growth of a drop of initial radius r_o by condensation at a constant supersaturation and by coalescence in a cloud of smaller droplets.

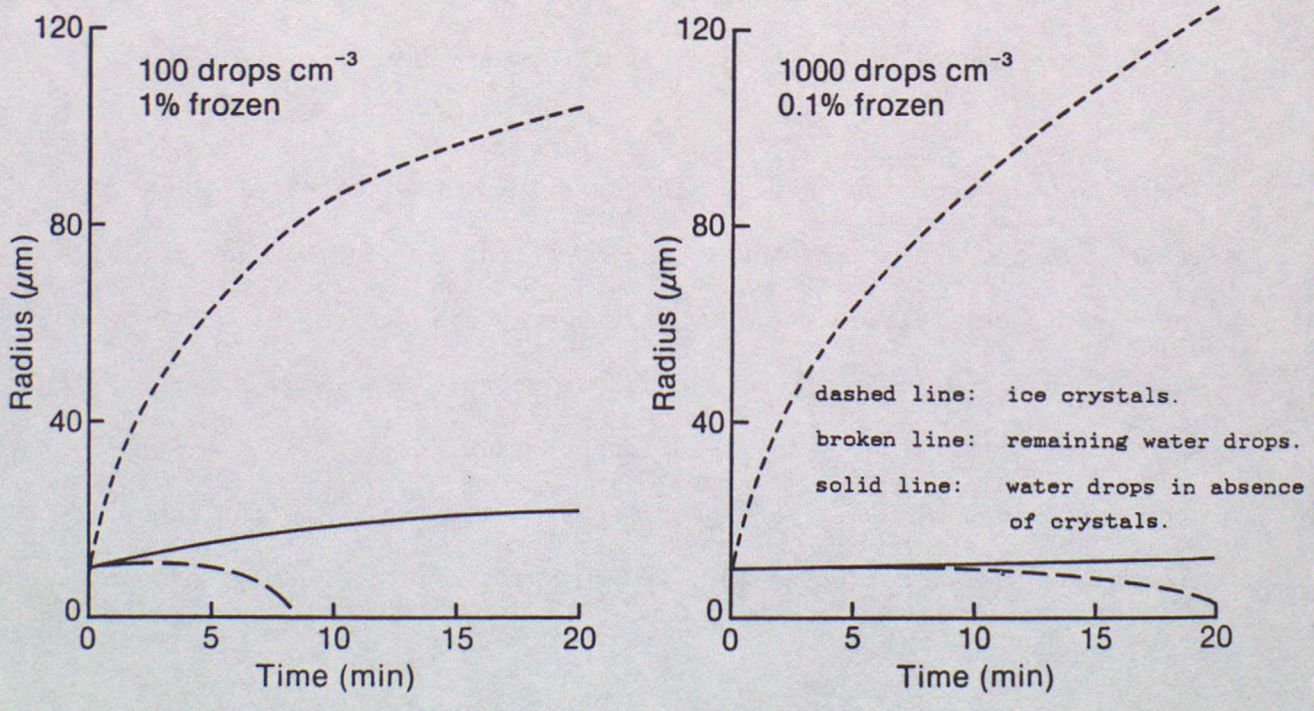

Figure 3.2. The growth of ice crystals in a cloud of droplets of the same initial radius initially at water saturation and in an updraught typical of those in moderate cumulus. The concentration of ice crystals is shown.

of which condition, are more common in maritime air, the larger droplets will grow by collecting the smaller ones to a sufficient size to fall to the surface as rain.

If the cloud grows tall enough to exceed the height of the freezing level the droplets will normally supercool down to temperatures of about -20°C. Ultimately however, and always before they reach -40°C, the droplets freeze. Alternatively, ice crystals may form directly from the vapour upon sublimation nuclei. As soon as ice particles of any form appear in the presence of supercooled water droplets, the cloud becomes colloidally unstable because the saturation vapour pressure over ice is less than that over water at the same temperature and hence ice particles grow rapidly at the expense of the water droplets (see figure 3.2). While the concentration of ice particles remains small in comparison to that of water droplets, the former will grow quite large and subsequently collide with and collect water-droplets and other particles in their path. Provided the cloud depth is sufficient, the particles will grow large enough to precipitate to the surface.

These two natural precipitation processes are of immediate interest to the weather modifier because, by adding quite small concentrations of giant condensation nuclei or of ice nuclei to clouds where their low natural concentration renders the development of precipitation inefficient, it may be possible to augment the amount of precipitation which would otherwise occur.

There is another situation which is of interest from the viewpoint of weather modification. This is where growth of a supercooled convective cloud is limited by atmospheric stability conditions but where comparatively small increases in cloud buoyancy could result in considerably enhanced cloud growth. In growth-limited supercooled clouds the addition of large numbers of artificial ice nuclei in the upper levels can result in complete glaciation of substantial regions of supercooled water; the consequent release of the latent heat of freezing can produce sufficient buoyancy to produce considerable cloud growth as seen in Figure 3.3 leading to significant increases in precipitation.

These mechanisms have all been explored with varying degrees of success. It is important to realize that the increases that can be expected from precipitation enhancement techniques are relatively modest and are often well within the natural variability of the precipitation it is hoped to change. Hence quite sophisticated statistical techniques are essential to determine whether any observed changes in precipitation are associated with the modification treatment or merely part of the natural fluctuation.

In this lecture emphasis will be given to attempts to enhance surface precipitation but other forms of weather modification, based on the above physical principles will also be discussed. These include artificial dispersal of fogs and the suppression of hail.

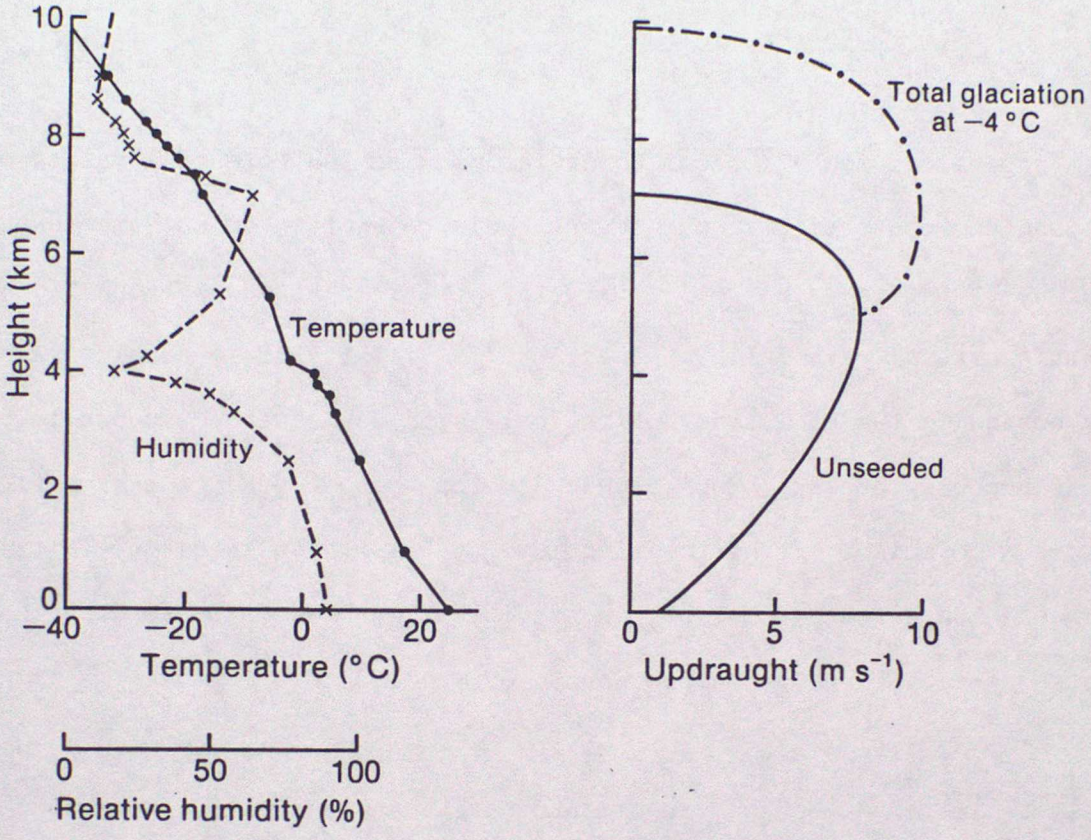

Figure 3.3. Enhanced ascent of a thermal due to instantaneous release of latent heat of fusion caused by artificial glaciation. The calculations are for an entraining thermal using a sounding typical of those observed on some cloud seeding experiments.

3.2 PRECIPITATION ENHANCEMENT

3.2.1 Warm clouds

In tropical or semi-tropical countries many of the potential rain-producing clouds are convective in nature and their tops often do not exceed the height of the freezing level; this is particularly true in conditions when little natural rain falls. Hence, the possibility of increasing rainfall by enhancing the efficiency of the collision-coalescence process is of considerable concern. When clouds develop whose tops do not significantly exceed the height of the freezing level, it may be possible to initiate or enhance the effectiveness of the precipitation process by seeding them with water droplets or hygroscopic particles.

Only a limited number of experiments have been carried out to test the effectiveness of such techniques because it is clear that large masses of seeding material are necessary. If seeding is to be carried out with 10 μm diameter salt particles of density 2 g cm^{-3} and each particle ultimately grows to a 2.5 mm diameter raindrop, the original particles will increase in mass by a factor of nearly 10^7. One millimeter of rain over an area of 1000 km^2 has a mass of 10^9 kg so that if it is to be induced by seeding, it would be necessary to employ 100 kg of seeding material. The situation will however be more favourable if a "chain reaction" occurs, in which drops break up after first growing by coalesence and the fragments then serve as growth centres for new large droplets. However, little evidence exists that such a process occurs extensively in natural clouds. Seeding

using water droplets requires even larger masses of seeding material because of the difficulty in dispersing small droplets and the slower growth by condensation compared with growth on a salt particle. In spite of these limitations, a few experiments have been carried out.

Braham et al (1957) carried out experiments in which up to 400 gallons of water was released from an aircraft into the tops of individual clouds. In each case the seeded cloud was chosen at random from a pair of essentially similar clouds and the differences studied between the behaviour of each cloud of the pair. In most cases both treated and untreated clouds produced rain at some time after they were first examined. The treated clouds rained much earlier than those untreated but the amount of rain they produced appeared the same.

Some experiments in the United States have examined seeding of warm clouds with sodium chloride. Such seeding apparently resulted in the formation of rain only from the seeded portion of a line of shallow clouds. Rain lasting about 1 hour was observed to reach the ground about 20 min after seeding. The total mass of water reaching the ground was about 3.5×10^8 kg for a mass of salt of 160 kg; results which are comparable with those expected theoretically.

Indian workers have carried out by far the greatest number of salt seeding experiments aimed at increasing precipitation from convective clouds. They used salt as a seeding material, ground to about 10 μm diameter and dispersed by blowers at a rate of about 2.5 kg min^{-1}. Figure 3.4 shows the areas used for some of the experiments with a dense network of raingauges

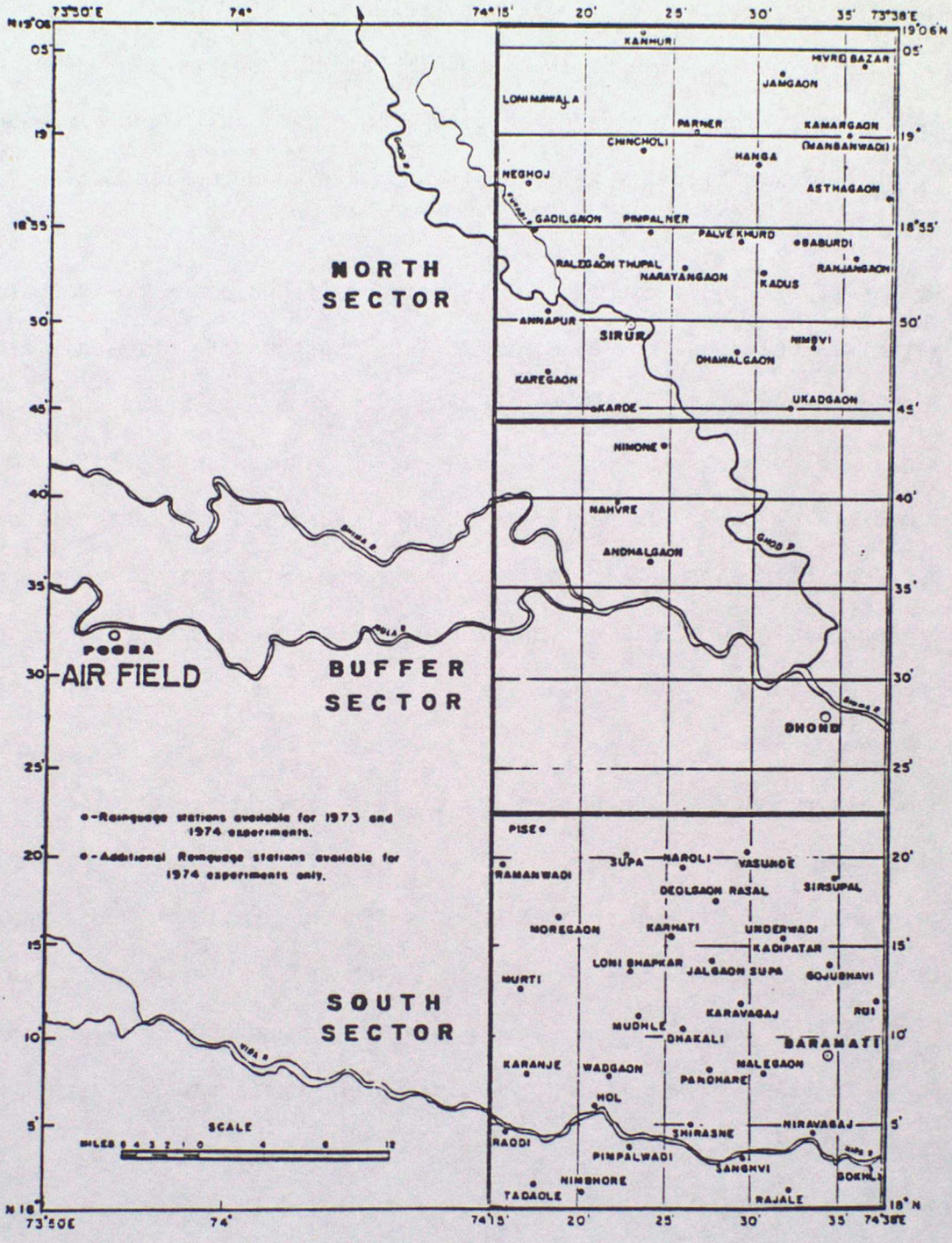

Figure 3.4. The area covered by the early Indian warm rain experiments showing the dense rain gauge network.

(1 per 56 km^2). As shown in Table 3.1 many of the experiments showed large increases in rainfall in the target areas but, despite the magnitude of the apparent effects of seeding the effects are not statistically significant in view of the large natural variations in rainfall. It is interesting to note that seeding tended to cause shallow clouds (less than 500 m deep) to dissipate, presumably due to increased entrainment of air from outside the cloud. There is some suggestion that during seeding the temperature and water content in the clouds increased as can be seen in the successive cloud traverses shown in Figure 3.5 although the reasons for the increases are not certain.

3.2.2 Cold Clouds

3.2.2.1 Seeding for microphysical effects

In is the most commonly employed technique for seeding cold clouds (those rising above the height of the freezing level), moderate concentrations of ice forming nuclei have been introduced in order to enhance the efficiency of the microphysical process described earlier. As the simplest possible hypothesis of the effect of seeding, it might be assumed that one ice nucleus produces one raindrop. Depending upon the seeding material employed and the temperature level at which it is introduced or becomes effective, one gram of material may result in the production of 10^{12} to 10^{15} ice nuclei. Hence, if each nucleus results in the formation of a 2.5 mm diameter raindrop, less than 100 g, and possibly less than 0.1 g of material could suffice to produce 1 mm of rain over an area of 1000 km^2.

Pair	North-seeded days mean rainfall in mm per station Date	Target (T)	Control (C)	South-seeded days mean rainfall in mm per station Date	Target (T')	Control (C')	$\left(\frac{T}{C}X\frac{T'}{C'}\right)^{1/2}$	Result
1	June 28	3.65	3.85	June 26	6.84	4.75	1.168	Positive
2	July 1	0.29	0.63	30	0.43	0.07	1.682	Positive
3	July 5	3.11	0.52	July 4	1.42	1.98	2.051	Positive
4	July 7	0.32	0.26	8	0.38	1.54	0.551	Negative
5	July 11	4.81	0.39	15	0.27	0.06	7.451	Positive
6	July 23	0.11	0.21	21	0.02	0.00	Indeterminate	Inconclusive
7	July 28	5.88	5.24	27	3.43	0.68	2.371	Positive
8	July 30	25.37	11.68	29	6.98	11.72	1.137	Positive
9	Aug. 29	1.01	1.46	Aug. 30	0.16	0.47	0.485	Negative
10	Aug. 31	0.00	0.00	Sept 1	0.06	0.14	Indeterminate	Inconclusive
11	Sept 2	0.08	0.14	3	0.12	0.00	Infinity	Positive

NOTE: When the mean rainfall is 0.05 mm or less, it is considered as zero.

Table 3.1. The results of a series of experiments in which clouds were seeded with salt on a random basis in India. The double ratio test is used to remove effects of natural variability in the rainfall between target and control areas.

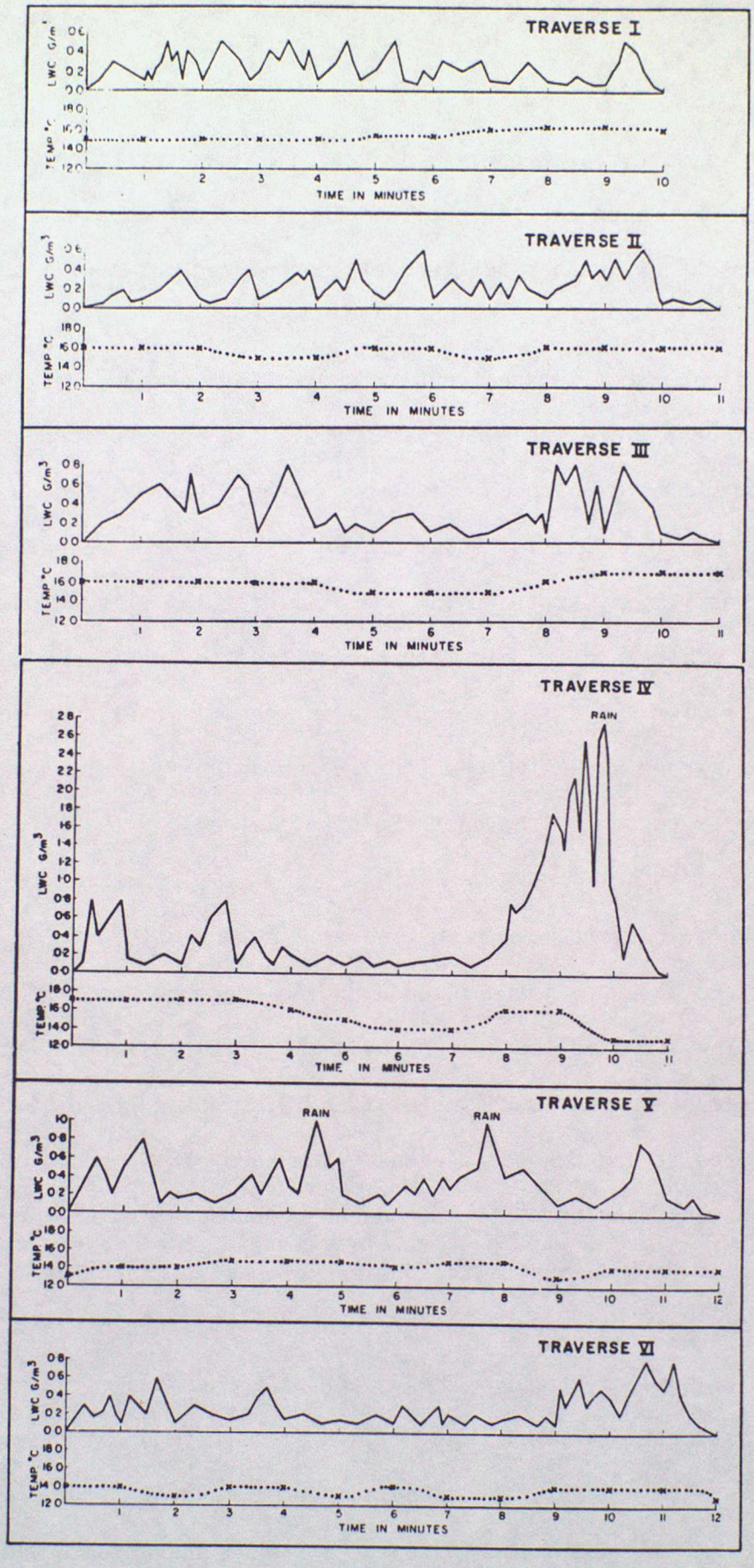

Figure 3.5. Sucessive traverses of a cloud following seeding with salt. The increase in mean temperature following seeding can be seen as can the formation of regions of high liquid water content.

It is impossible to review the very many precipitation enhancement projects which have been carried out throughout the world using this technique in the past few decades but two well documented cases will be examined.

The first Israeli experiment commenced in 1961 and continued in all subsequent winter seasons until 1967. A cross-over design was employed in which either a northern area or a southern one was seeded on a random basis with a buffer zone in between never being seeded. Seeding was from an aircraft flying just off the coast, dispersing silver iodide smoke into the bases of the clouds which approached from the west. An increase in rainfall of 15%, significant at about the 5% level, was achieved over the whole target area with greater and more significant increases in the interior region of the northern area.

In the second and more recent Israeli experiments, the seeding line for the northern area was moved inland, and some ground based generators were used allowing a control area to be available for statistical analysis. The experimental area is shown in Figure 3.6. Using this control area in the analyses it was concluded that an increase of the order of 15%, significant at better than the 5% level, occurred in the northern target area. The increase in the important catchment of Lake Kinneret was 21%. The increase was found to be greatest when cloud top temperatures were between -15 and -21°C. When the temperature was outside this range the effects were statistically insignificant. It is also of interest that most of the increase in rainfall was associated with days of light or moderate rainfall (< 15 mm) and is not dominated by a few unusual events. Microphysical observations suggest that in this area natural clouds have very low

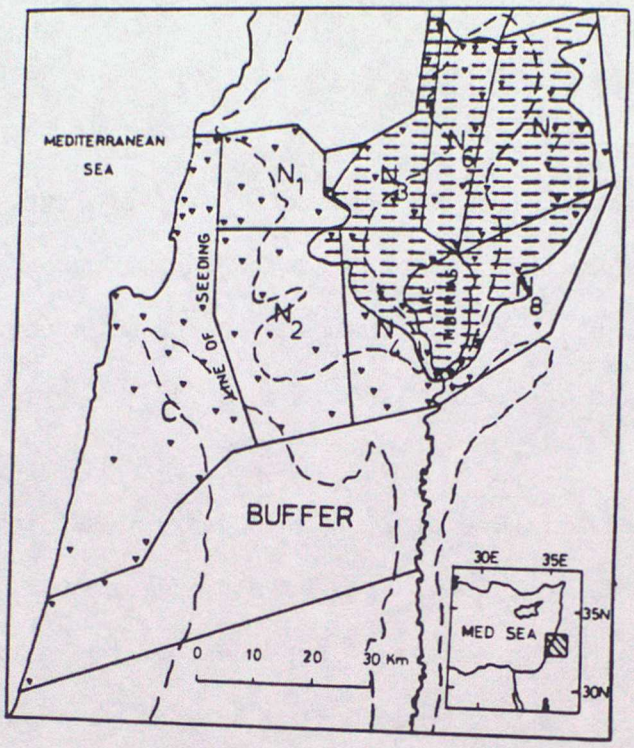

Figure 3.6. Map showing the area of the Israeli cloud seeding experiments. The hatched area is the catchment of lake Kinneret and triangles denote rainguage locations. The 200 m contour is shown dashed and the line of aircraft seeding is also shown.

concentrations of ice nuclei at temperatures higher than -21°C. Ascent of the air over the coastal slope in the prevailing north-westerly wind at the time of experiment ensures a plentiful supply of water vapour so that conditions are possible for seeding to be effective. However at temperatures above -15°C the rate of ice crystal growth by diffusion is sufficiently slow that ice particles cannot grow on artificial nuclei in the time available. A full analysis of the microphysical data is required to fully explain the rainfall observations.

A long-term randomized experiment was carried out in Tasmania between 1964 and 1970 over the catchment area of a hydroelectric authority. There were 54 seeded and similar number of unseeded periods each of 10-18 days duration with the experiment running only in alternate years. Seeding of frontal layer cloud systems having tops colder than -5°C with silver iodide smoke was carried out from aircraft either at cloud base or at the -5°C level or above. Results were analysed separately season by season. It was concluded that seeding increased autumn rainfall by 20-40%, significant at the 2-4% level, that the winter rainfall increased by about 10%, significant at about the 10% level, but that any changes during spring or summer were not significant.

The results demonstrate however the difficulty of interpreting the data. Analysis of data from 16 raingauges in the target area and 38 in control areas reveals that the total rainfall in the target area was 8% less in the seeded periods compared with the unseeded periods (see Table 3.2) with a marked seasonal dependence of the ratio of rainfall in seeded and unseeded periods. However comparison between target and control areas using the

	N	T	C_1	C_2	T/C_1	T/C_2	$T/\frac{1}{2}(C_1+C_2)$	T_s† / T_u	Double ratios = $\frac{T_s}{C_s} \Big/ \frac{T_u}{C_u}$		
									$C=C_1$	σ	$C=\frac{1}{2}(C_1+C_2)$
Totals all 4 years	S 54	84·76	85·84	66·95	0·99	1·27	1·11	0·92	1·04		1·06
	U 54	92·15	97·47	79·31	0·95	1·16	1·04				
Autumn	S 14	20·46	19·06	14·47	1·07	1·41	1·22	0·84	1·25	0·05	1·25
	U 11	19·21	22·43	17·36	0·86	1·11	0·97				
Winter	S 14	22·03	26·11	19·82	0·84	1·11	0·96	0·81	1·02	0·5	1·07
	U 14	27·28	33·11	27·46	0·82	0·99	0·90				
Spring	S 16	30·67	30·09	22·99	1·02	1·33	1·16	1·28	0·98	0·6	0·99
	U 18	27·02	25·99	20·40	1·04	1·32	1·17				
Summer	S 10	11·60	10·58	9·67	1·10	1·20	1·15	0·68	0·94	0·8	0·93
	U 11	18·64	15·94	14·09	1·17	1·32	1·24				

T = target, C_1 = control area 1, C_2 = control area 2, σ = statistical significance level, S = seeded period, U = unseeded (control) period, N = number of periods, † Calculated per period.

Table 3.2. Analysis of the results of the Tasmanian seeding experiments in which silver iodide was used to seed supercooled clouds.

double ratio (target seeded/target unseeded)/(control seeded/control unseeded) indicates positive effects of 25% in autumn. The results are therefore rather inconclusive; the high autumn double ratio being largely due to the control area rainfall being less on seeded than on unseeded occasions.

3.2.2.2 Seeding for dynamical effects

It was noted very early in the experiments in which cumulus clouds were seeded that occasionally marked growth occurred. However, it is only comparatively recently that deliberate attempts have been made to cause such growth by massive seeding of convective clouds with a view to obtaining greatly enhanced precipitation. The physical principle on which the experiments are based is simply that when large quantities of supercooled water can rapidly be caused to freeze, the release of the latent heat of freezing will produce sufficient buoyancy to enable the cloud to grow much taller than would otherwise be the case. Greater cloud depth will in turn allow greater growth to take place on precipitation particles, giving longer cloud lifetimes and more precipitation.

In the Florida Area Cumulus Experiment individual cumuli forming over an area of more than 10^4 km^2 (see Figure 3.7) were seeded by dropping pyrotechnic flares containing large quantities (100 — 1000 g per cloud) of silver iodide into the upper levels of active supercooled clouds on days for which a simple numerical model suggested that such a procedure would result in significant cloud growth. Rainfall was obtained using a

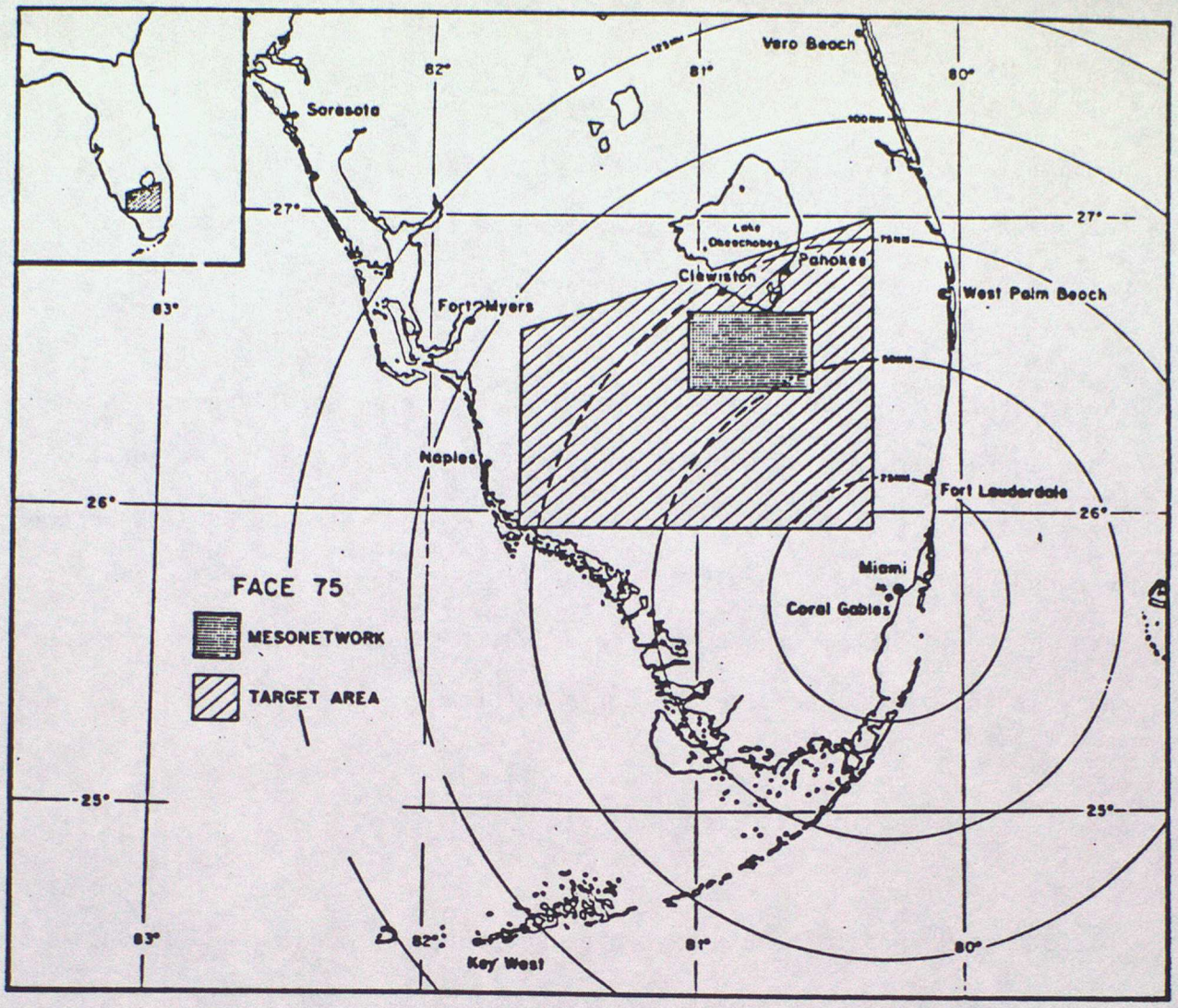

Figure 3.7. Field design for the Florida Area Cumulus Experiment showing the target area and the area of detailed surface measurements (including radar) of rainfall, wind, temperature, humidity and pressure.

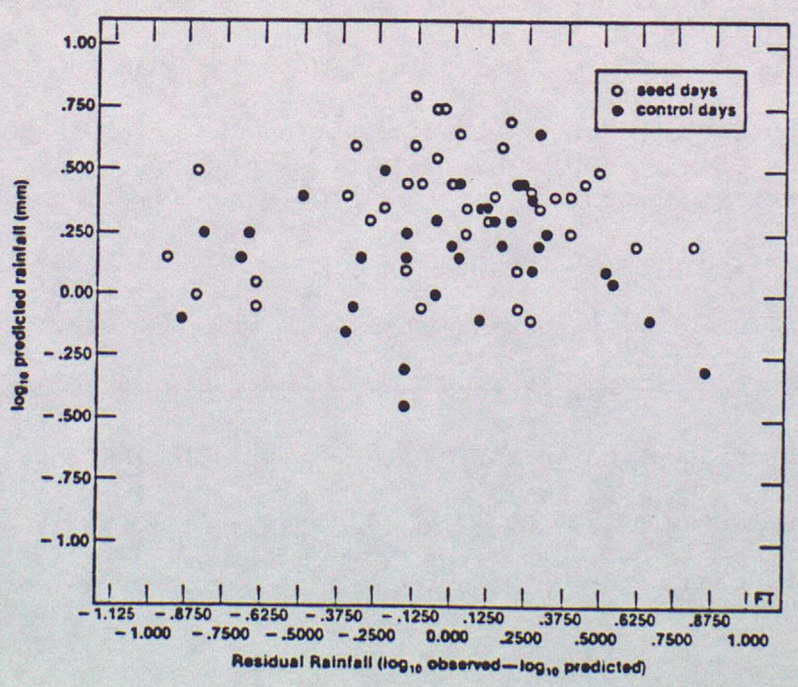

Figure 3.8. Comparison of rainfall predictions on the target area using a statistical model with observations of rainfall. Model input variables include input from a 1-d cloud model, the atmospheric profile and the rainfall prior to seeding.

combination of raingauges and 10 cm radar. It was claimed that significant increases in precipitation were observed, particularly in cases where merging of adjacent clouds followed seeding.

The rainfall predictions from the model were in resonable agreement with observed rainfall at the surface as is shown in Fig 3.8 and from these results it was claimed that rainfall in the seeded days was 50 ± 90% higher than on unseeded days. However the results were dominated by heavy rain on less than one-fifth of the seeded days and if these are excluded from the analysis the overall results are not significant.

3.2.2.3 Orographic cloud seeding

Persistent orographic clouds have been subjected to seeding and in this case results are more positive. The clouds are naturally shallow and do not often create precipitation but if they are seeded by particles formed at high levels in convective clouds these can grow by accretion producing heavy precipitation at the surface. Some randomised experiments have been conducted in Colorado in which seeding agents are injected into the upwind edge of the supercooled cloud. The resulting ice crystals grow rapidly, provided there is not competition for the available water. Before they reach the downwind edge of the cloud the seeded particle fall speed is sufficiently large for it to fall through the cloud accreting supercooled droplets (see Figure 3.9). It has been demonstrated that provided the cloud top temperature was in the range -11 to -20°C increases in surface precipitation averaging 25% could be produced. This result has withstood rigorous statistical tests. However, the number of occasions on which

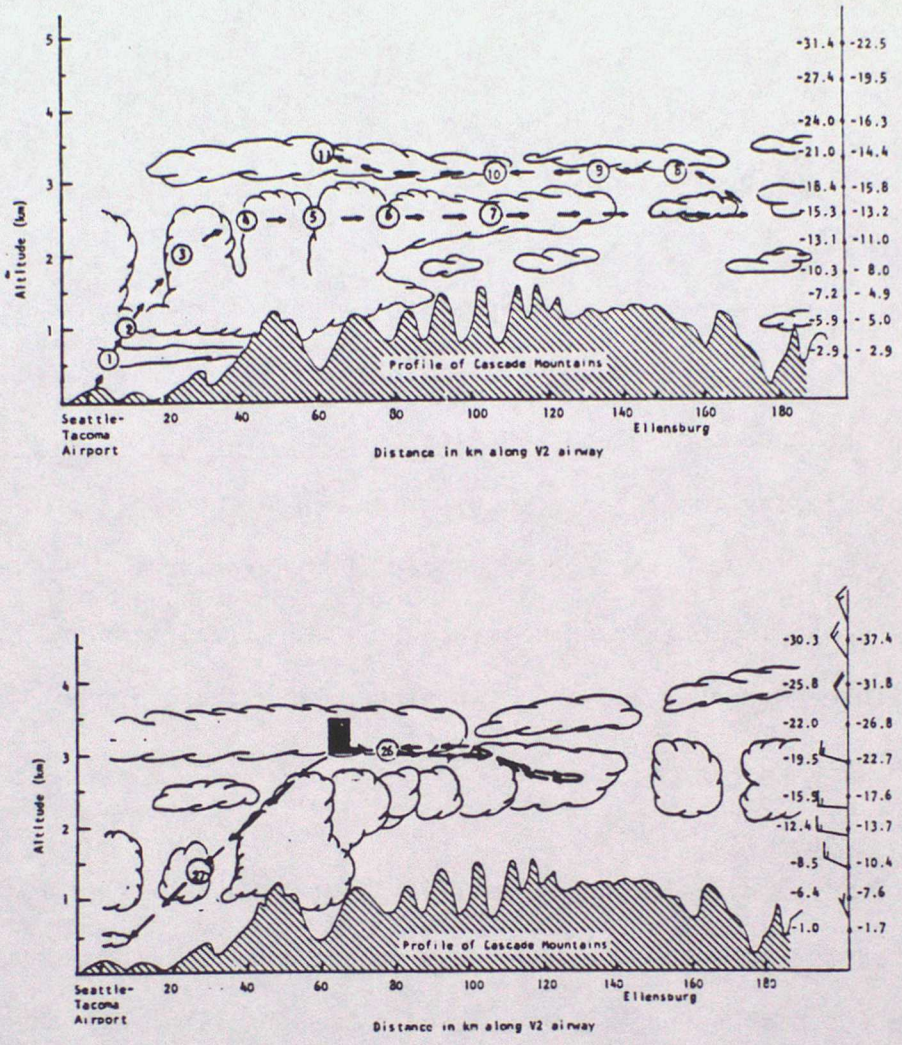

Figure 3.9. Schematic diagrams showing the rationale for seeding of wintertime orographic clouds to modify snowfall at the surface. Aircraft observations were made at the positions indicated. The upper figure shows runs prior to seeding and the lower figure the runs after seeding which took place within the region shown heavily shaded.

clouds form under favourable conditions of cloud depth, temperature and wind speed (which determines the time available for particle growth and the rate of release of moisture) is probably rather restricted.

3.2.2.4 Conclusions

Of the many large-scale area experiments (order of $10^3 - 10^4$ km^2) in which moderate concentrations of artificial ice nuclei were dispersed in clouds, only a few have demonstrated at a satisfactory statistical significance level that seeding increased precipitation. The increases in precipitation were typically 10-20% when averaged over the target area for the full operating season. In many experiments no statistically significant increases were observed and in a few experiments there appear to have been decreases in precipitation following seeding.

These contradictory results may well relate to the fact that clouds supercooled to the same extent but having different microstructures and different ice budgets could be expected to respond in a different manner to a given seeding technique. The high colloidal stability of the winter stratiform clouds in Tasmania, of winter orographic clouds in the central USA and the winter continental cumuli of Israel seem to render these clouds more favourable to seeding for microphysical effects than is true for maritime cumuli. These latter clouds have been found to produce naturally high ice particle concentrations at some stage in their life cycle; the addition of additional ice nuclei is detrimental, resulting in either no change in precipitation or possibly a decrease. Figure 3.10 shows how ice particle growth is reduced when the concentration is increased. It now

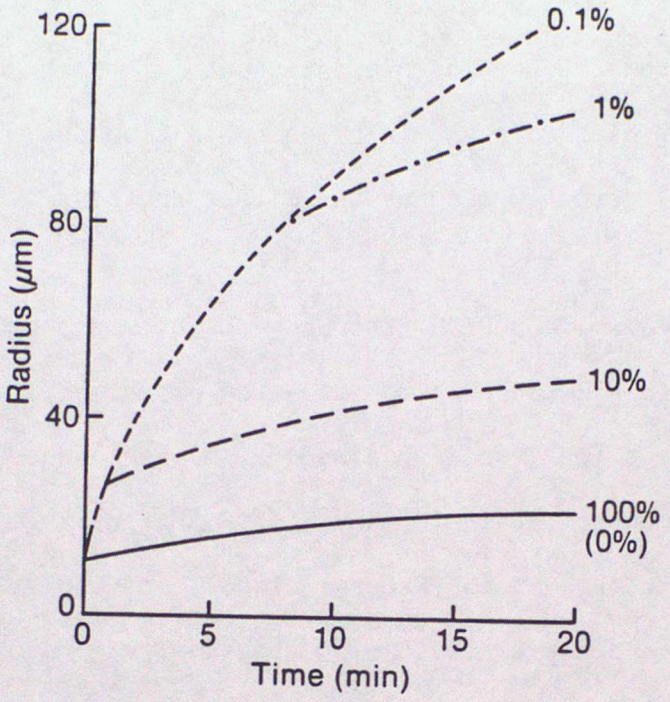

Figure 3.10. The effect on growth by sublimation onto ice crystals in a mixed phase cloud of the number of ice crystals present. This shows the effect of "overseeding" giving much reduced ice crystal growth.

Total number of particles: 100 cm^{-3}

Growth of drops in water cloud indistinguishable from growth of crystals in an ice cloud

seems that the water-ice budget of the clouds is probably one of the more crucial fctors governing the release of precipitation. Thus it is in those

cases when the processes of ice nucleation and particle growth are slower than the rate at which moisture is released in clouds by the updraught that seeding can be expected to produce positive effects.

In an attempt to clarify some of the problems and to provide guidance to governments considering weather modification experiments a Precipitation Enhancement Project (PEP) was organised by the World Meteorological Organization in central Spain (Figure 3.11). Extensive measurements of the microphysical structure of the natural clouds, concentrating on the water-ice budget and the precipitation processes have demonstrated the natural variability and the difficulty in predicting the likely effects of seeding. It is clear that in many cases the natural concentration of ice crystals was sufficiently high that seeding was unlikely to produce an increase in precipitation although the mechanism for the generation of such high ice particle concentrations is as yet unexplained. A major factor in determining the seedability of clouds is the supercooled water content; instruments are being developed to measure this parameter remotely and this could help in the selection of cases amenable to seeding.

The PEP showed that, in the project area, seeding might produce increases in rainfall over an area of 5-30% but that such changes would require seeding experiments over 5-10 years to demonstrate effects significant at the 5% level. The project has also shown the potential of detailed numerical models to study the effects of seeding (Figure 3.12) although at

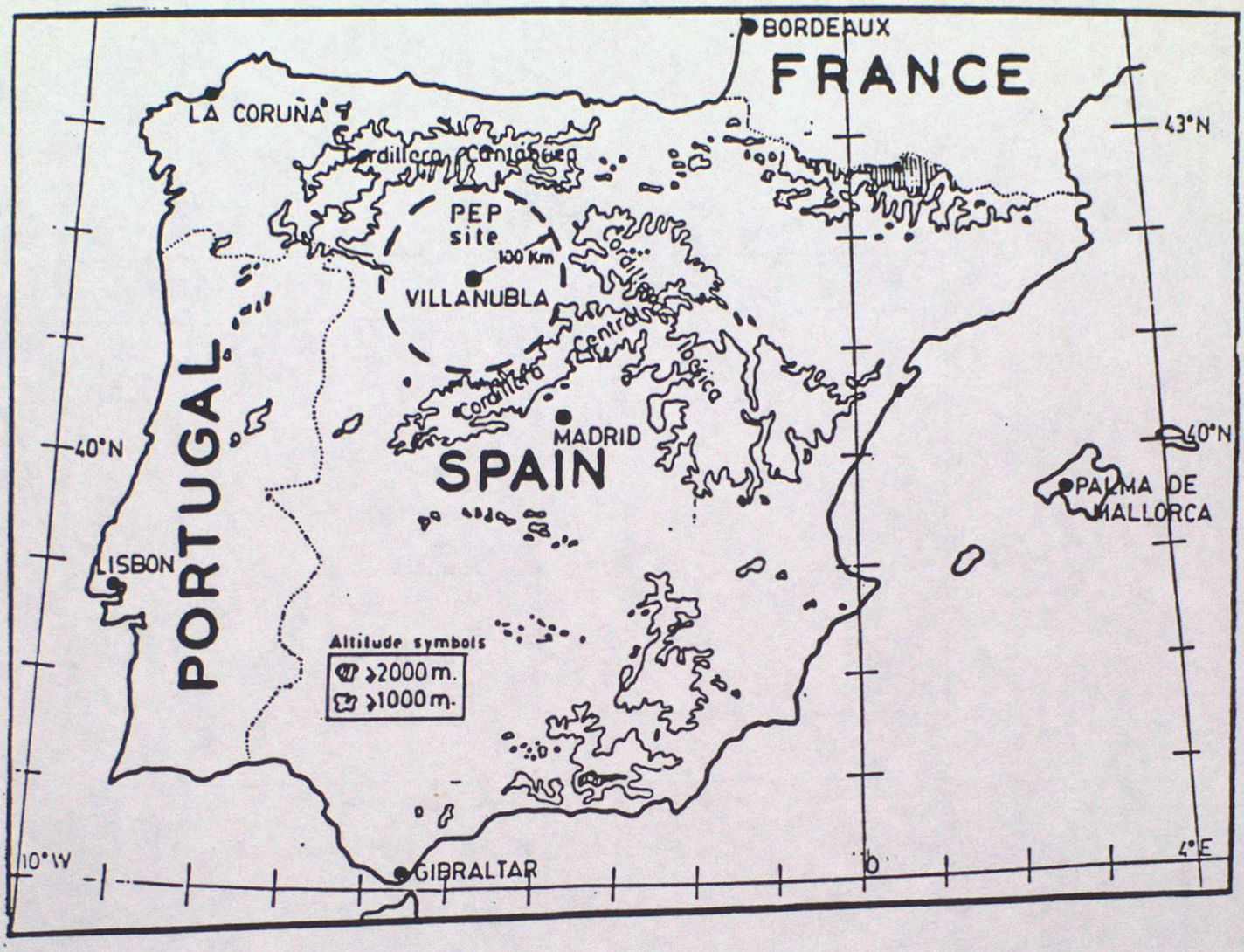

Figure 3.11. The area covered by the WMO Precipitation Enhancement Project.

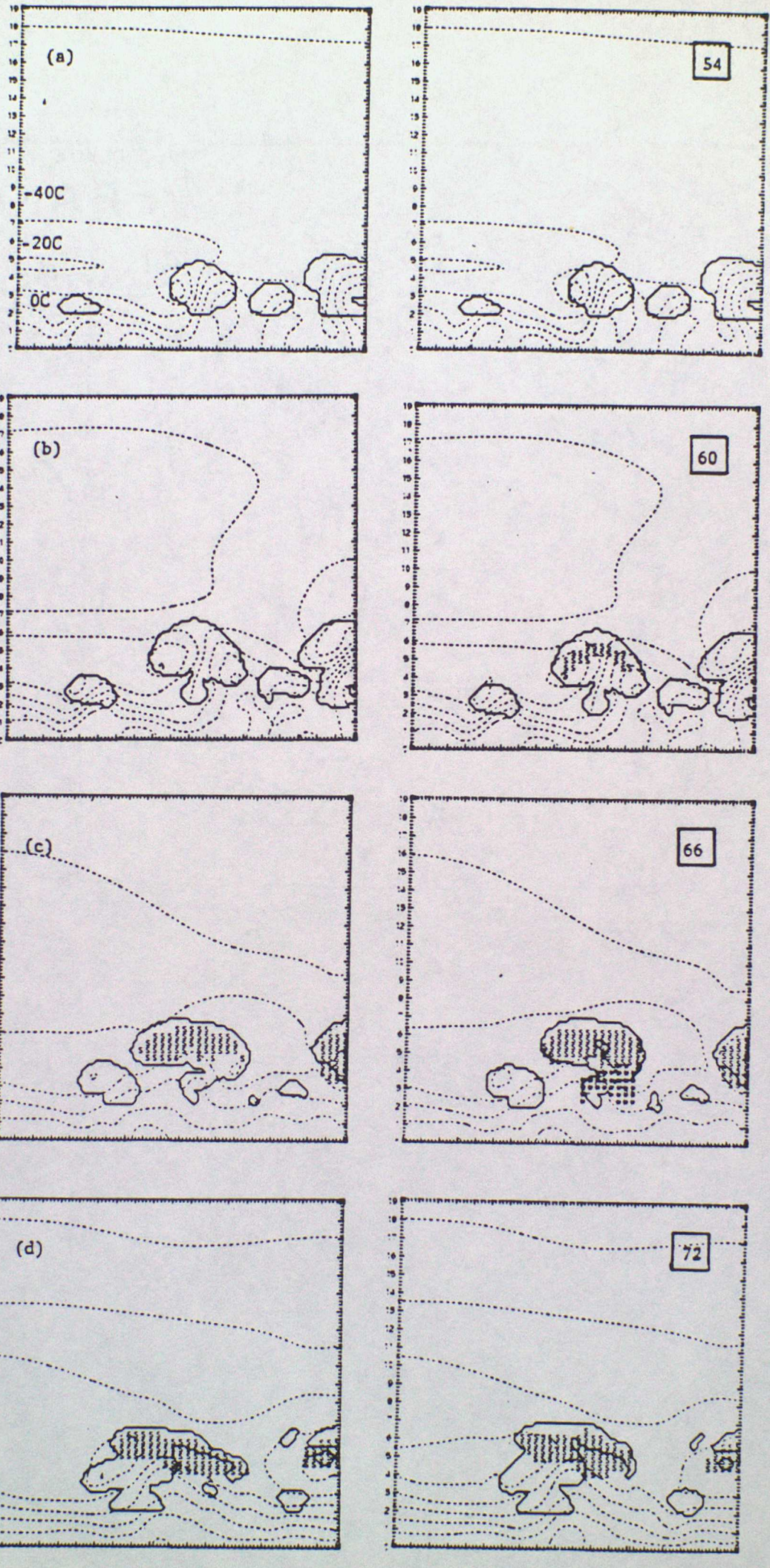
(a)
-40C
-20C
0C
54
(b)
60
(c)
66
(d)
72

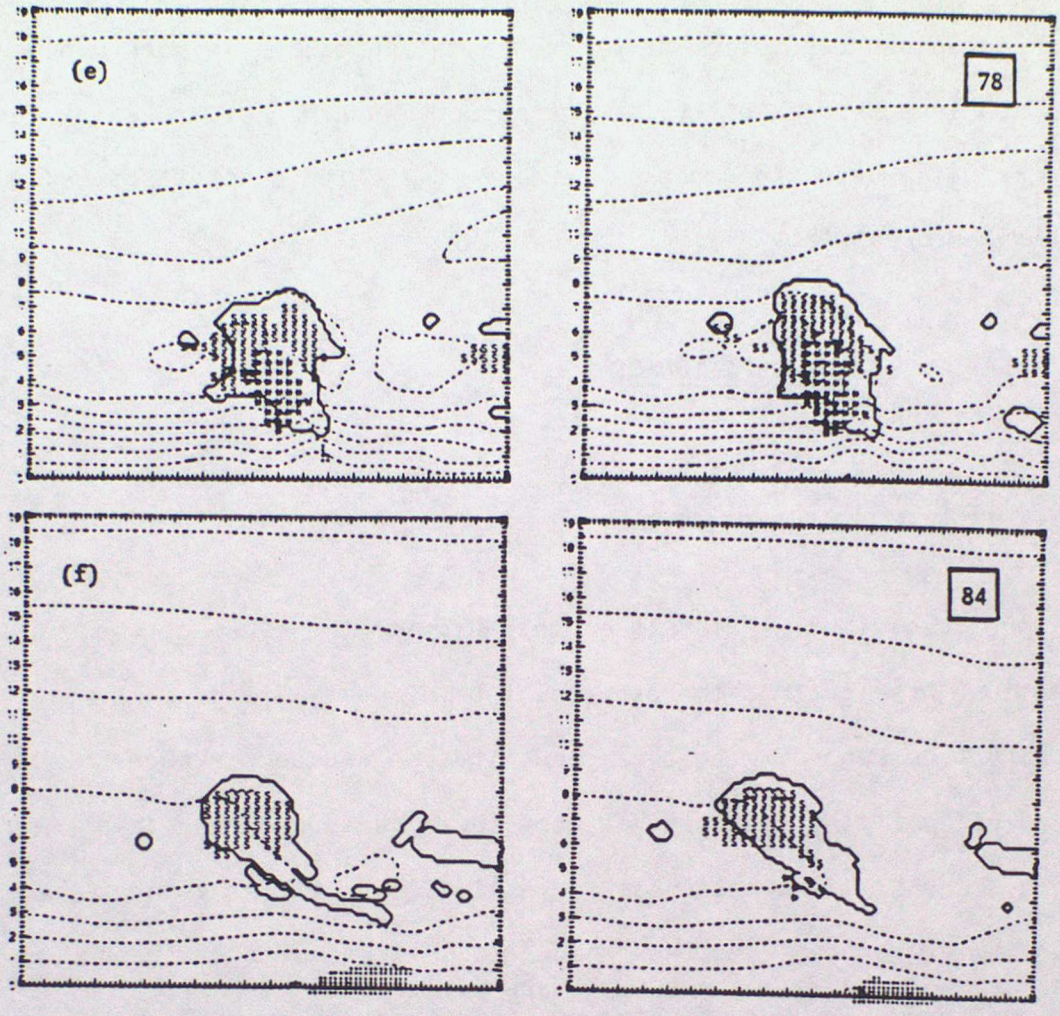

Figure 3.12. Sequence of 2d numerical model simulation fields from, left, unseeded and right, seeded clouds at the indicated times (min). Snow rain and hail are indicated by S, open circles and asterisks respectively. Streamlines are shown dotted and the solid line indicates the cloud boundary.

present the representation of microphysical processes in rather elementary. Such models appear to offer, in the future, a method of assessing the factors which determine whether seeding is likely to be effective on particular occasions.

3.3 ARTIFICIAL DISSIPATION OF FOG

3.3.1 Supercooled and ice fogs

Fogs are traditionally classified according to the cause of their formation; however from the standpoint of dispersal it is more relevant to classify them according to their constitution and temperature, since the method of modifying them depends upon these factors rather than the fog's origin. Ice fog is a suspension of small ice particles generally only occurring at temperatures less than -30°C. Studies of this fog have been made and these have resulted in some practical recommendations for decreasing its occurrence by minimizing the production of moisture from human activities. However, no practical method has yet been found for modifying an ice fog once it has formed.

Supercooled fog is composed of water droplets which remain unfrozen although their temperature is below 0°C. Provided the temperature is not too low and there is a relative absence of ice nuclei to stimulate freezing, such fogs are naturally stable. They can be modified quite readily by introducing artificial nuclei.

The dissipation of a supercooled fog is achieved by seeding it with material which produces ice crystals which, because of the difference in vapour pressure over ice and water at the same temperature, grow by deposition of vapour supplied by the fog droplets which thereby decrease in size. The reduction in fog droplet size increases the visibility but the main effect occurs when the ice crystals grow to such a size that they fall out. A number of operational procedures for clearing supercooled fog have been developed, including seeding from aircraft with dry ice or silver iodide or from extensive ground installations in which the expansion of propane gas produces sufficient cooling to generate large quantities of ice crystals. These methods of modifying supercooled fogs are in fairly wide use, but are limited to the relatively few regions of the world where supercooled fog is a sufficiently important operational hazard. Operational clearing is conducted in France, Germany and Norway as well as in the USA and USSR.

3.3.2 Warm fogs

Warm fog consists of water droplets at above, freezing temperature. It is the most common type of fog and is difficult to disperse artifically: nevertheless, a number of methods have been developed which are successful.

Considerable effort has been devoted by many groups to the development of warm fog dissipation techniques based upon seeding with hygroscopic chemicals. The basic idea is that if hygroscopic substances in the form of

either dry particles or solution droplets are released within a fog they absorb water vapour from the air, causing the fog droplets to evaporate. The hygroscopic particles themselves grow large enough to precipitate out of the system. Kunkel and Silverman (1970) have explored the best chemicals to be used for this purpose and have considered methods of encapsulation of the material. Theoretical models have been used to determine the optimum particle size and seeding strategy. Environmental considerations are also of major importance in hygroscopic seeding, since a large quantity of material may be necessary which ultimately is precipitated to the surface, and encapsulated urea has been put forward as the optimum choice. Successful development of a seeding agent and its use in small-scale field trials has not yet been followed by similar success over a large airport runway. Delivery of the seeding material at the right time and place to effect clearing more-or-less continuously of a runway some distance downwind from the seeding line has not proved reliable. More widespread seeding, which might be effective in clearing fog, is economically not practicable.

Another method that has been developed for clearing warm fog involves mixing of the relatively dry air often found above radiation fogs or stratus decks down into the fog or cloud layer. The method involves the use of the downwash from a large helicopter stationed just above the top of the fog. It has successfully created holes and clear lines in fogs up to 100-150 m thick. It has had operational success in special circumstances, such as helicopter rescues and supply operations in which the helicopter is able to land through holes in the cloud which it has cleared for itself.

At the present time the only major warm fog dissipation technique being used operationally is the thermal system in which sufficient thermal energy is used to evaporate fog droplets and to raise the temperature of the air sufficiently to accomodate the additional water. Operational systems involve large, permanent, expensive installations; they consume large amounts of fuel and are practical for only the busiest and largest airports where fogs are common. In addition to two French installations a prototype system has been constructed in the USA, after extensive small-scale testing and engineering trials. A key attribute of this new system is the use of propellors to distribute the heated air.

Warm fog dissipation methods based upon the use of artificial electrification to increase the natural rate of coalescence and precipitation of fog droplets or the use of laser heating have not so far led to practical applications.

3.4 HAIL SUPPRESSION

Worldwide losses of agricultural production due to hail damage are estimated to be in excess of 10^{10} dollars annually. However, in contrast to other weather-related disasters such as drought, floods, hurricanes, etc, hail losses tend to be very localized. The interest in hail suppression is worldwide as shown by the results of a survey conducted by WMO (1986).

Hailstorms are complex meteorological phenomena which have extreme variability in time and space and this makes it very difficult to assess the results of any programmes aimed at their modification, several efforts in operational hail suppression have been carried out over the last three decades. However, because of the fundamental difficulty of evaluation, it has only been possible to provide a limited assessment of the effectiveness of such programmes.

Many hypotheses have been proposed for suppressing hail. Those which have received widest discussion are:

(i) Enhancement of competition among hailstone embryos;

(ii) Glaciation of the medium on which hailstones grow;

(iii) Promotion of coalescence, followed by freezing; and

(iv) Dynamic effects, e.g. destruction of cumulonimbus clouds by initiation of downdraughts.

Glaciation, meaning conversion of supercooled cloud water to cloud ice requires unrealistically large amounts of ice nucleating agents, and promotion of coalescence needs very large amounts of hygroscopic material since the clouds are much larger than the nonprecipitating cumulus considered earlier. Dynamic effects, while potentially very important, have not been sufficiently studied to yield a useful working hypothesis. This leaves enhanced competition among hailstone embryos as the only

hypothesis which is generally accepted as showing promise for success based on the current understanding of hailstorms. This hypothesis can be simple stated as follows:

"If the number of growing hailstone embryos can be increased by a large factor (~ 100), then the competition for the available water supply prevents any embryos from growing large and thus the resulting hailstones either melt before reaching the ground or are too small to cause any damage". It should be noted that the total amount of precipitation at the surface may not be reduced but the damage depends on hail size not on total precipitation.

To implement this hypothesis it is necessary to increase the concentration of hail embryos in the hail growth zone. To produce this effect by means of seeding with ice nuclei requires the production of additional hail embryos to compete with the natural embryos for the available supply of supercooled water in the hailstone growth region. The seeding agent must act when and where the embryos form, and this may be at some distance from the hailstone growth region.

The most favourable regions for rapid growth of large hailstones are those with moderate to strong updraughts (> 12 m s^{-1}), appreciable liquid water concentrations (> 2 g m^{-3}), and low temperatures ($\leq -15°C$). Embryo formation on the other hand is favoured by weaker updraughts, say 5 m s^{-1}. In much stronger updraughts, newly formed ice particles would be carried up to the cloud top before growing large enough to become hail embryos. Two types of embryos have been distinguished. One type results from the freezing of supercooled raindrops, the other from the growth of graupel.

Which type predominates in a storm depends upon cloud-base temperature, updraught speed, liquid water concentration, cloud droplet size spectrum and activity of the ice nuclei which are present. Analysis of hail suggests there is a higher percentage of frozen-drop embroys in the large stones compared with small stones.

Nearly all hail suppression projects rest upon the assumption that hail is due, at least sometimes, to a deficiency of natural ice nuclei in the atmosphere. Nevertheless, no correlation between hail occurrences and variations in the concentration of natural ice nuclei, which often vary by a factor of ten or more, has been noted. While it is still possible that there is a threshold concentration required to suppress hail, the threshold (if it exists) probably exceeds the maximum observed concentration of natural ice nuclei. Therefore, if hail processes are to be modified by addition of ice nuclei, the concentration of artificial nuclei must be larger than the typical concentration of natural ice nuclei by a large factor. Such changes have in fact been produced.

In cases where hail forms on graupel embryos, the concentration of graupel can in principle, be increased by seeding early in the lifetime of new convective cells. A generalized concept of seeding new growth regions for this purpose has emerged independently in several hail projects, despite lack of precision in estimating the subsequent trajectories of such additional graupel particles and in ignorance of whether they in fact would enter the important regions to compete with the natural embryos.

Important questions have been raised about the required dispersion of the nuclei. For example, line sources (rockets, droppable pyrotechnics and airborne generators) offer an advantage over point sources (exploding shells). However, rockets and shells offer a chance for very rapid response to threatening situations. Also, problems of deactivation of nuclei by sunlight and by wetting in warm cloud have been raised, but these problems can be avoided when the seeding agent is injected directly. When airborne or ground-based generators are used, deactivation can be reduced by careful control of the chemical composition of the seeding agent.

The implementation of the seeding concepts in specific hailstorm situations requires very careful attention to the storm structure. In storms where each cell has a simple vertical structure and the hail embryos grow into hailstones near their place of origin, seeding in each new cell before the natural hail embryos appear offers a possibility of suppressing damaging hail. In more complex and persistent storms, where hail embryos may move in a continuous stream from the embryo growth region to a quite distinct hail growth region, more subtle techniques are likely to be required.

In spite of very intensive efforts by many groups in many countries seeding effects have not been clearly identified in the physical parameters of hailstorms. It is therefore still necessary to rely mainly on statistical evaluation of a hail suppression experiment to determine the likelihood that the variations are not simple chance fluctuations. Crop damage is ultimately the most relevant parameter, but due to the great variations among crops and their different rates of maturing during the growing

season, crop damage is not recommended as a primary response variable. The relation between the variables derived from hailstone number and sizes (e.g. mass or kinetic energy) and crop damage need to be better established.

In many regions where hail damage occurs, it is the same storms which produce much of the rainfall needed by agriculture. There is no observational evidence to show whether or not seeding for hail suppression increases or decreases rainfall in the defined target area or in nearby areas. However, this is a potential problem which needs further investigation and should be built into the design of future hail suppression experiments.

3.5 REFERENCES

Braham, R.R., L.J. Battan and Byers, H.R 1957 Artificial nucleation of cumulus clouds", Meteor.Monog. 2, 11, 47-85.

Kunkel, B.A. and B.A. Silverman 1970 A comparison of the warm fog clearing capabilities of some hygroscopic materials, J.Appl.Meteor., 9, 634-638.

WMO 1986 Trends in weather modification 1975-1983. Weather Modification Programme, Report No 7.

3.6 BIBLIOGRAPHY

Biswas, K.R., Kapoor, K.K. and Ramana Murity, Bh. V. 1967 Cloud seeding experiments using common salt. J. Appl. Meteorol., 6, 914-923.

Braham, R.R. 1986 The cloud physics of weather modification. Part 1 - Scientific basis. WMO Bulletin, 35, 215-222.

Changnon, S.A., 1980 The rationale for future weather modification research. Bull. Am. Meteorol. Soc., 61, 546-551.

Federer, B. and others 1986 Main results of Grossversuch IV J. Clim. Appl. Meteorol., 25, 917-957.

Foote, G.B. and ;Knight, C.A.(eds) 1977 Hail: A review of hail science and hail suppression. Meteorol. Mag., 38, Am. Meteorol. Soc.

Hess, W.N. (ed) 1979 Weather and climate modification. Wiley, New York.

Hobbs, P.V. 1975 The nature of winter clouds and precipitation in the Cascade Mountains and their modification by artificial seeding. Parts I-III. J. Appl. Meteorol., 14, 783-858.

List, R. 1978 The WMO precipitation enhancement project — PEP. WMO Bulletin, 27, 237-242.

Mason, B.J. 1982 Personal reflections on 35 years of cloud seeding. Contemp. Phys., 23, 311-327.

WMO 1986 Review of present status of weather modification. WMO Bulletin, 35, 140-144.